AD-A119 827 NATIONAL AERONUATICS AND SPACE ADMINISTRATION MOFFET--ETC F/G 20/4
AN EXPERIMENTAL STUDY OF DYNAMIC STALL ON ADVANCED AIRFOIL SECT--ETC(U)
JUL 82 W J MCCROSKEY, K W MCALISTER, L W CARR
UNCLASSIFIED NASA-A-8924-VOL-1 NASA-TM-84245-VOL-1 NL

NASA Technical Memorandum 84245

USAAVRADCOM TR-82-A-8

(12)

An Experimental Study of Dynamic Stall on Advanced Airfoil Sections Volume 1. Summary of the Experiment

W. J. McCroskey, K. W. McAlister, L. W. Carr, and S. L. Pucci

July 1982

NASA
National Aeronautics and
Space Administration

United States Army
Aviation Research
and Development
Command

NASA Technical Memorandum 84245 USAAVRADCOM TR-82-A-8

12

An Experimental Study of Dynamic Stall on Advanced Airfoil Sections Volume 1. Summary of the Experiment

W. J. McCroskey
K. W. McAlister
L. W. Carr
S. L. Pucci. Aeromechanics Laboratory
AVRADCOM Research and Technology Laboratories
Ames Research Center, Moffett Field, California

NASA
National Aeronautics and Space Administration
Ames Research Center
Moffett Field. California 94035

United States Army
Aviation Research and Development Command
St. Louis, Missouri 63166

TABLE OF CONTENTS

	Page
LIST OF TABLES	v
LIST OF FIGURES	vii
SYMBOLS	ix
SUMMARY	1
1. INTRODUCTION	1
2. DESCRIPTION OF THE EXPERIMENT	2
Test Apparatus	2
Instrumentation	3
Data Analysis and Measurement Accuracy	4
Test Conditions	7
3. GUIDE TO THE DATA	8
4. RESULTS AND DISCUSSION	10
Static Data	10
Dynamic Data	12
Comments on Wind-Tunnel Effects	14
5. SUMMARY AND CONCLUSIONS	14
REFERENCES	16
TABLES	19
FIGURES	55

LIST OF TABLES

		Page
1	Harmonic Coefficients of the Oscillation Mechanism	19
2	Airfoil Coordinates: NACA 0012 and Ames A-01 Airfoils	20
3	Airfoil Coordinates: Wortmann FX-098 and Sikorsky SC-1095 Airfoils	21
4	Airfoil Coordinates: Hughes HH-02 (-5° Tab) and Vertol VR-7 (-3° Tab) Airfoils	22
5	Airfoil Coordinates: NLR-1 and NLR-7301 Airfoils	23
6	Transducer Locations on the Airfoils	24
7	Static Drag Coefficients at $M_\infty = 0.30$ based on Wake Surveys	25
8	Summary of the Measured Static Airfoil Characteristics at $M_\infty = 0.30$, including Wind Tunnel Wall Corrections	25
9	List of Test Points with Unusual Zero Drift of Pressure Transducers	26
10	Coefficients of Linear Curve-Fit of Static Lift Data, without Wind-Tunnel Corrections	27
11	List of Data Frames	28
12	List of Static Data	44
13	Mach Number Sweep at $\alpha = 15° + 10° \sin \omega t$, $k = 0.10$	45
14	Frequency Sweep at $M_\infty = 0.29$, $\alpha = 15° + 10° \sin \omega t$	45
15	Frequency Sweep at $M_\infty = 0.30$, $\alpha = 10° + 10° \sin \omega t$	46
16	Frequency Sweep at $M_\infty = 0.30$, $\alpha = 15° + 5° \sin \omega t$	46
17	Frequency Sweep at $M_\infty = 0.30$, $\alpha = 10° + 5° \sin \omega t$	46
18	Stall Onset at $M_\infty = 0.30$, $\alpha = \alpha_o + 10° \sin \omega t$, $k = 0.10$	47
19	Stall Suppression at $M_\infty = 0.30$, $\alpha = \alpha_o + 10° \sin \omega t$	47
20	Stall Suppression at $M_\infty = 0.18$, $\alpha = \alpha_o + 10° \sin \omega t$	47
21	Pitch Damping Studies at $M_\infty = 0.30$, $\alpha = \alpha_o + 2° \sin \omega t$	48
22	No Separation: $M_\infty = 0.30$, $\alpha = 5° + 5° \sin \omega t$	50
23	Dynamic Boundary-Layer Trip Data	50

		Page
24	Miscellaneous Dynamic Data	51
25	Test Cases for Numerical Analysis (ref. 1)	54

LIST OF FIGURES

		Page
1	Airfoils tested in the experiment	55
2	Model installation in the test section	56
3	Photograph of the oscillation mechanism	57
4	Sketch of the wooden model shells surrounding the steel spar	58
5	Pressure transducer and hot-wire installation: view from inside the upper-surface shell	59
6	Coordinate axes for the airfoils	59
7	Sketch of the shadowgraph system for visualizing the leading-edge region	60
8	Representative shadowgraphs before (upper) and during (lower) dynamic stall: Sikorsky SC-1095 airfoil, $M_\infty = 0.30$, $\alpha = 10° + 10° \sin \omega t$, $k = 0.10$	61
9	Static lift and moment data on the NACA 0012 airfoil at $M_\infty = 0.3$; shaded bands represent uncertainty limits of data corrected for wind-tunnel-wall effects	62
10	Static lift and moment data on the Wortmann FX-098 airfoil at $M_\infty = 0.11$	63
11	Static lift and moment data on the Vertol VR-7 airfoil at $M_\infty = 0.30$	64
12	Comparison of measured lift-drag polars for the NACA 0012 airfoil at $M_\infty = 0.30$, including wind-tunnel-wall corrections	65
13	Comparison of lift-curve slopes on the NACA 0012 and SC-1095 airfoils, including wind-tunnel-wall corrections	65
14	Typical data presentation from volume 2; no wall corrections	66
15	Typical data presentation from volume 3	67
16	Static characteristics of the NACA 0012 airfoil at $M_\infty = 0.30$, including wind-tunnel-wall corrections	67
17	Static characteristics of the Ames A-01 airfoil at $M_\infty = 0.30$, including wind-tunnel-wall corrections	69
18	Static characteristics of the Wortmann FX-098 airfoil at $M_\infty = 0.30$, including wind-tunnel-wall corrections	71

Page

19 Static characteristics of the Sikorsky SC-1095 airfoil at $M_\infty = 0.30$, including wind-tunnel-wall corrections 73

20 Static characteristics of the Hughes HH-02 airfoil at $M_\infty = 0.30$, including wind-tunnel-wall corrections 75

21 Static characteristics of the Vertol VR-7 airfoil at $M_\infty = 0.30$, including wind-tunnel-wall corrections 77

22 Static characteristics of the NLR-1 airfoil at $M_\infty = 0.30$, including wind-tunnel-wall corrections 79

23 Static characteristics of the NLR-7301 airfoil at $M_\infty = 0.30$, including wind-tunnel-wall corrections 81

24 Comparison of maximum static lift on the NACA 0012 airfoil 83

25 Comparison of maximum static lift on the Ames A-01 airfoil 83

26 Comparison of maximum static lift on the Wortmann FX-098 airfoil 84

27 Comparison of maximum static lift on the Sikorsky SC-1095 airfoil 84

28 Comparison of maximum static lift on the Hughes HH-02 airfoil 85

29 Comparison of maximum static lift on the Vertol VR-7 airfoil 85

30 Comparison of maximum static lift on the NLR-1 airfoil 86

31 Comparison of maximum static lift on the NLR-7301 airfoil 86

32 Maximum unsteady lift on the eight airfoils: solid symbols = stall onset; open symbols = deep stall 87

33 Comparison of maximum lift on the eight airfoils at $M_\infty = 0.30$ 88

34 Comparison of maximum lift on the NACA 0012 airfoil under deep-dynamic-stall conditions: $\alpha = 15° + 10° \sin \omega t$, $k = 0.10$ 89

35 Comparison of the lift hysteresis on the NACA 0012 airfoil: $M_\infty \cong 0.1$, $\alpha = 15° + 10° \sin \omega t$, $k = 0.10$ 89

36 Comparison of maximum airloads on the NACA 0012 airfoil at $M_\infty = 0.30$ and $\alpha_1 k^2 \cong$ constant 90

37 Comparison of maximum airloads on the Sikorsky SC-1095 airfoil at $M_\infty = 0.30$ and $\alpha_1 k^2 \cong$ constant 91

38 Comparison of maximum airloads on the NLR-1 airfoil at $M_\infty = 0.3$ and $\alpha_{max} = 20°$ 92

SYMBOLS

A	static lift coefficient at $\alpha = 0$ (see table 10)
B	static $C_{L_\alpha}\sqrt{1 - M_\infty^2}$ (see table 10)
C_C	chord force coefficient
C_D	form drag coefficient derived from surface pressure measurements
C_{D_W}	total drag coefficient derived from wake survey (see table 7)
C_L	lift coefficient
C_{L_α}	lift-curve slope at low α, per deg
C_M	quarter-chord pitching moment coefficient
C_{M_o}	static pitching-moment coefficient at zero angle of attack
C_N	normal force coefficient
C_p	pressure coefficient
c	airfoil chord, m
k	reduced frequency, $\omega c/2U_\infty$
L/D	ratio of lift to drag
M_∞	free-stream Mach number (also M in table 11 and fig. 14)
M_{max}	maximum local Mach number on the airfoil
q_∞	free-stream dynamic pressure, N/m^2 (also Q, psi, in table 11)
Re	Reynolds number based on chord and free-stream conditions
r_o	leading-edge radius, m
t	time, sec
U_∞	free-stream velocity, m/sec
$X_{a.c.}$	chordwise location of the aerodynamic center of pressure at zero lift
x	chordwise coordinate, m (see fig. 6)
y	normal coordinate, m (see fig. 6)
α	angle of attack, deg
$\alpha_{C_{min}}$	angle of attack for maximum negative chordwise force, deg

$\alpha_{L_{max}}$	angle of attack for maximum lift, deg
$\alpha_{M_{max}}$	angle of attack for maximum local Mach number, deg
α_o	mean angle, deg (also A0 in computer printouts); also angle for zero lift in table 8 and figs. 9-11
α_{ss}	static-stall angle, corresponding to $C_{L_{max}}$, deg
α_1	amplitude, deg (also A1 in table 11 and fig 14)
α_2	magnitude of second harmonic of α, deg
β	$\sqrt{1 - M_\infty^2}$
ζ	aerodynamic pitch damping coefficient, $-\frac{1}{4\alpha_1^2}\oint C_M \, d\alpha$
ϕ_2	phase of second harmonic component of α, deg
ω	circular frequency, rad/sec

AN EXPERIMENTAL STUDY OF DYNAMIC STALL ON ADVANCED AIRFOIL SECTIONS

VOLUME 1. SUMMARY OF THE EXPERIMENT

W. J. McCroskey, K. W. McAlister, L. W. Carr, and S. L. Pucci

U.S. Army Aeromechanics Laboratory (AVRADCOM), Ames Research Center

SUMMARY

The static and dynamic characteristics of seven helicopter sections and a fixed-wing supercritical airfoil were investigated over a wide range of nominally two-dimensional flow conditions, at Mach numbers up to 0.30 and Reynolds numbers up to 4×10^6. Details of the experiment, estimates of measurement accuracy, and test conditions are described in this volume (the first of three volumes). Representative results are also presented and comparisons are made with data from other sources. The complete results for pressure distributions, forces, pitching moments, and boundary-layer separation and reattachment characteristics are available in graphical form in volumes 2 and 3.

The results of the experiment show important differences between airfoils, which would otherwise tend to be masked by differences in wind tunnels, particularly in steady cases. All of the airfoils tested provide significant advantages over the conventional NACA 0012 profile. In general, however, the parameters of the unsteady motion appear to be more important than airfoil shape in determining the dynamic-stall airloads.

1. INTRODUCTION

Retreating-blade stall limits the high-speed performance of most modern helicopters. In the past decade, numerous new airfoils have been designed in attempts to improve the stall characteristics of rotors without compromising the advancing-blade performance. Only a few of these have been tested under unsteady conditions, and some have not been tested at all. Furthermore, there is almost no overlap between the existing data sets with regard to the important parameters of oscillatory motion.

The motivation of the present experimental investigation was the obvious need for a standard data base for a series of modern rotor-blade sections. The primary objective was to measure the unsteady airloads, over an extensive matrix of test conditions, on the eight profiles shown in figure 1. Other investigations were also overlapped as much as possible. The NACA 0012 served primarily as a standard reference section; the six modern helicopter sections were chosen as representative of contemporary designs from several different companies and research organizations. A modern fixed-wing supercritical profile was also included to extend the range of leading-edge geometries and to provide a basis for comparison with oscillating-airfoil results obtained in other wind tunnels.

Secondary objectives were to investigate the type of stall and boundary-layer separation characteristics for each profile, to provide guidelines for estimating the dynamic-stall characteristics of new airfoils in the future, to supplement the conventional lift and pitching-moment measurements with unsteady drag data and

stall-flutter boundaries, and to determine the effects of leading-edge roughness that is comparable to the erosion of blades in service or in incipient icing conditions.

Dynamic stall depends on a large number of parameters. Consequently, a very large number of unsteady test points (more than 600) plus 44 sets of static data were required to fulfill the objectives of this investigation. As a result, the complete report consists of three volumes. The present volume summarizes the experiment and some of the principal results, including comparisons with data from other sources. It also contains a comprehensive index of the individual unsteady data points. Volume 2 (Pressure and Force Data) contains the pressure, force, and moment data in graphical form. These data are also available upon request on digital computer tapes, one tape for each airfoil, as explained in volume 2. In addition, there is a single tape containing only the 10 test cases that were discussed in reference 1 for the NACA 0012, Vertol VR-7, and NLR-7301 airfoils. Boundary-layer transition, flow reversal, and reattachment results appear in volume 3 (Hot-Wire and Hot-Film Measurements).

This report is primarily intended to assist the users of the data; therefore, the results are not discussed at length. The principal results have been published in references 1 and 2.

2. DESCRIPTION OF THE EXPERIMENT

Test Apparatus

The experiment was performed in the 2- by 3-m atmospheric-pressure, solid-wall Wind Tunnel at the U.S. Army Aeromechanics Laboratory. The tests were conducted in essentially the same manner as those in a previous experiment (refs. 3,4), except that the free-stream Mach number was extended to 0.3, the model chord c was reduced to 0.61 m (except for the Hughes HH-02 airfoil, $c = 0.69$ m), the frequency of oscillation was extended to 11 Hz, and the data processing was refined considerably. The models spanned the 2.13-m vertical dimension of the wind tunnel, as indicated in figure 2, and were oscillated sinusoidally in pitch about the quarter chord. A gap of approximately 2 mm existed between the ends of the model and the wind-tunnel walls.

The drive mechanism used (fig. 3) was the same one described in references 3 and 4, with some notable improvements. In some cases, the connecting push rod was fitted with a remotely controlled jackscrew mechanism that allowed the mean angle, α_o, to be varied continuously while the tunnel was operating. Discrete amplitudes of oscillation of 2°, 5°, 6°, 8°, 10°, or 14° could be set between runs. The motion of the airfoils was given by $\alpha \cong \alpha_o + \alpha_1 \sin \omega t$, with maximum higher harmonic distortion approximately 2% of α_1. Table 1 gives the harmonic content of the mechanism for various values of α_o and α_1. The frequency of oscillation could be varied between approximately 0.02 and 12 Hz.

The models of the eight airfoils (fig. 1) consisted of interchangeable shells constructed of wood and fiberglass. These shells surrounded a stainless steel spar that contained the instrumentation and wiring, as indicated schematically in figures 2 and 4. The shells contained special fittings for the pressure transducers and hot-wire or hot-film sensors (fig. 5) that facilitated model changes without disconnecting the instrumentation.

Each set of shells was precision-machined, while mounted on the spar, to a design accuracy of ±0.1 mm. However, measurements after the test revealed that the rms standard deviation of the coordinates from the design values was about 0.4 mm, or 0.06% of chord, and that the maximum error was about 0.8 mm. The nominal design coordinates of the airfoils are given in tables 2-5, referred to the standard coordinate system sketched in figure 6. The coordinates were taken originally from references 5-9 and from Amer (K. Amer, private communication, 1977).

A limited amount of static and dynamic data were obtained on each airfoil at $M_\infty = 0.185$ and 0.29 with a boundary-layer trip, consisting of a 3-mm-wide band of 0.10-mm-diam glass spheres glued to the leading edge. The purpose of the trip was to eliminate the laminar separation bubble that would normally form near the leading edge as the stall angle was approached. It also approximately simulated surface abrasion on helicopter blades operating under severe field conditions, as well as roughness caused by incipient icing conditions.

Instrumentation

The primary data were obtained from 26 Kulite differential pressure transducers, types YCQH-250-1 and YCQL-093-15. Those of the latter type were used in the leading- and trailing-edge regions, because of their smaller size. The locations of the transducers for each airfoil are given in table 6. The back side of each transducer was referenced to the total pressure of the wind tunnel; total pressure was measured about 1.5 m upstream of the model. The measuring side of the transducers mated with the fittings shown in figure 5, which had 0.79-mm-diam orifices. The transducers thus installed had flat amplitude versus frequency responses of 250 Hz or better and typical cavity resonance frequencies of about 850 Hz.

Special on-line analog computers that calculated and displayed the instantaneous normal force, pitching moment, pitch damping, and pressure distributions proved to be extremely valuable in assessing the dynamic-stall behavior, as well as the performance of the instrumentation, while the tests were in progress. These devices also enabled the unsteady parameters to be adjusted until some desired result was obtained, such as the maximum lift condition in the absence of moment stall or neutral aerodynamic damping in pitch.

Boundary-layer transition, flow reversal, separation, and reattachment were studied with a variety of surface hot films and hot-wire sensors (single-, double-, and triple-element probes), using the techniques described in references 4, 10, and 11. Six sensors were used on the upper surface of each airfoil, at the locations given in table 6. In addition, a hot-wire probe protruding just outside the boundary layer was mounted near the leading edge of the NLR-1 profile to aid in diagnosing the local supersonic zone that was frequently inferred at high incidence.

The leading-edge region was also examined with a shadowgraph flow visualization system (fig. 7). The high-intensity strobe light was fired at selected phase angles during the oscillation, and the pattern that developed on the Scotchlite high-gain reflective sheeting on the floor of the tunnel was photographed by the pulse camera above the test section. A representative photograph is shown in figure 8.

Finally, a traversing pitot-static probe was used to survey the wake behind each airfoil under steady-flow conditions. The steady drag of the airfoils at $M_\infty = 0.30$ was derived from these measurements; these drag coefficients are listed in table 7.

Data Analysis and Measurement Accuracy

For quantitative purposes, the pressure transducer and hot-wire signals were amplified and recorded on a 32-channel analog tape recorder with 2500-Hz flat frequency response. In addition, the average free-stream dynamic pressure, the instantaneous angle of attack of the model, and 1/cycle and 200/cycle timing indicators were recorded simultaneously. Calibrations of the pressure transducers were recorded at the beginning and end of each analog tape. The unsteady data tapes were digitized and ensemble-averaged off line. At least 50 cycles of data were normally sampled 200 times per cycle; however, for the NACA 0012 airfoil at very low frequencies, that is, $k < 0.002$, only about 10 cycles were recorded. Reference and calibration signals and the steady pressure data were acquired with the same system and were digitally sampled 100 times over a 5-sec interval. The averaged pressure data were then processed and integrated numerically by trapezoidal rule to determine the unsteady lift, moment, and pressure drag.

End-to-end checks of the data acquisition and processing system indicated that the pressure signals were reproduced to within an rms error of approximately 70 N/m^2 (0.01 psi), and that the transducer calibrations were reliable to better than ±150 N/m^2 (0.02 psi) or ±3% of the reading, whichever was greater, over the range of tunnel speeds and temperatures. The model temperature, measured inside the shells, was closely monitored and not allowed to vary more than 3°C between records of no-flow pressure readings. Transducer zero drift was normally controlled to within the greater value of either ±150 N/m^2 (0.02 psi) or ±5% of free-stream dynamic pressure. However, some exceptions are noted later in this section.

The hot-wire and hot-film signals were recorded as consecutive, separate data frames, and individual cycles of the analog records were examined to determine the boundary-layer characteristics, as discussed in references 4, 10, and 11. For these data, the results from three to eight cycles were averaged to obtain the relative times within the cycle, ωt, at which the various boundary-layer events occurred.

The instantaneous angle of attack was measured with a potentiometer attached to the tubular portion of the model spar (fig. 3). The angle-of-attack signal was calibrated for each data point based on the value of α_1, which was set by the oscillation linkage, and physical measurements of α_{max} and α_{min} that were obtained from the trailing-edge position relative to the centerline of the tunnel with the wind off. The maximum absolute error in α was estimated to be ±0.2°, with a relative uncertainty of ±0.05° over the cycle. The maximum torsional deflection of the model at the centerline was calculated to be ±0.3°. Table 1 gives the amplitude and phase of the second harmonic component of α for various nominal values of α_1. The frequency of the oscillation was maintained and measured to an estimated accuracy of ±0.03 Hz.

The tunnel dynamic pressure was measured with a conventional pitot-static probe mounted approximately 1.5 m upstream of the model and connected to a pressure transducer and amplifier system with a net accuracy of approximately ±14 N/m^2 (0.002 psi) under steady conditions. The measured values ranged from 90 N/m^2 (0.013 psi) at $M_\infty = 0.04$ to 6200 N/m^2 (0.90 psi) at $M_\infty = 0.3$. The output of this transducer was recorded by hand and on the 32-channel analog tape recorder. An average of these two values, which rarely differed by more than 2%, was used to compute q_∞, except in a few cases in the early stages of the test program in which the tape-recorded value was obviously in error and was therefore ignored. The 25-mm-thick ground plane shown in figure 2 caused a 1% reduction in tunnel cross-sectional area between the pitot-static tube and the model; this was ignored except as noted in connection with the steady lift results presented in section 4 under the heading Static Data.

A detailed examination of the digitized data revealed that the 200/cycle sampling of the analog signals was not always synchronized perfectly with the 200/cycle timing indicators. That is, the effective time base of the digitized data was in error, the cumulative effect of which was either to leave a small gap in the data at the end of the cycle or to overlap the 200th sample of a given cycle with the first sample of the next cycle. Consequently, a corrected time base for the digital data arrays was obtained by least-squares curve-fitting a first- and second-harmonic sine wave to the angle-of-attack signal, α. All of the pressure data were then linearly interpolated onto the new time base at 200 even intervals per cycle and stored in new arrays, with the first data point in each array corresponding to $\omega t = 0$. The end result is that the final data appear at the desired times, but suffer an effective "smearing" that would be, at worst, equivalent to sampling at a rate of 100 points per cycle instead of 200 per cycle.

Experimental uncertainty of the airloads- For the purposes of comparing the static and dynamic-stall characteristics of the eight airfoil sections, the absolute accuracy of the measurements and the consequences of wind-tunnel blockage, circulation interference, and sidewall boundary-layer interference are less important than the random experimental errors outlined above. However, an attempt was made to assess all of these, as described below.

The total measurement uncertainty in the pressure, force, and moment coefficients depends on the operating conditions. For example, the probable error in C_p based on the instrumentation characteristics quoted above varies from less than ±0.07 at $M_\infty = 0.3$ and $\alpha = 0$ to about ±0.4 near the leading edge at $M_\infty = 0.11$ and α approaching the stall angle. For most of the static data at $M_\infty = 0.3$, the measurement uncertainty is estimated at ±0.03 for $C_{L_{max}}$, ±0.005 for C_M, and ±0.0005 for C_D derived from the wake measurements. However, the uncertainty in the SC-1095 lift and moment data is thought to be at least twice as large, because of some unresolved difficulties with the pressure measurements. These values increase with decreasing Mach number, rising by a factor of about 5 in the extreme case $M_\infty = 0.035$, where the pressure signals were very small.

Some representative examples of static C_L and C_M versus α are given in figures 9-11, and the primary characteristics of each airfoil at $M_\infty = 0.30$ are presented in table 8. The symbols in the figures indicate the individual uncorrected data points, as presented in volume 2 of this report; the shaded bands denote the estimated bounds of the airfoil characteristics. The bounds of the airfoil characteristic include static wind-tunnel-wall corrections according to Allen and Vincenti (ref. 12) and a 1% correction due to the reduction in test-section area at the model caused by the steel plate on the floor of the tunnel (fig. 2). (This wall correction method is only valid below stall, where the corrections are about 1% for α and 1.5% for C_L.) These boundaries were derived based on the measurement uncertainties described above, on data that were obtained with the on-line analog computers, and on the dynamic data obtained at $k \leq 0.01$. It should be noted that the scatter in the data and the uncertainty bounds increase considerably for conditions above the stall angle. The last line in table 8 indicates the experimental uncertainties for the various quantities listed. The static data are discussed further in section 4.

A novel feature of the present experiment was the determination of unsteady pressure drag, $C_D = C_C \cos\alpha + C_N \sin\alpha$, where C_C and C_N are the chordwise and normal force coefficients derived from the upper and lower surface-pressure distributions. The two terms in this expression for C_D are approximately equal and opposite at high angles of attack below stall, so that the probable percentage errors of

C_D are much greater than for C_C, C_N, C_L, or C_M. Figure 12 shows a typical static lift-drag polar based on pressure measurements and on the more accurate wake survey of the total drag (table 7). The measured pressure drag, which neglects the contribution due to skin friction, is less than the total drag at low lift coefficients, but it incorrectly exceeds the wake measurements by as much as 0.02 near the stall angle, that is, by as much as 100%. (It may be noted that Woodward (ref. 13) reported similar, unexplained discrepancies between measured pressure drag and C_D based on wake surveys.) However, the percentage errors are much less in the stall regime, where the magnitude of C_C decreases considerably and the maximum drag coefficient becomes of the order of $C_L \tan \alpha$ (i.e., of the order of unity) for the deep-dynamic-stall cases studied.

The measurement uncertainty of the unsteady data is probably comparable to that of the static data, but fewer independent checks were available to assess the random experimental errors and the wind-tunnel interference, especially in the post-stall regime. Fromme and Golberg (ref. 14) have indicated that unsteady wall corrections can be greater than the corresponding static corrections, but it is not clear to what extent their potential flow analysis can be applied to the present measurements. Likewise, it is not possible to estimate reliably the post-stall tunnel sidewall effects nor how these vary from one airfoil to another, but tuft flow visualization and experience suggested that these problems became less important as the frequency of oscillation is increased. It is the authors' judgment that for $M_\infty \geq 0.2$, the unsteady data in the deep-dynamic-stall regime should be in error by no more than ± 0.2 for C_L, ± 0.05 for C_M, and ± 0.10 for C_D, except as noted in the next section. The results are thought to be about twice this accurate below stall and in light stall, whereas the accuracy was seriously degraded for $M_\infty < 0.1$ because of the small values of the pressure signals.

Special cases of questionable accuracy- Despite efforts to monitor the performance of the pressure instrumentation during the test and to control and minimize the measurement uncertainties, various problems sometimes arose that only became evident during the post-test reduction and analysis of the data. In most cases, it was possible to correct these problems on an individual basis, using redundant information or by interpolating in time or space between neighboring values, without significantly compromising the accuracy of the results. In other instances, the measurements appeared to be qualitatively correct, but the experimental uncertainty was likely to have been outside the normal bounds discussed in the previous section. These cases are identified below by data-point or "frame" number.

Frame 10202 for the NACA 0012 airfoil had an unusually large number of random irregularities, a total of 44 in the 5,200 pressure data samples. These were eliminated by linearly interpolating between data at preceding and succeeding time increments. Because some of these irregularities occurred during rapid fluctuations of the flow, the time-histories of part of the pressure data for this particular frame may have been degraded. However, the effect on the integrated force and moment coefficients was probably small.

Table 9 lists the frames for which the "zero" drift of one or more of the transducers appeared to have exceeded by a significant amount the nominal values quoted in the previous section. Also included are the low Mach-number cases for which the no-flow pressure readings taken before and after recording data varied by more than 50% of free-stream dynamic pressure, even though this drift amounted to less than the nominal measurement uncertainty of 150 N/m^2 (0.02 psi). It should be mentioned that in all cases the differences between these pretest and post-test zeros were linearly interpolated with respect to elapsed time to obtain effective zeros for the individual

data frames. In principle, this should have reduced the effects of the transducer drift; however, the actual improvement in the measurement accuracy because of this technique remains unknown.

For the Hughes HH-02 airfoil, the responses of pressure transducers No. 1 (leading edge) and No. 25 ($x/c = 0.0081$, lower surface) were rather sluggish, possibly because the orifices were partially clogged. Therefore, the unsteady data from these two transducers are suspect. In calculating the force and moment data for this airfoil, transducer No. 25 was ignored and the pressure integrals

$$C_N = -\oint C_p \, dx/c \qquad \text{etc.}$$

were replaced by

$$C_N = -2 \oint C_p \xi \, d\xi \qquad \text{etc.}$$

where $\xi = \sqrt{x/c}$, thereby eliminating the influence of transducer No. 1, since $C_{p_1}\sqrt{x_1} = 0$. Another problem with the HH-02 force and moment data is that the trailing-edge transducers were at $x/c = 0.925$ instead of 0.98, so that the error in extrapolating to $x/c = 1.0$ is greater for this airfoil. The net effect of these modifications is difficult to assess, but it probably increased the experimental uncertainties for the lift, pressure drag, and pitching moment data by no more than 50%.

The NLR-7301 airfoil had a large amount of concave curvature on the lower surface downstream of $x/c = 0.5$, which produced larger pressure gradients there than existed on the other airfoils. Therefore, the relatively sparse distribution of pressure transducers in that region may have led to larger errors in determining the forces and moments than the nominal values quoted in the preceding section.

The reduced data for the Sikorsky SC-1095 airfoil under static conditions and at low frequencies consistently exhibited values of maximum lift coefficient and lift-curve slope that appeared to be about 5% too large, based on comparisons with the other airfoils and with the results obtained from the special on-line analog computer described above under Instrumentation. In particular, the comparison with the present NACA 0012 data (fig. 13) contrasts significantly with the steady results of Noonam and Bingham (ref. 15) and Jepson (ref. 16), who found C_{L_α} to be approximately the same for both airfoils. A detailed examination of the present data and the transducer calibrations revealed somewhat erratic performance in a few cases, but no systematic behavior emerged that could explain the apparent problem. Therefore, the conclusion is that the SC-1095 results should be viewed with caution, even though they appear to be qualitatively correct.

Test Conditions

The primary reference conditions for the initial comparisons of the various airfoils were static and deep-dynamic stall at $M_\infty = 0.3$, with the nominal unsteady motion given by $\alpha = 10° + 10° \sin \omega t$ and $k = \omega c/2U_\infty = 0.10$. Limited but systematic variations in Mach number and the unsteady parameters were explored for all airfoils as indicated below and in section 3, where the specific test points are indexed and cross-referenced.

Static data- Pressure measurements were recorded at discrete values of α between -5° and 20° for M_∞ = 0.11, 0.185, 0.25, and 0.30 for all airfoils except the NACA 0012. In the latter case, static data were recorded only at M_∞ = 0.30; quasi-steady data were obtained for a continuous range of $\alpha = \alpha_0 + 10° \sin \omega t$ for $k \cong 0.001$ for nine values of M_∞ between 0.035 and 0.30. A number of the static conditions were repeated with a boundary-layer trip at the leading edge. Wake surveys for static drag were obtained at $M_\infty = 0.3$ for α between -5° and the static stall angle.

Unsteady data- The parameters that were varied under dynamic-stall conditions were Mach number, reduced frequency, mean angle, and amplitude of the oscillation. The effect of Mach number was studied between M_∞ = 0.035 and 0.30, primarily in the deep-stall regime for $\alpha = 15° + 10° \sin \omega t$ and $k = 0.10$. In these cases, the Reynolds number also varied, proportional to Mach number, according to the relation $Re \cong 14\times10^6\ M_\infty$.

The principal ranges of reduced frequency, mean angle, and amplitude were $0.01 \leq k \leq 0.20$, α_0 = 10° and 15°, and α_1 = 2°, 5°, and 10°, respectively; the effects of these parameters were studied primarily at M_∞ = 0.30. Additional variations in k and α_0 were effected to achieve specific dynamic effects, such as no stall, stall onset, stall suppression because of unsteady effects, and neutral aerodynamic damping in pitch.

Finally, additional test points were selected that duplicated some of the conditions of references 3 and 17-19 as closely as possible. A complete list of the unsteady test conditions and descriptions of the parametric variations are given in the following section.

3. GUIDE TO THE DATA

A very large data base was generated in this investigation. As mentioned in the Introduction, summary graphs of the pressure, force, and moment coefficients and selected results from the boundary-layer studies are contained in separate volumes. The airloads data are also stored on digital computer tapes, one for each airfoil, as explained in volume 2. This section describes briefly the data presentations to be found in the subsequent volumes and indicates by test point, or "frame number," the various types of data that are available.

Figure 14 illustrates the format of volume 2 for the unsteady pressure, force, and moment coefficient data, that is, C_L, C_M, and C_D versus α and ωt, and the upper-surface pressure distributions throughout the cycle. Additional information is listed at the top of the graphs. Following the airfoil name is the identification number for each test point. As explained in volume 2, these frame numbers comprise data at a single angle of attack for the steady data, and data at 200 evenly spaced time intervals throughout the cycle for the unsteady cases. The quantities A0 and A1 are the mean value and the first-harmonic amplitude, respectively, of the instantaneous angle of attack, α; M_{max} is the estimated maximum value of the local Mach number at any time in the cycle, calculated from the classical gas-dynamic equations for steady isentropic flow and the measured pressure coefficient, $-C_{p_{min}}$ (cf. ref. 2); $\alpha_{L_{max}}$, $\alpha_{C_{min}}$, and $\alpha_{M_{max}}$ are the angles of attack corresponding to maximum lift, minimum chord force (cf. ref. 3), and M_{max}, respectively; and ζ is

the aerodynamic damping in pitch. The asterisk on the ordinate of the pressure-coefficient graph represents sonic conditions.

The dotted line in the C_L vs α curve in figure 14 is an approximation to the quasi-static lift behavior for this flow condition, according to the relation

$$C_L = A + \frac{B\alpha}{\sqrt{1 - M_\infty^2}}$$

where α is in degrees and A and B were obtained from the relevant steady and very low-frequency data, that is, for $k \leq 0.01$. The values of A and B are given in table 10. Finally, it should be mentioned that in contrast to the data in table 8 and the static results presented in section 4 under the heading Static Data, wind-tunnel wall corrections have not been applied to A and B, to the data in volume 2, nor to the numerical data tapes.

Figure 15 shows two representative examples of the boundary-layer "flow reversal" information contained in volume 3. The abscissa in the figures show the position on the airfoil where the surface instrumentation first indicated a breakdown of the attached boundary-layer flow at the beginning of dynamic stall, as explained and discussed in volume 3 and in references 4, 10, and 11. This event either signifies or is closely associated with the separation that accompanies the beginning stages of dynamic stall. The ordinate indicates the nondimensional time in the cycle, ωt, at which this event occurred.

Tables 11-24 provide a comprehensive summary and index of the entire experimental program. Table 11 lists the frame numbers of all the pressure data, in the sequence in which they appear on the data tapes. The airfoil and pertinent test conditions are also listed, and the conditions for which boundary-layer data were recorded are indicated in the last column. The letter "Y" in the "TRIP" column indicates the use of the boundary-layer trip; "N" denotes the standard smooth condition. The notations "ST" and "US" denote steady and unsteady data, respectively, and the frequency of oscillation in Hertz is given in the column labeled "FREQ."

Table 12 is an index of the steady-data sets, arranged by airfoil and Mach number. The use of a boundary-layer trip is indicated by the letter "T." The notation "Quasi-steady" indicates the data that were acquired on the NACA 0012 airfoil as unsteady data, but at very low frequency, $k \leq 0.002$.

A cross-reference index that groups the unsteady data by types for each of the eight airfoils is given in tables 13-24. There are some duplicate entries in these tables, in order to facilitate the identification of data sets with variations in the individual parameters of the unsteady motion. There are also blank entries, since not all conditions were recorded for all airfoils. The principal types of unsteady conditions are outlined below.

Variations in Mach number- Table 13 lists the test points concerned with the effect of Mach number on deep dynamic stall, for $\alpha = 15° + 10° \sin \omega t$ and $k = 0.10$. Although the NLR-7301 airfoil was only tested at three values of M_∞ with $\alpha_o = 15°$, it was also tested with $\alpha_o = 10°$ at $M_\infty = 0.11$, 0.18, 0.22, and 0.30; these frames are given in table 24. Stall-suppression conditions, tables 19 and 20, and the effects of leading-edge trips, table 23, were studied at $M_\infty = 0.18$ and 0.30 for various values of α_o and k. As stated in section 2 under Test Conditions, the variation of Reynolds number with Mach number was $Re \cong 14\times10^6\, M_\infty$.

Reduced frequency sweeps- The test points concerned with the effect of frequency on dynamic stall are given in tables 14-17. These data cover the range $0.01 \le k \le 0.20$ at $M_\infty = 0.3$, with mean angles of 10° and 15° and amplitudes of 5° and 10°. In addition, the NACA 0012 airfoil was tested over an extensive range of other values of α_o (table 24).

Stall onset- This condition, defined in references 1 and 2 as obtaining the maximum possible lift without moment stall occurring at any time throughout the cycle of oscillation, was studied at $M_\infty = 0.30$, $k = 0.10$, $\alpha_1 = 10°$, and variable mean angle, as indicated in table 18.

Stall suppression caused by unsteady effects- With α_1 fixed at 10°, α_o was varied so that α_{max} was slightly greater than the static-stall angle. Data were then recorded (tables 19 and 20) at various reduced frequencies to study whether stall would diminish or increase with increasing k.

Pitch damping boundaries- Stall conditions relevant to small-amplitude flutter boundaries are listed in table 21, at $\alpha_1 = 2°$ and $M_\infty = 0.30$. Mean angle and reduced frequency were varied to obtain approximate boundaries of neutral aerodynamic damping in pitch and to obtain the maximum negative value of pitch damping, $-\zeta_{min}$. However, no data of this type were recorded for the NACA 0012 airfoil.

No separation- A limited number of test points were recorded at $M_\infty = 0.30$ and $\alpha = 5° + 5° \sin \omega t$, as indicated in table 22. Some additional conditions for the NLR-1 and NLR-7301 profiles without separation are given in table 24.

Boundary-layer trip- Data with the leading-edge trip were obtained statically for α between 0° and 20° and dynamically for $\alpha = 15° + 10° \sin \omega t$ at two values of Mach number, 0.18 and 0.30. The values of k for the dynamic data are given in table 23; the static data with trip are so indicated in table 12. An exception was the NLR-7301 section at $M_\infty = 0.30$, for which $\alpha = 10° + 5° \sin \omega t$ (table 24). In addition, the NLR-1 section with trip was studied with $\alpha_o = 2.5°$ (table 24).

Miscellaneous- These test points are included in table 24. In addition to the cases mentioned above, the unsteady test conditions of references 3 and 17 for the NACA 0012, of reference 18 for the Sikorsky SC-1095, and of reference 19 for the NLR-1 airfoil were reproduced insofar as possible. Also, for the Vertol VR-7 airfoil, k was varied from 0.01 to 0.25 at $M_\infty = 0.18$ with $\alpha_o = 10°$ and 15° and $\alpha_1 = 10°$. Finally, dynamic stall on the NLR-1 profile at negative incidence was studied at $M_\infty = 0.30$ for $\alpha = -2° + 10° \sin \omega t$ and $0.01 \le k \le 0.10$.

Selected test cases- Finally, table 25 lists the unsteady data that were proposed in reference 1 as specific test cases for evaluating unsteady viscous flow theories and computational methods. These data were obtained on the NACA 0012, Vertol VR-7, and NLR-7301 airfoils. They include conditions of no-stall, stall-onset, light-stall, and deep-dynamic-stall, all at $M_\infty = 0.3$.

4. RESULTS AND DISCUSSION

Static Data

The measurements performed under steady or quasi-static flow conditions provide a frame of reference for the dynamic-stall results and a basis for comparison with

data from other wind tunnels. Some of the highlights of the static data are presented below, with particular reference to the force and moment coefficients at $M_\infty = 0.3$. With the exception of the drag data listed in table 7, wind-tunnel-wall corrections have been applied to all of the static results presented in this section, using the formulae of reference 12.

As noted earlier, table 8 gives a summary of the primary static characteristics of each airfoil at $M_\infty = 0.30$, and figures 16-23 show the basic variations of lift, pitching moment, and drag coefficients for the eight sections. The dashed lines in the "a" parts of figures 17-23 represent curve-fits of the lift data in the linear $C_L - \alpha$ regime. The drag data derived from the wake surveys are listed in table 7. In the following discussions, some comparisons are made for each airfoil between the present measurements and data obtained elsewhere.

NACA 0012 airfoil- This profile has been tested by many investigators, with a wide range of results. Figure 24 shows the variation in $C_{L_{max}}$ with Mach number, including results reported or summarized in references 3, 5, 15-17, and 20-24 over a wide range of Reynolds numbers. The present values of $C_{L_{max}}$ increase with increasing Mach number for $M_\infty < 0.22$, probably because of the effects of increasing Reynolds number, whereas compressibility effects are thought to be responsible for the decrease in $C_{L_{max}}$ for $M_\infty > 0.22$. The boundary-layer trip was found to be relatively unimportant for this airfoil at the Mach and Reynolds numbers of the test.

The present $C_{L_{max}}$ data tend to lie near the upper range of the values from other sources. The same is true for the lift-curve slopes in the linear regime, C_{L_α}, which is not shown.

Ames A-01 airfoil- Figure 25 compares the data from the present test with measurements made in a transonic wind tunnel at somewhat lower Reynolds numbers (ref. 6) for the A-01 airfoil. Although the lift-curve slopes for $C_L < 1.0$ were not significantly different in the two tests, the airfoil stalled at lower angles of attack in the transonic tunnel. Consequently, lower values of maximum lift coefficient were measured and reported in reference 6 at $M_\infty = 0.2$ and 0.3, which was near the lower operating limit of that facility.

Wortmann FX-098 airfoil- Maximum-lift data from several investigations (refs. 8, 24-26) are compared with the present data in figure 26 for the FX-098 airfoil. All of the data agree reasonably well over the Mach-number range of the present test. However, there are marked differences at higher Mach numbers.

Sikorsky SC-1095 airfoil- Steady results for this section are shown in figure 27, where the comparison is generally unfavorable. The suspicious nature of the present lift data was mentioned earlier in section 2 under Data Analysis and Measurement Accuracy; here the open circles indicate the present data analyzed in the normal way and the solid symbols represent what are thought to be the true values. The latter, somewhat lower, values are based primarily on the on-line measurements. It should be mentioned that the data of Noonan and Bingham (ref. 15) were obtained on a modified profile with a reflex training edge that reduced C_{M_0} to approximately zero, compared with the present value of -0.027 at $M_\infty = 0.3$ (cf. table 8). Also, the data of Jepson (ref. 16) in figure 27 came from a slotted-wall tunnel with 12.5% porosity, which was thought to yield somewhat lower values of C_L than comparable tests in solid-wall tunnels. Furthermore, the Reynolds numbers in references 15 and 16 were

lower than those of the present tests. Nevertheless, the discrepancies in figure 27 seem to be too large to be attributed to these factors or to measurement uncertainties. It will be shown later that dynamic data on the SC-1095 section are generally in better agreement.

Hughes HH-02 airfoil- Figure 28 shows the measured maximum lift coefficients for the present HH-02 airfoil, in comparison with data from a section that is almost identical except for a slightly smaller leading-edge radius (ref. 27). Although the Mach number range does not overlap, the two sets of results seem consistent.

Vertol VR-7 airfoil- Results from four sources are plotted in figure 29 for the VR-7 profile. The present data are somewhat higher than those of Coulomb (ref. 28), primarily because the stall occurred at slightly higher angles of attack, but the lift-curve slopes (not shown) and the effect of a boundary-layer trip were approximately the same. The value of $C_{L_{max}}$ at $M_\infty = 0.3$ is slightly lower than that of Dadone (ref. 5), whose measurements at higher Mach numbers exceed considerably those of Bingham et al. (ref. 29).

NLR-1 airfoil- Figure 30 shows the good agreement of the present measurements with those of Dadone (ref. 19) for the NLR-1 airfoil. It should be mentioned, however, that the details of the pitching-moment behavior in the vicinity of $C_{L_{max}}$ (not shown) were somewhat different. As in the previous example, the data of Noonan and Bingham (ref. 24) for $C_{L_{max}}$ at $M_\infty \geq 0.35$ tend to be lower than the data of Dadone (ref. 19). This airfoil appears to be more sensitive to Mach number than any of the other modern helicopter sections.

NLR-7301 airfoil- As shown in figure 31, the maximum static lift for the NLR-7301 airfoil exceeded that of the other sections by a considerable margin; however, C_{M_O} was -0.083 (cf. table 8). The values of $C_{L_{max}}$ shown are also greater than those obtained at NLR under virtually identical conditions (ref. 30). This was obtained at a significantly larger stall angle, more than 1° larger at $M_\infty = 0.18$, than in the NLR experiments, apparently because of different boundary-layer separation characteristics and sidewall interferences.

Dynamic Data

Although the static data described above comprised an essential part of the investigation, the primary objective was to obtain a common data base of unsteady characteristics for helicopter applications. In this section some representative examples are presented and comparisons made with other investigations. More complete discussions of the basic phenomena and of the results obtained are given in references 1 and 2.

The unsteady stall-onset and dynamic-stall counterparts of the static $C_{L_{max}}$ results discussed above are shown in figures 32 and 33, reproduced from reference 2 with some minor corrections. The dashed lines in figure 33 indicate the estimated deep-stall $C_{L_{max}}$ for the NLR-7301 airfoil; data were not obtained for this condition for $M_\infty > 0.25$. These results have not been corrected for wind-tunnel-wall interference.

Figures 32 and 33 illustrate an important general result of the investigation: the parameters of the unsteady motion tend to be more important than the airfoil geometry. For example, the differences in the values of $C_{L_{max}}$ for the Wortmann, Sikorsky, and Hughes airfoils can hardly be discerned within the experimental uncertainty, but the unsteady stall-onset and deep-stall results are much higher than the static values shown in figures 26-28 and 33. It is also interesting to note that at least for $M \leq 0.25$, the deep-stall $C_{L_{max}}$ values for the NLR-1 and NLR-7301 airfoils are almost identical. In contrast, the static and unsteady stall-onset results for these two very different profiles are considerably different and represent the lower and upper bounds, respectively, of all the airfoils tested.

In view of the aforementioned scatter in the static results from different wind tunnels, it is logical to inquire how different sets of dynamic data might compare. Because of the large number of parameters that affect dynamic stall and the tendency for past investigators to select different combinations of these parameters, the possibilities for direct comparison of unsteady results are much more limited. However, some examples are given below.

<u>NACA 0012 airfoil</u>- The first comparison for this profile is shown in figures 34 and 35, where data from reference 3 were obtained in the same wind tunnel as the present results, but with a model whose chord was twice as large. Figure 34 shows that the large values of $C_{L_{max}}$ reported in reference 3 were not realized in the present experiment. Figure 35 shows C_L versus α, where the two results are seen to differ by approximately 10% during the portion of the cycle when α is increasing but before dynamic stall begins. This is approximately the same as the difference in the lift-curve slopes for the corresponding static data, and it is consistent with the differences that would be predicted for static wind-tunnel-wall corrections (ref. 12) for the two chord-to-height ratios. However, it can be inferred from the differences in the peaks of the lift curves in figure 35 that the organized vortex-shedding phenomenon was more pronounced on the larger model after stall began. Also, reattachment of the boundary layer on the downstroke occurred earlier. These do not seem to be solely Reynolds-number effects; rather, it is suspected that in the earlier tests there was excessive interference between the boundary layers on the upper and lower walls of the tunnel and the unsteady viscous flow on the ends of the vertically mounted airfoil.

St. Hilaire and Carta (ref. 17) have reported on dynamic-stall tests of the NACA 0012 airfoil at UTRC under conditions similar to those in the present experiment. Figure 36 compares some of the data from the two investigations. The format and choice of unsteady parameters is based on an extension of the observation in reference 2, that for sinusoidal pitching oscillations the values of α_{max} and the product $\alpha_1 k^2$ seem to be particularly important in determining the detailed time-history of the unsteady airloads during dynamic stall. In order to compare as many test points as possible, data were selected that satisfied the criterion $0.0014 < \alpha_1 k^2 < 0.0022$, where α_1 is in radians. The variations in $C_{L_{max}}$ and $C_{M_{min}}$ in figure 36 are seen to correlate reasonably well on this basis, and the results from the two sources are in fairly good agreement. Some of the $C_{L_{max}}$ data from the UTRC wind tunnel are slightly higher than the present measurements.

<u>SC-1095 airfoil</u>- Gangwani (ref. 18) has reported data that were obtained on the SC-1095 section in the same facility that was used by St. Hilaire and Carta (ref. 17) to obtain the NACA 0012 data described in the preceding paragraph. The results are

compared with the present data in figure 37, following the same format as above. Fewer data points are available, but the degree of correlation is approximately comparable to that of the NACA 0012 results in figure 36. In contrast with that figure, however, the present values of $C_{L_{max}}$ tend to be slightly higher than the UTRC data (ref. 18). In any case, the discrepancies generally appear to be within the measurement uncertainty, and the agreement is better than for the static results (fig. 27).

NLR-1 airfoil- This profile was tested by Dadone (ref. 19) over a wide range of Mach numbers, mean angles, and amplitudes. Based on the considerations outlined above regarding α_{max} and $\alpha_1 k^2$, his results are compared with the present data in figure 38 as functions of $\alpha_1 k^2$ at a constant value $\alpha_{max} = 20°$, where α_1 is also in degrees. The lift data are in better agreement than in the previous examples, but more scatter appears in the pitching-moment results than before.

No unsteady results from other sources are presently available from other sources for comparison with the data obtained on the Wortmann FX-098, Ames A-01, Hughes HH-02, Vertol VR-7, and NLR 7301 airfoils.

Comments on Wind-Tunnel Effects

It is well known that testing the same airfoil in different wind tunnels often gives different results, especially for the static-stall characteristics. This is borne out in figures 24-31. In fact, if the results from these eight figures were overlaid, the real differences between the individual airfoils would be almost completely obscured by the differences attributable to the test facilities.

Although more limited in scope, the comparisons of dynamic-stall data shown in figures 36-38 are more encouraging than the static results. Since all of these data came from tests with either high aspect-ratio models or sidewall boundary-layer control, this suggests that the present dynamic data may be relatively free of wind-tunnel-wall contamination and other three-dimensional effects. A detailed examination of the complete time-histories of the unsteady airloads and further studies on models of various aspect ratios would be required to confirm this speculation.

A special feature of the present experiment is that a large number of airfoils were studied over a wide range of unsteady flow conditions in the same facility. This provides the basis for meaningful comparisons, even though wind-tunnel interference effects were not completely negligible. However, as stated in reference 1, it is recommended that the wind-tunnel walls be included or considered in any quantitative uses of the data.

5. SUMMARY AND CONCLUSIONS

A large amount of steady and unsteady data has been obtained on eight airfoil sections over a wide range of test conditions, at Mach numbers up to 0.30. The details of the experimental arrangements, estimates of the measurement accuracy, and the test conditions are described in this volume. Some comparisons are also made with data from other sources. Volume 2 (Pressure and Force Data) presents the results in graphical form and describes the digital computer tapes that contain the extensive numerical data. Volume 3 (Hot-Wire and Hot-Film Measurements) describes the boundary-layer studies performed with surface-mounted hot wires and hot films.

The results of the experiment show important differences between airfoils, differences that would otherwise tend to be masked by differences in wind tunnels, particularly in steady cases. All of the airfoils tested offer significant advantages over the standard NACA 0012 profile. In general, however, the parameters of the unsteady motion appear to be more important than airfoil shape in determining the dynamic-stall airloads.

REFERENCES

1. McCroskey, W. J.; and Pucci, S. L.: Viscous-Inviscid Interaction on Oscillating Airfoils in Subsonic Flow. AIAA J., vol. 20, no. 2, Feb. 1982, pp. 167-174.

2. McCroskey, W. J.; McAlister, K. W.; et al.: Dynamic Stall on Advanced Airfoil Sections. J. American Helicopter Soc., vol. 26, no. 3, July 1981, pp. 40-50.

3. McAlister, K. W.; Carr, L. W.; and McCroskey, W. J.: Dynamic Stall Experiments on the NACA 0012 Airfoil. NASA TP-1100, 1978.

4. Carr, L. W.; McAlister, K. W.; and McCroskey, W. J.: Analysis of the Development of Dynamic Stall Based on Oscillating Airfoil Experiments. NASA TN D-8382, 1977.

5. Dadone, L. U.: U.S. Army Helicopter Design Datcom. Vol. I - Airfoils. NASA CR-153247, 1976.

6. Hicks, R. M.; and McCroskey, W. J.: An Experimental Evaluation of a Helicopter Rotor Section Design by Numerical Optimization. NASA TM-78622, 1980.

7. Balch, D. T.: Helicopter Blade. U.S. Patent 3,728,045, 1973.

8. Kemp, L. D.: An Analytical Study for the Design of Advanced Rotor Airfoils. NASA CR-112297, 1973.

9. Barche, J., ed.: Experimental Data Base for Computer Program Assessment. AGARD Advisory Report 138, Advisory Group for Aerospace Research and Development, Neuilly-sur-Seine, France, 1979.

10. Carr, L. W.; and McCroskey, W. J.: A Directionally Sensitive Hot-Wire Probe for Detection of Flow Reversal in Highly Unsteady Flows. International Congress on Instrumentation in Aerospace Facilities, 1979 Record, Sept. 1979, pp. 154-162.

11. McCroskey, W. J.; McAlister, K. W.; and Carr, L. W.: Dynamic Stall Experiments on Oscillating Airfoils. AIAA J., vol. 14, no. 1, Jan. 1976, pp. 57-63.

12. Allen, H. J.; and Vincenti, W. G.: Wall Interference in a Two-Dimensional Flow Wind Tunnel with Consideration of the Effect of Compressibility. NACA Report 782, 1944.

13. Woodward, D. S.: The Twodimensional Characteristics of a 12.2% Thick R.A.E. Aerofoil Section. RAE Technical Report 68303, Royal Aircraft Establishment, Farnborough Hants, England, Jan. 1969.

14. Fromme, J. A.; and Golberg, M. A.: Unsteady Two-Dimensional Airloads Acting on Oscillating Airfoils in Subsonic Ventilated Wind Tunnels. NASA CR-2914, 1977.

15. Noonan, K. W.; and Bingham, G. J.: Aerodynamic Characteristics of Three Helicopter Rotor Airfoil Sections at Reynolds Numbers from Model Scale to Full Scale at Mach Numbers from 0.35 to 0.90. NASA TP-1701, 1980.

16. Jepson, W. D.: Two Dimensional Test of Four Airfoil Configurations with an Aspect Ratio of 7.5 and a 16 Inch Chord up to a Mach Number of 1.1. Report SER-50977, Sikorsky Aircraft, Stratford, Conn., Apr. 1977.

17. St. Hilaire, A. L.; and Carta, F. O.: The Influence of Sweep on the Aerodynamic Loading of an Oscillating NACA 0012 Airfoil. Vol. II - Data Report. NASA CR-145350, 1979.

18. Gangwani, S. T.: Prediction of Dynamic Stall and Unsteady Airloads for Rotor Blades. American Helicopter Society Paper 81-01, May 1981.

19. Dadone, L. U.: Two-Dimensional Wind Tunnel Test of an Oscillating Rotor Airfoil. NASA CR-2915, 1977.

20. Lizak, A. A.: Two-Dimensional Wind Tunnel Tests of an H-34 Main Rotor Airfoil Section. TREC Technical Report 60-53, U.S. Army Transportation Research Command, Ft. Eustis, VA, 1960.

21. Prouty, R. W.: A State-of-the-Art Survey of Two-Dimensional Airfoil Data. J. American Helicopter Soc., vol. 20, no. 4, Oct. 1975, pp. 14-25.

22. Bevert, A.: Essais Comparatifs en Courant Plan des Profils "G.1" et NACA 0012. ONERA Doc. No. 76/1157.AN, Office National d'Etudes et de Recherches Aérospatiales, Châtillon, France, Mar. 1970.

23. Harris, C. D.: Two-Dimensional Aerodynamic Characteristics of the NACA 0012 Airfoil in the Langley 8-Foot Transonic Pressure Tunnel. NASA TM-81927, 1981.

24. Noonan, K. W.; and Bingham, G. J.: Two-Dimensional Aerodynamic Characteristics of Several Rotorcraft Airfoils at Mach Numbers from 0.35 to 0.90. NASA TM X-73990, Jan. 1977.

25. Bingham, G. J.; and Noonan, K. W.: Low-Speed Aerodynamic Characteristics of Five Helicopter Blade Sections at Reynolds Numbers from 2.4×10^6 to 8.4×10^6. NASA TM X-2467, 1972.

26. Wortmann, F. X.: Design of Airfoils with High Lift at Low and Medium Subsonic Mach Numbers. Paper No. 7, AGARD Conference Proceedings CP-102, Advisory Group for Aerospace Research and Development, Neuilly-sur-Seine, France, 1972.

27. Prouty, R. W.: Airfoil Section Data Report. Report No. 150-A-1012, Hughes Helicopters, Culver City, Calif., Mar. 1978.

28. Coulomb, J.: Caractéristiques Stationnaires du Profil VR 7. Procès-verbal No. 102 B/SC, Centre d'Essais Aéronautique de Toulouse, Toulouse, France, June 1979.

29. Bingham, G. J.; Noonan, K. W.; and Jones, H. E.: Results of an Investigation of Several New Rotorcraft Airfoils as Related to Airfoil Requirements. Paper No. 8, NASA Conference Publication 2046, Mar. 1978.

30. Joosen, C. J. J.; and Kho, C. G.: Two Dimensional Low-Speed Wind Tunnel Investigation on a NLR 73-108-10 Airfoil with Fowler Type Flap, Part 1: Text, Tables, and Figures. NLR TR 74058 C, National Lucht- en Ruimtevaartlabotorium, Amsterdam, The Netherlands, Sept. 1975.

TABLE 1.- HARMONIC COEFFICIENTS OF THE OSCILLATION MECHANISM

$$\alpha = \alpha_o + \alpha_1 \sin \omega t + \alpha_2 \sin(\omega t + \phi_2)$$

α_o	Nominal α_1	α_1	α_2	ϕ_2
5	5	5.00	0.05	(a)
10	5	4.90	.05	(a)
0	10	10.20	.20	(a)
5	10	10.05	.20	(a)
10	10	9.90	.20	260°
15	10	9.90	.20	(a)
15	14	14.10	.38	200°

[a]Not measured.

TABLE 2. - AIRFOIL COORDINATES: NACA 0012 AND AMES A-01 AIRFOILS

x/c	NACA 0012, y/c		AMES A-01, y/c	
	upper	lower	upper	lower
0.0000	0.00000	0.00000	0.00000	0.00000
0.0005	0.00395	-0.00395	0.00377	-0.00338
0.0010	0.00556	-0.00556	0.00541	-0.00472
0.0020	0.00781	-0.00781	0.00766	-0.00651
0.0035	0.01027	-0.01027	0.01013	-0.00844
0.0050	0.01221	-0.01221	0.01214	-0.00994
0.0065	0.01386	-0.01386	0.01388	-0.01120
0.0080	0.01531	-0.01531	0.01543	-0.01227
0.0100	0.01704	-0.01704	0.01732	-0.01350
0.0125	0.01894	-0.01894	0.01945	-0.01481
0.0160	0.02127	-0.02127	0.02214	-0.01634
0.0200	0.02360	-0.02360	0.02490	-0.01777
0.0250	0.02615	-0.02615	0.02801	-0.01922
0.0350	0.03043	-0.03043	0.03335	-0.02137
0.0500	0.03555	-0.03555	0.03991	-0.02365
0.0650	0.03966	-0.03966	0.04523	-0.02549
0.0800	0.04307	-0.04307	0.04961	-0.02710
0.1000	0.04683	-0.04683	0.05421	-0.02902
0.1250	0.05055	-0.05055	0.05829	-0.03104
0.1500	0.05345	-0.05345	0.06098	-0.03277
0.2000	0.05737	-0.05737	0.06344	-0.03551
0.2500	0.05941	-0.05941	0.06431	-0.03727
0.3000	0.06002	-0.06002	0.06446	-0.03828
0.3500	0.05949	-0.05949	0.06409	-0.03866
0.4000	0.05803	-0.05803	0.06316	-0.03848
0.4500	0.05581	-0.05581	0.06154	-0.03782
0.5000	0.05294	-0.05294	0.05924	-0.03665
0.5500	0.04952	-0.04952	0.05623	-0.03501
0.6000	0.04563	-0.04563	0.05249	-0.03297
0.6500	0.04132	-0.04132	0.04792	-0.03056
0.7000	0.03664	-0.03664	0.04246	-0.02785
0.7500	0.03160	-0.03160	0.03600	-0.02486
0.8000	0.02623	-0.02623	0.02860	-0.02153
0.8500	0.02053	-0.02053	0.02064	-0.01786
0.9000	0.01448	-0.01448	0.01260	-0.01374
0.9250	0.01132	-0.01132	0.00899	-0.01144
0.9500	0.00807	-0.00807	0.00598	-0.00888
0.9750	0.00472	-0.00472	0.00392	-0.00603
0.9900	0.00265	-0.00265	0.00322	-0.00421
1.0000	0.00126	-0.00126	0.00299	-0.00300
	$r_o/c = 0.0158$		$r_o/c = 0.012$	

TABLE 3. - AIRFOIL COORDINATES: WORTMANN FX-098 AND SIKORSKY SC-1095 AIRFOILS

x/c	WORTMANN FX-098, y/c		SIKORSKY SC-1095, y/c	
	upper	lower	upper	lower
0.0000	0.00000	0.00000	0.00000	0.00000
0.0005	0.00293	-0.00249	0.00307	-0.00257
0.0010	0.00426	-0.00343	0.00443	-0.00368
0.0020	0.00619	-0.00471	0.00640	-0.00535
0.0035	0.00837	-0.00609	0.00865	-0.00724
0.0050	0.01017	-0.00717	0.01054	-0.00880
0.0065	0.01175	-0.00807	0.01221	-0.01016
0.0080	0.01319	-0.00886	0.01374	-0.01138
0.0100	0.01494	-0.00978	0.01560	-0.01285
0.0125	0.01692	-0.01079	0.01771	-0.01450
0.0160	0.01944	-0.01202	0.02041	-0.01657
0.0200	0.02204	-0.01321	0.02320	-0.01865
0.0250	0.02501	-0.01451	0.02635	-0.02092
0.0350	0.03021	-0.01664	0.03140	-0.02454
0.0500	0.03681	-0.01913	0.03677	-0.02842
0.0650	0.04234	-0.02111	0.04070	-0.03108
0.0800	0.04705	-0.02277	0.04374	-0.03295
0.1000	0.05222	-0.02464	0.04680	-0.03464
0.1250	0.05714	-0.02658	0.04963	-0.03619
0.1500	0.06073	-0.02819	0.05174	-0.03739
0.2000	0.06491	-0.03059	0.05447	-0.03884
0.2500	0.06650	-0.03198	0.05548	-0.03933
0.3000	0.06630	-0.03251	0.05524	-0.03918
0.3500	0.06515	-0.03242	0.05437	-0.03858
0.4000	0.06336	-0.03184	0.05299	-0.03760
0.4500	0.06097	-0.03096	0.05105	-0.03622
0.5000	0.05798	-0.02982	0.04854	-0.03446
0.5500	0.05445	-0.02843	0.04555	-0.03234
0.6000	0.05040	-0.02678	0.04212	-0.02985
0.6500	0.04586	-0.02487	0.03819	-0.02702
0.7000	0.04085	-0.02273	0.03375	-0.02384
0.7500	0.03543	-0.02034	0.02887	-0.02034
0.8000	0.02962	-0.01768	0.02362	-0.01658
0.8500	0.02337	-0.01473	0.01808	-0.01265
0.9000	0.01642	-0.01134	0.01235	-0.00865
0.9250	0.01253	-0.00932	0.00943	-0.00664
0.9500	0.00856	-0.00702	0.00642	-0.00454
0.9750	0.00476	-0.00423	0.00328	-0.00233
0.9900	0.00255	-0.00237	0.00132	-0.00093
1.0000	0.00110	-0.00110	0.00000	0.00000
	$r_o/c = 0.007$		$r_o/c = 0.008$	

TABLE 4. - AIRFOIL COORDINATES: HUGHES HH-02 (-5° TAB) AND VERTOL VR-7 (-3° TAB) AIRFOILS

x/c	HUGHES HH-02, y/c		VERTOL VR-7, y/c	
	upper	lower	upper	lower
0.0000	0.00000	0.00000	0.00000	0.00000
0.0005	0.00283	-0.00284	0.00337	-0.00330
0.0010	0.00405	-0.00388	0.00483	-0.00460
0.0020	0.00594	-0.00532	0.00696	-0.00633
0.0035	0.00819	-0.00683	0.00943	-0.00800
0.0050	0.01009	-0.00800	0.01149	-0.00919
0.0065	0.01176	-0.00895	0.01330	-0.01010
0.0080	0.01327	-0.00978	0.01494	-0.01086
0.0100	0.01510	-0.01072	0.01695	-0.01172
0.0125	0.01717	-0.01172	0.01923	-0.01263
0.0160	0.01975	-0.01290	0.02213	-0.01367
0.0200	0.02237	-0.01404	0.02512	-0.01467
0.0250	0.02531	-0.01524	0.02846	-0.01575
0.0350	0.03029	-0.01714	0.03423	-0.01751
0.0500	0.03640	-0.01943	0.04144	-0.01966
0.0650	0.04137	-0.02127	0.04759	-0.02154
0.0800	0.04553	-0.02276	0.05299	-0.02320
0.1000	0.05012	-0.02432	0.05922	-0.02516
0.1250	0.05468	-0.02575	0.06565	-0.02709
0.1500	0.05828	-0.02675	0.07091	-0.02855
0.2000	0.06328	-0.02793	0.07887	-0.03055
0.2500	0.06608	-0.02843	0.08378	-0.03186
0.3000	0.06738	-0.02834	0.08592	-0.03273
0.3500	0.06750	-0.02755	0.08574	-0.03308
0.4000	0.06640	-0.02600	0.08365	-0.03271
0.4500	0.06391	-0.02377	0.07984	-0.03148
0.5000	0.06008	-0.02104	0.07451	-0.02952
0.5500	0.05504	-0.01797	0.06781	-0.02712
0.6000	0.04891	-0.01482	0.05996	-0.02464
0.6500	0.04174	-0.01176	0.05171	-0.02207
0.7000	0.03344	-0.00952	0.04322	-0.01929
0.7500	0.02403	-0.00851	0.03442	-0.01639
0.8000	0.01436	-0.00889	0.02527	-0.01346
0.8500	0.00481	-0.00984	0.01575	-0.01050
0.9000	-0.00431	-0.01041	0.00558	-0.00744
0.9250	-0.00394	-0.00777	0.00117	-0.00609
0.9500	-0.00203	-0.00583	-0.00016	-0.00512
0.9750	-0.00006	-0.00387	0.00115	-0.00380
0.9900	0.00112	-0.00269	0.00194	-0.00300
1.0000	0.00190	-0.00190	0.00247	-0.00247
	$r_o/c = 0.008$		$r_o/c = 0.011$	

TABLE 5. - AIRFOIL COORDINATES: NLR-1 AND NLR-7301 AIRFOILS

x/c	NLR-1, y/c		NLR-7301, y/c	
	upper	lower	upper	lower
0.0000	0.00000	0.00000	0.00000	0.00000
0.0005	0.00359	-0.00288	0.00730	-0.00748
0.0010	0.00499	-0.00388	0.01051	-0.01020
0.0020	0.00687	-0.00518	0.01518	-0.01373
0.0035	0.00890	-0.00643	0.02030	-0.01735
0.0050	0.01053	-0.00730	0.02424	-0.02016
0.0065	0.01194	-0.00799	0.02756	-0.02252
0.0080	0.01321	-0.00858	0.03043	-0.02455
0.0100	0.01475	-0.00929	0.03375	-0.02688
0.0125	0.01648	-0.01006	0.03729	-0.02935
0.0160	0.01868	-0.01101	0.04140	-0.03225
0.0200	0.02097	-0.01196	0.04514	-0.03502
0.0250	0.02358	-0.01301	0.04873	-0.03794
0.0350	0.02799	-0.01477	0.05372	-0.04264
0.0500	0.03328	-0.01688	0.05920	-0.04806
0.0650	0.03750	-0.01859	0.06321	-0.05229
0.0800	0.04093	-0.02007	0.06636	-0.05576
0.1000	0.04435	-0.02179	0.06985	-0.05962
0.1250	0.04701	-0.02363	0.07347	-0.06358
0.1500	0.04905	-0.02522	0.07648	-0.06689
0.2000	0.05200	-0.02775	0.08115	-0.07194
0.2500	0.05386	-0.02958	0.08441	-0.07527
0.3000	0.05489	-0.03082	0.08649	-0.07713
0.3500	0.05528	-0.03154	0.08755	-0.07763
0.4000	0.05511	-0.03185	0.08764	-0.07672
0.4500	0.05443	-0.03176	0.08678	-0.07412
0.5000	0.05327	-0.03126	0.08495	-0.06934
0.5500	0.05164	-0.03025	0.08206	-0.06237
0.6000	0.04948	-0.02882	0.07789	-0.05386
0.6500	0.04677	-0.02707	0.07212	-0.04397
0.7000	0.04348	-0.02503	0.06458	-0.03316
0.7500	0.03892	-0.02276	0.05551	-0.02227
0.8000	0.03172	-0.02028	0.04523	-0.01221
0.8500	0.02368	-0.01756	0.03415	-0.00409
0.9000	0.01562	-0.01427	0.02269	0.00108
0.9250	0.01179	-0.01199	0.01696	0.00228
0.9500	0.00811	-0.00903	0.01129	0.00246
0.9750	0.00454	-0.00511	0.00577	0.00153
0.9900	0.00244	-0.00253	0.00258	0.00042
1.0000	0.00103	-0.00103	0.00055	-0.00055
	$r_o/c = 0.007$		$r_o/c = 0.055$	

TABLE 6.- TRANSDUCER LOCATIONS ON THE AIRFOILS

Transducer Number[a]	Nominal[b] x/c		Actual pressure transducer location							
	Pressure	Hot wire	0012	A-01	FX-098	SC-1095	VR-7	NLR-1	NLR-7301	HH-02
1 LE	0. (0.)		0.	0.	0.0002U	0.	0.	0.	0.0015U	0.
2 U	.005 (.004)		.0060	.0054	.0038	.0040	.0044	.0054	.0101	.0050
3	.010 (.010)		.0103	.010	.0067	.0110	.0083	.0108	.0165	.0087
4	.025 (.030)	0.025 (.025)	.0242	.024	.0196	.0275	.0225	.028	.0335	.0326
5	.050 (.06)		.052	.050	.051	.053	.050	.051	.0512	.0581
6	.100 (.12)	.10 (.12)	.102	.100	.101	.1025	.100	.101	.102	.1167
7	.175 (.18)		.176	.175	.177	.178	.175	.177	.177	.183
8	.25 (.25)		.252	.250	.252	.252	.250	.250	.252	.250
9	.325 (.32)		.326	.325	.326	.325	.325	.325	.326	.317
10	.40 (.38)	.40 (.38)	.40	.40	.40	.40	.40	.40	.40	.383
11	.50 (.48)		.50	.50	.50	.50	.50	.50	.50	.472
12	.60 (.56)	.60 (.56)	.60	.60	.60	.60	.60	.60	.60	.561
13	.70 (.65)		.70	.70	.70	.70	.70	.70	.70	.650
14	.80 (.74)	.80 (.74)	.80	.80	.80	.80	.80	.80	.80	.739
15	.90 (.84)		.899	.90	.90	.90	.90	.90	.90	.840
16 U	.98 (.93)		.98	.98	.98	.98	.98	.98	.98	.925
17 L	.98 (.93)		.979	.98	.98	.98	.98	.98	.98	.925
18	.90 (.84)		.90	.90	.90	.90	.90	.90	.90	.840
19	.70 (.65)		.70	.70	.70	.70	.70	.70	.70	.650
20	.50 (.48)		.50	.50	.50	.50	.50	.50	.50	.472
21	.30 (.29)		.30	.30	.30	.30	.30	.30	.30	.294
22	.15 (.16)		.153	.150	.153	.150	.150	.150	.155	.161
23	.05 (.072)		.0504	.050	.051	.052	.050	.051	.0517	.0730
24	.025 (.030)		.023	.026	.027	.028	.0246	.0220	.0194	.0293
25	.010 (.010)		.0093	.0130	.0125	.009	.0094	.0108	.0051	.0081
26 L	.005 (.004)		.0049	.0073	.0061	.005	.0040	.0062	.0021	.0044

[a]LE = leading edge; U = upper surface; L = lower surface.
[b]Locations for HH-02, for which c = 68.6 cm, are shown in parentheses; for all other airfoils shown, c = 61.0 cm.

TABLE 7. - STATIC DRAG COEFFICIENTS AT M = 0.30 BASED ON WAKE SURVEYS

α, deg	N-0012	AMES-01	W-098	SC-1095	HH-02	VR-7	NLR-1	NLR-7301
-5.0	0.00843	0.00851	0.00886	0.00739	0.00846	0.00899	0.02602	0.00952
-2.0	0.00729	0.00832	0.00771	0.00713	0.00719	0.00759	0.00743	0.00780
0.0	0.00711	0.00794	0.00683	0.00708	0.00679	0.00723	0.00710	0.00968
2.0	0.00718	0.00662	0.00664	0.00670	0.00655	0.00707	0.00745	0.00891
5.0	0.00865	0.00767	0.00755	0.00807	0.00816	0.00800	0.00831	0.01011
8.0	0.01031	0.00965	0.01142	0.01013	0.01112	0.01059	0.01086	0.01305
10.0	0.01190	0.01248	0.01405	0.01127	0.01382	0.01353	0.01322	0.01569
12.0	0.01711	0.01600	0.01773	0.01586	0.01849	0.02156	0.02006	0.02022
13.0	- -	- -	- -	0.02015	0.02236	- -	- -	- -
14.0	0.02901	- -	0.08922	- -	- -	- -	- -	- -
-4.0	- -	- -	- -	- -	- -	- -	0.00773	0.00843
-1.75	- -	- -	- -	- -	- -	- -	- -	0.00874
-1.0	- -	- -	- -	- -	- -	- -	- -	0.00962
1.0	- -	0.00738	- -	- -	- -	- -	- -	0.00973
1.5	- -	- -	- -	- -	- -	- -	- -	0.00910
2.5	- -	- -	- -	- -	- -	- -	- -	0.00896
3.0	- -	0.00702	- -	- -	- -	- -	- -	- -
4.0	- -	0.00712	- -	- -	- -	- -	- -	- -
6.0	- -	0.00791	- -	- -	- -	- -	- -	- -
9.9	- -	0.01218	- -	- -	- -	- -	- -	- -

TABLE 8.- SUMMARY OF THE MEASURED STATIC AIRFOIL CHARACTERISTICS AT M_∞ = 0.30, INCLUDING WIND TUNNEL WALL CORRECTIONS

Airfoil	C_{L_α}	α_o	C_{M_o}	$C_{D_{min}}$	$X_{a.c.}$	$C_{L_{max}}$	α_{ss}	$(L/D)_{max}$
NACA 0012	0.109	-0.1°	-0.007	0.0072	0.24	1.33	13.7°	90
Ames-01	.111	-.6	-.005	.0070	.25	1.45	13.6	100
FX-098	.109	-1.3	-.026	.0066	.24	1.43	13.1	94
SC-1095	(.110)[a]	-.9	-.027	.0073	.245	(1.46)[a]	13.5	(98)[a]
HH-02	.114	-.6	-.002	.0066	.255	1.42	13.2	92
VR-7	.117	-1.6	-.016	.0071	.26	1.51	12.6	107
NLR-1	.102	-1.0	-.025	.0071	.22	1.29	12.4	87
NLR-7301	.117	-1.9	-.083	.0078	.25	(1.83)[a]	(17.2)[a]	89
Nominal uncertainty	±.003	.2	.005	.0005	.005	.03	.3	5

[a]Uncertainty larger than nominal value in table.

TABLE 9.- LIST OF TEST POINTS WITH UNUSUAL ZERO DRIFT OF PRESSURE TRANSDUCERS

Airfoil	Frame	M_∞	Type[a]	Problem transducers	Airfoil	Frame	M_∞	Type[a]	Problem transducers
NACA 0012	8019	0.035	U	All	Wortmann				
	8021				FX-098	18414	.11	S	20,22
	8023					19401	.25		2,3,4
	8102					19402	.25		
	8104					19405	.25		
	8106					19406	.25		
	8114	.07		23		20103	.25		2,3
	8116	.07		23		20104	.25		
	8118	.07		23		20122	.30		
	8210	.11		4		20123	.30		
	12118	.26	Q.S.	3		20203	.30		
	13107	.11		1,4,20		20204	.30		
	13115	.07		Many	Sikorsky				
	13120	.07		1,3,4,18, 24,26	SC-1095	33022	.07	U	1,17,18,25
						33106	.11	U	Many
	13205	.035		Many		33110	.11	U	Many
	13217	.035		Many		34409	.29	U	2,3
	14104	.18	U	3,8		35021	.30	S	11
	14106	.18	U	3,8		35023	.30		11
	14108	.18	U	3,8		35100	.30		11
Ames A-01	26306	.30	S	2,3		35102	.30		11
	26307	.30		2,3		35103	.30		11
	28019	.11		1,20		36209	.11		1,20,22
	28021			1,20		36210	.11		1,20,22
	28023			1,20		35211	.11		1,20,22
	28101			1,20		35212	.11		1,20,22
	28106			All		35213	.11		1,20,22
	28107				Hughes				
	28109				HH-02	42309	.22	U	6
	28110					42313	.25		6
	28115					43308	.30		13
	28116					43309	.30		13
	28117				Vertol				
	28119				VR-7	47213	.18		1,4,24
	28120					47217	.22		1,4,24
	29317	.035	U	5,12,14,23		47301	.25		3,24
Wortmann						47305	.28		3,24
FX-098	16019	.035	U	Many	NLR-1	62020	.07		1,16,18
	16200	.18	U	4,11		63018	.30		2
	17220	.30	U	2		63019	.30		2
	18102	.18	S	2,3,4		63020	.30		2
	18106	.18		2,3,4		63021	.30		2
	18108	.18		2,3,4		65207	.20		2,3,4
	18410	.11		20,22		65209	.30		2,3,4
	18411	.11		20,22	NLR-7301	66616	.11	S	Many
	18413	.11		20,22	NLR-7301	66617	.11	S	Many

[a]S = steady; U = unsteady; Q = quasi-steady, $k \leq 0.002$.

TABLE 10.- COEFFICIENTS OF LINEAR CURVE-FIT OF STATIC LIFT DATA WITHOUT WIND-TUNNEL CORRECTIONS

$$C_L = A + \frac{B\alpha}{\sqrt{1 - M_\infty^2}}$$

Airfoil	$A = C_L(0)$	$B = \beta C_{L_\alpha}$
NACA 0012	0	0.110
Ames 01	.15	.108
Wortmann FX-098	.07	.111
Sikorsky SC-1095	.11	.110
Hughes HH-02	.07	.116
Vertol VR-7	.19	.117
NLR-1	.11	.102
NLR-7301	.24	.116

TABLE 11.- LIST OF DATA FRAMES

(a) NACA 0012 airfoil.

A FRAME	TRIP	TYPE	A0	A1	Q	M	RE	K	FREQ	B FRAME
4019	N	ST	-5.0	0.0	.875	.301	3957803.	0.0000	0.00	4020
4100	N	ST	-2.0	0.0	.877	.301	3932537.	0.0000	0.00	4101
4102	N	ST	0.0	0.0	.877	.301	3923848.	0.0000	0.00	4103
4109	N	ST	2.0	0.0	.877	.302	3910221.	0.0000	0.00	4110
4111	N	ST	4.0	0.0	.885	.299	3931136.	0.0000	0.00	4112
4113	N	ST	8.0	0.0	.877	.302	3898235.	0.0000	0.00	4114
4119	N	ST	10.0	0.0	.877	.301	3900622.	0.0000	0.00	4120
4123	N	ST	12.0	0.0	.877	.302	3876047.	0.0000	0.00	4200
4201	N	ST	13.0	0.0	.877	.302	3870568.	0.0000	0.00	4202
4203	N	ST	13.5	0.0	.879	.301	3867132.	0.0000	0.00	4204
4209	N	ST	14.0	0.0	.877	.302	3861326.	0.0000	0.00	4210
4211	N	ST	14.5	0.0	.868	.305	3822671.	0.0000	0.00	4212
4213	N	ST	15.0	0.0	.877	.302	3843407.	0.0000	0.00	4214
4215	N	ST	15.5	0.0	.784	.284	3628769.	0.0000	0.00	4216
4217	N	ST	16.0	0.0	.688	.266	3398340.	0.0000	0.00	4218
4219	N	ST	17.8	0.0	.717	.271	3462550.	0.0000	0.00	4220
4301	N	ST	20.0	0.0	.700	.266	3449278.	0.0000	0.00	4302
4401	N	ST	13.0	0.0	.877	.302	3795037.	0.0000	0.00	4402
4403	N	ST	11.0	0.0	.877	.302	3783629.	0.0000	0.00	
4404	N	ST	8.0	0.0	.877	.302	3780176.	0.0000	0.00	
4405	N	ST	5.0	0.0	.877	.302	3781319.	0.0000	0.00	
4410	N	ST	2.0	0.0	.877	.302	3783016.	0.0000	0.00	
4411	N	ST	0.0	0.0	.877	.302	3781623.	0.0000	0.00	
4412	N	ST	-2.0	0.0	.877	.302	3775643.	0.0000	0.00	
11018	N	ST	-5.0	0.0	.875	.302	3998937.	0.0000	0.00	
11019	N	ST	-2.0	0.0	.875	.301	3969548.	0.0000	0.00	
11020	N	ST	0.0	0.0	.875	.302	3978509.	0.0000	0.00	
11101	N	ST	2.0	0.0	.875	.302	3974780.	0.0000	0.00	
11102	N	ST	4.0	0.0	.875	.301	3958541.	0.0000	0.00	
11105	N	ST	8.1	0.0	.876	.301	3938660.	0.0000	0.00	
11110	N	ST	10.0	0.0	.875	.301	3936424.	0.0000	0.00	
11111	N	ST	12.3	0.0	.875	.301	3921945.	0.0000	0.00	
11112	N	ST	13.4	0.0	.875	.301	3912483.	0.0000	0.00	
11113	N	ST	13.8	0.0	.875	.301	3904607.	0.0000	0.00	
11118	N	ST	14.0	0.0	.875	.301	3913072.	0.0000	0.00	
11121	N	ST	14.6	0.0	.875	.302	3929975.	0.0000	0.00	
11122	N	ST	15.0	0.0	.867	.304	3925323.	0.0000	0.00	
11123	N	ST	15.5	0.0	.811	.289	3745403.	0.0000	0.00	
11200	N	ST	16.0	0.0	.911	.290	3733699.	0.0000	0.00	
11201	N	ST	17.0	0.0	.841	.295	3793167.	0.0000	0.00	
11204	N	ST	17.9	0.0	.803	.288	3725491.	0.0000	0.00	
11205	N	ST	20.0	0.0	.764	.280	3616412.	0.0000	0.00	
11208	N	ST	24.9	0.0	.610	.249	3252565.	0.0000	0.00	
11209	N	ST	30.0	0.0	.561	.239	3105558.	0.0000	0.00	
11210	N	ST	25.0	0.0	.619	.251	3254780.	0.0000	0.00	
11211	N	ST	20.0	0.0	.725	.273	3515071.	0.0000	0.00	
11213	N	ST	18.0	0.0	.764	.280	3628495.	0.0000	0.00	
11214	N	ST	16.0	0.0	.875	.302	3866108.	0.0000	0.00	
11215	N	ST	15.0	0.0	.875	.302	3861556.	0.0000	0.00	
11216	N	ST	14.0	0.0	.869	.301	3846733.	0.0000	0.00	
11221	N	ST	13.1	0.0	.875	.302	3884818.	0.0000	0.00	
11222	N	ST	11.0	0.0	.875	.302	3876254.	0.0000	0.00	
11223	N	ST	8.0	0.0	.875	.302	3870718.	0.0000	0.00	
11304	N	ST	5.0	0.0	.875	.302	3896492.	0.0000	0.00	
11305	N	ST	2.0	0.0	.875	.302	3885782.	0.0000	0.00	
11308	N	ST	0.0	0.0	.875	.301	3870607.	0.0000	0.00	
11309	N	ST	-2.0	0.0	.875	.301	3870953.	0.0000	0.00	
7019	N	US	9.0	5.0	.878	.297	3894008.	.0508	2.70	7020
7021	N	US	9.0	5.0	.886	.299	3962010.	.1004	5.40	7022
7023	N	US	9.0	5.0	.886	.299	3944777.	.2005	10.80	7100

A FRAME	TRIP	TYPE	A0	A1	Q	M	RE	K	FREQ	B FRAME
7101	N	US	9.0	5.0	.878	.301	3909814.	.1496	8.10	7102
7104	N	US	9.0	5.0	.878	.301	3901884.	.0249	1.35	7105
7108	N	US	8.0	5.0	.878	.301	3920784.	.0250	1.35	
7110	N	US	8.0	5.0	.878	.301	3903187.	.0997	5.40	
7111	N	US	8.0	5.0	.877	.301	3894727.	.1992	10.80	
7112	N	US	10.0	5.0	.877	.301	3879891.	.0252	1.37	
7113	N	US	10.0	5.0	.877	.301	3877295.	.0994	5.40	
7114	N	US	10.0	5.0	.877	.301	3869051.	.1987	10.80	
7117	N	US	11.0	5.0	.878	.301	3891815.	.0249	1.35	
7118	N	US	11.0	5.0	.878	.301	3875085.	.0497	2.70	
7119	N	US	11.0	5.0	.877	.301	3865664.	.0993	5.40	
7120	N	US	11.0	5.0	.877	.301	3860258.	.1488	8.10	
7121	N	US	11.0	5.0	.878	.301	3852461.	.1983	10.80	
7200	N	US	12.0	5.0	.878	.301	3878632.	.0249	1.35	7201
7205	N	US	12.0	5.0	.877	.302	3853339.	.0991	5.40	7206
7207	N	US	12.0	5.0	.877	.302	3845471.	.1981	10.80	7208
7212	N	US	8.8	5.0	.877	.302	3864684.	.1488	8.10	7213
7214	N	US	8.8	5.0	.877	.302	3659691.	.0992	5.40	7215
7216	N	US	8.8	5.0	.877	.302	3856685.	.0496	2.70	7217
7300	N	US	10.0	5.0	.877	.300	3986300.	.1513	8.10	7301
7302	N	US	10.0	5.0	.877	.300	3957627.	.0745	4.00	
7305	N	US	12.0	5.0	.877	.300	3966326.	.1510	8.10	
8019	N	US	10.0	10.0	.013	.035	465897.	.1038	.66	8020
8021	N	US	10.0	10.0	.013	.035	486001.	.1515	.97	8022
8023	N	US	10.0	10.0	.013	.035	485755.	.2529	1.62	8024
8102	N	US	15.0	10.0	.013	.036	485630.	.1032	.66	8103
8104	N	US	15.0	10.0	.013	.036	484039.	.1529	.98	8105
8106	N	US	15.0	14.0	.013	.036	493453.	.1039	.67	8107
8114	N	US	15.0	10.0	.054	.072	980395.	.0992	1.30	8115
8116	N	US	15.0	10.0	.054	.072	979893.	.1487	1.95	8117
8118	N	US	15.0	10.0	.054	.072	978493.	.2477	3.25	8119
8123	N	US	15.0	14.0	.054	.072	980066.	.0991	1.30	8200
8203	N	US	10.0	10.0	.054	.072	978307.	.2476	3.25	8204
8210	N	US	10.0	10.0	.122	.109	1491495.	.2497	4.90	
8214	N	US	15.0	10.0	.122	.109	1490389.	.0996	1.96	
8220	N	US	15.0	10.0	.339	.184	2432854.	.0993	3.30	8221
8222	N	US	15.0	10.0	.339	.184	2423357.	.1487	4.95	8223
8306	N	US	15.0	14.0	.339	.184	2404523.	.0988	3.30	8307
9022	N	US	15.0	6.0	.339	.184	2358259.	.2352	7.92	
9101	N	US	15.0	5.0	.339	.184	2358620.	.2842	9.57	
9106	N	US	10.0	10.0	.339	.184	2365336.	.2453	8.25	
9110	N	US	8.0	10.0	.339	.184	2476299.	.0100	.33	9111
9112	N	US	8.0	10.0	.341	.183	2475104.	.0500	1.65	9113
9118	N	US	8.0	10.0	.339	.184	2449160.	.1990	6.60	9119
9202	N	US	15.0	10.0	.479	.220	2847551.	.0985	3.93	
9203	N	US	15.0	10.0	.610	.249	3187113.	.0984	4.46	
9208	N	US	15.0	10.0	.762	.280	3520275.	.0975	4.98	
9210	N	US	15.0	10.0	.842	.295	3672459.	.0098	.53	
9213	N	US	15.0	10.0	.831	.294	3596380.	.0243	1.31	
9214	N	US	15.0	10.0	.821	.292	3566725.	.0489	2.62	
9217	N	US	15.0	10.0	.812	.290	3549571.	.0983	5.24	
9218	N	US	15.0	10.0	.773	.283	3450727.	.1509	7.86	
9221	N	US	10.0	10.0	.876	.302	3672528.	.0098	.54	
9222	N	US	10.0	10.0	.876	.302	3660134.	.0241	1.34	
9223	N	US	10.0	10.0	.876	.302	3652176.	.0481	2.68	
9302	N	US	10.0	10.0	.876	.302	3659205.	.0963	5.36	
9307	N	US	10.0	10.0	.877	.302	3670847.	.1447	8.04	
10022	N	US	12.0	10.0	.878	.301	3769502.	.0976	5.36	
10101	N	US	20.0	10.0	.688	.265	3303441.	.1102	5.36	
10104	N	US	12.0	8.0	.877	.302	3711352.	.0485	2.68	

TABLE 11.- Continued.

(a) Concluded.

A FRAME	TRIP	TYPE	A0	A1	Q	M	RE	K	FREQ	B FRAME
10105	N	US	12.0	8.0	.878	.302	3694271.	.0968	5.36	
10108	N	US	12.0	8.0	.847	.296	3635889.	.1253	6.81	
10113	N	US	15.0	5.0	.876	.302	3896846.	.0098	.53	
10114	N	US	15.0	5.0	.841	.295	3801337.	.0252	1.34	
10118	N	US	15.0	5.0	.823	.291	3748526.	.1020	5.36	
10120	N	US	15.0	5.0	.843	.294	3785165.	.1511	8.04	
10123	N	US	15.0	5.0	.532	.293	3758528.	.2024	10.72	
10202	N	US	10.0	5.0	.877	.301	3858103.	.0098	.54	
10203	N	US	10.0	5.0	.877	.301	3847481.	.0246	1.34	
10204	N	US	10.0	5.0	.870	.300	3826614.	.0493	2.68	
10207	N	US	10.0	5.0	.877	.302	3834629.	.0740	4.02	
10208	N	US	10.0	5.0	.870	.300	3959785.	.0990	5.36	
10211	N	US	10.0	5.0	.870	.300	3863353.	.1486	8.04	
10212	N	US	10.0	5.0	.870	.300	3850737.	.1979	10.72	
10218	N	US	5.0	5.0	.880	.300	3933484.	.0098	.53	
10221	N	US	5.0	5.0	.878	.301	3925387.	.0993	5.36	
10222	N	US	5.0	5.0	.878	.301	3912114.	.1983	10.72	
10303	N	US	5.0	10.0	.877	.301	3910580.	.0991	5.36	
10305	N	US	3.8	10.0	.877	.301	3911328.	.0991	5.36	
10309	N	US	2.8	10.0	.877	.301	3896361.	.0989	5.36	
12020	N	US	20.0	10.0	.718	.270	3490909.	.0010	.05	12023
12102	N	US	5.0	10.0	.882	.302	3820000.	.0009	.05	12105
12109	N	US	6.0	10.0	.756	.279	3455765.	.0010	.05	12112
12118	N	US	20.0	10.0	.676	.262	3246704.	.0010	.05	12121
12203	N	US	20.0	10.0	.531	.231	2887477.	.0011	.05	12121
12208	N	US	7.0	10.0	.587	.244	3269975.	.0010	.05	12212
12300	N	US	20.0	10.0	.421	.204	2706734.	.0011	.04	12301
12305	N	US	20.0	10.0	.292	.169	2252844.	.0011	.03	12306
12310	N	US	7.0	10.0	.350	.186	2469266.	.0010	.03	
13021	N	US	7.0	10.0	.120	.108	1502757.	.0017	.03	13104
13107	N	US	20.0	10.0	.113	.105	1421201.	.0017	.03	13108
13115	N	US	20.0	10.0	.048	.068	918563.	.0027	.03	13116
13120	N	US	5.0	10.0	.053	.072	962303.	.0025	.03	13202
13205	N	US	5.0	10.0	.014	.036	488772.	.0025	.02	13213
13217	N	US	20.0	10.0	.013	.036	485631.	.0026	.02	
13222	N	US	20.0	10.0	.749	.276	3656957.	.0010	.05	
13303	N	US	7.0	10.0	.603	.247	3298109.	.0010	.05	
13308	N	US	7.0	10.0	.461	.215	2894310.	.0010	.04	
13310	N	US	7.0	10.0	.466	.216	2884723.	.0010	.04	
13313	Y	US	7.0	10.0	.332	.181	2404990.	.0010	.03	13316
13321	Y	US	7.0	10.0	.639	.294	3740954.	.0009	.05	13405
14019	Y	US	15.0	10.0	.339	.183	2453890.	.0499	1.65	14020
14021	Y	US	15.0	10.0	.336	.182	2434182.	.1001	3.30	14022
14023	Y	US	15.0	10.0	.335	.182	2426579.	.1504	4.95	14100
14104	Y	US	15.0	10.0	.338	.183	2448651.	.0499	1.65	14105
14106	Y	US	15.0	10.0	.340	.184	2449389.	.0994	3.30	14107
14108	Y	US	15.0	10.0	.339	.183	2443079.	.1493	4.95	14109
14117	Y	US	15.0	10.0	.837	.293	3843264.	.0257	1.35	14118
14119	Y	US	15.0	10.0	.836	.293	3818432.	.0509	2.68	14120
14200	Y	US	15.0	10.0	.843	.294	3822179.	.0253	1.34	14201
14202	Y	US	15.0	10.0	.839	.293	3792702.	.0506	2.68	14203
14208	Y	US	15.0	10.0	.828	.291	3764396.	.1019	5.36	14209
14210	Y	US	15.0	10.0	.832	.292	3760353.	.1014	5.36	14211
14218	N	US	15.0	10.0	.830	.292	3762798.	.0254	1.34	
14219	N	US	15.0	10.0	.824	.291	3735990.	.0509	2.68	
14220	N	US	15.0	10.0	.805	.287	3683317.	.1031	5.36	14221
15218	N	US	15.0	10.0	.818	.290	3678973.	.0994	5.24	
10117	N	US	15.0	5.0	.843	.295	3802563.	.0504	2.68	
7202	N	US	12.0	5.0	.877	.302	3861194.	.0496	2.70	7201
7222	N	US	10.0	5.0	.876	.298	3975490.	.0509	2.70	7223

TABLE 11.- Continued.

(b) Ames A-01 airfoil.

A FRAME	TRIP	TYPE	A0	A1	Q	M	RE	K	FREQ	B FRAME
26020	N	ST	-5.0	0.0	.880	.301	3921512.	0.0000	0.00	26021
26022	N	ST	-2.0	0.0	.881	.302	3907918.	0.0000	0.00	
26023	N	ST	0.0	0.0	.882	.302	3900668.	0.0000	0.00	26100
26101	N	ST	2.0	0.0	.878	.302	3878703.	0.0000	0.00	
26107	N	ST	4.0	0.0	.879	.302	3839303.	0.0000	0.00	
26108	N	ST	8.0	0.0	.880	.302	3839762.	0.0000	0.00	
26109	N	ST	10.0	0.0	.879	.302	3826626.	0.0000	0.00	26113
26114	N	ST	12.0	0.0	.884	.303	3832104.	0.0000	0.00	26115
26122	N	ST	13.0	0.0	.857	.298	3737465	0.0000	0.00	26123
26200	N	ST	13.5	0.0	.833	.293	3667954.	0.0000	0.00	26201
26205	N	ST	14.0	0.0	.857	.298	3720572.	0.0000	0.00	26206
26207	N	ST	15.0	0.0	.882	.302	3754105.	0.0000	0.00	26208
26209	N	ST	16.0	0.0	.870	.300	3715585.	0.0000	0.00	26210
26215	N	ST	18.0	0.0	.815	.290	3589962.	0.0000	0.00	
26216	N	ST	20.0	0.0	.778	.282	3497091.	0.0000	0.00	26217
26218	N	ST	25.0	0.0	.626	.252	3129086.	0.0000	0.00	
26219	N	ST	20.0	0.0	.773	.281	3465882.	0.0000	0.00	
26220	N	ST	16.0	0.0	.832	.293	3591634.	0.0000	0.00	26222
26300	N	ST	14.0	0.0	.878	.302	3703082.	0.0000	0.00	
26301	N	ST	13.0	0.0	.828	.293	3590546.	0.0000	0.00	
26302	N	ST	11.0	0.0	.879	.302	3693921.	0.0000	0.00	
26306	N	ST	5.0	0.0	.883	.303	3706075.	0.0000	0.00	
26307	N	ST	0.0	0.0	.878	.302	3693264.	0.0000	0.00	
26313	N	ST	5.0	0.0	.614	.250	3126375.	0.0000	0.00	26314
26315	N	ST	-2.0	0.0	.612	.250	3113134.	0.0000	0.00	
26318	N	ST	0.0	0.0	.616	.250	3132011.	0.0000	0.00	26319
26320	N	ST	2.0	0.0	.614	.249	3118900.	0.0000	0.00	
26321	N	ST	4.0	0.0	.612	.250	3112889.	0.0000	0.00	
26414	N	ST	8.0	0.0	.618	.250	3371063.	0.0000	0.00	
26415	N	ST	10.0	0.0	.612	.249	3345903.	0.0000	0.00	26416
26417	N	ST	12.0	0.0	.614	.249	3336283.	0.0000	0.00	26418
26419	N	ST	13.0	0.0	.621	.251	3344961.	0.0000	0.00	26420
26421	N	ST	14.0	0.0	.615	.249	3327823.	0.0000	0.00	26422
27020	N	ST	15.0	0.0	.617	.250	3308153.	0.0000	0.00	27021
27022	N	ST	16.0	0.0	.616	.250	3293220.	0.0000	0.00	27023
27100	N	ST	18.0	0.0	.616	.250	3281426.	0.0000	0.00	
27101	N	ST	20.0	0.0	.618	.250	3281356.	0.0000	0.00	27102
27103	N	ST	25.0	0.0	.613	.249	3256106.	0.0000	0.00	
27107	N	ST	20.0	0.0	.630	.252	3304196.	0.0000	0.00	
27108	N	ST	16.0	0.0	.615	.249	3259565.	0.0000	0.00	
27109	N	ST	14.0	0.0	.617	.250	3265185.	0.0000	0.00	
27110	N	ST	13.0	0.0	.611	.249	3248047.	0.0000	0.00	
27111	N	ST	11.1	0.0	.612	.249	3246751.	0.0000	0.00	
27116	N	ST	5.0	0.0	.607	.248	3241861.	0.0000	0.00	
27117	N	ST	0.0	0.0	.615	.249	3258729.	0.0000	0.00	
27123	N	ST	-5.0	0.0	.344	.185	2448549.	0.0000	0.00	27200
27201	N	ST	-2.0	0.0	.343	.184	2440864.	0.0000	0.00	
27202	N	ST	0.0	0.0	.340	.184	2428683.	0.0000	0.00	27203
27204	N	ST	2.0	0.0	.343	.184	2436687.	0.0000	0.00	
27205	N	ST	4.0	0.0	.343	.185	2438037.	0.0000	0.00	
27211	N	ST	8.0	0.0	.347	.185	2460290.	0.0000	0.00	
27212	N	ST	10.0	0.0	.344	.185	2444426.	0.0000	0.00	27213
27214	N	ST	12.0	0.0	.345	.185	2441417.	0.0000	0.00	27215
27216	N	ST	13.0	0.0	.342	.184	24297[illegible]0.	0.0000	0.00	27217
27218	N	ST	14.0	0.0	.340	.184	2418565.	0.0000	0.00	27219
27220	N	ST	14.9	0.0	.347	.186	2445054.	0.0000	0.00	27221
27301	N	ST	16.0	0.0	.344	.185	2441091.	0.0000	0.00	27302
27303	N	ST	18.0	0.0	.343	.184	2429869.	0.0000	0.00	
27304	N	ST	20.0	0.0	.343	.185	2429178.	0.0000	0.00	27305
27306	N	ST	25.0	0.0	.342	.184	2422378.	0.0000	0.00	

A FRAME	TRIP	TYPE	A0	A1	Q	M	RE	K	FREQ	B FRAME
27307	N	ST	20.0	0.0	.342	.184	2418525.	0.0000	0.00	
27308	N	ST	16.0	0.0	.342	.184	2422139.	0.0000	0.00	
27309	N	ST	14.0	0.0	.342	.184	2422443.	0.0000	0.00	
27310	N	ST	13.0	0.0	.343	.185	2426821.	0.0000	0.00	
27311	N	ST	11.0	0.0	.341	.184	2422433.	0.0000	0.00	
27317	N	ST	5.0	0.0	.339	.184	2432586.	0.0000	0.00	
27318	N	ST	0.0	0.0	.342	.184	2434309.	0.0000	0.00	
27400	N	ST	-5.0	0.0	.121	.109	1536531.	0.0000	0.00	27401
27402	N	ST	-2.0	0.0	.123	.110	1550354.	0.0000	0.00	
27403	N	ST	0.0	0.0	.121	.108	1533751.	0.0000	0.00	27404
27405	N	ST	2.0	0.0	.122	.109	1536087.	0.0000	0.00	
27406	N	ST	4.0	0.0	.122	.109	1532038.	0.0000	0.00	
27413	N	ST	8.0	0.0	.122	.110	1527387.	0.0000	0.00	
27414	N	ST	10.0	0.0	.121	.109	1522167.	0.0000	0.00	27415
27416	N	ST	12.0	0.0	.122	.110	1525614.	0.0000	0.00	27417
28019	N	ST	13.0	0.0	.121	.109	1491021.	0.0000	0.00	28020
28021	N	ST	14.0	0.0	.121	.109	1485106.	0.0000	0.00	28020
28023	N	ST	15.0	0.0	.132	.114	1541856.	0.0000	0.00	28100
28101	N	ST	16.0	0.0	.129	.112	1526677.	0.0000	0.00	28102
28106	N	ST	18.0	0.0	.124	.110	14[illegible]8052.	0.0000	0.00	
28107	N	ST	20.0	0.0	.124	.110	1492163.	0.0000	0.00	28108
28109	N	ST	25.0	0.0	.122	.109	1479403.	0.0000	0.00	
28110	N	ST	20.0	0.0	.124	.109	1487571.	0.0000	0.00	
28115	N	ST	14.0	0.0	.122	.109	1476171.	0.0000	0.00	
28116	N	ST	13.0	0.0	.123	.110	1474187.	0.0000	0.00	
28117	N	ST	11.0	0.0	.121	.109	1466536.	0.0000	0.00	
28119	N	ST	0.0	0.0	.123	.110	1476082.	0.0000	0.00	
28120	N	ST	14.5	0.0	.121	.108	1459583.	0.0000	0.00	
28207	Y	ST	0.0	0.0	.341	.184	2441392.	0.0000	0.00	28208
28209	Y	ST	5.0	0.0	.338	.183	2424855.	0.0000	0.00	28210
28211	Y	ST	10.0	0.0	.342	.184	2439422.	0.0000	0.00	28212
28213	Y	ST	12.0	0.0	.343	.185	2439577.	0.0000	0.00	28214
28215	Y	ST	13.0	0.0	.343	.185	2439192.	0.0000	0.00	28216
28217	Y	ST	14.0	0.0	.342	.184	2432247.	0.0000	0.00	28218
28222	Y	ST	15.0	0.0	.341	.185	2427824.	0.0000	0.00	28223
28300	Y	ST	16.0	0.0	.342	.184	2426509.	0.0000	0.00	28301
28302	Y	ST	20.0	0.0	.342	.184	2423536.	0.0000	0.00	28303
28304	Y	ST	0.0	0.0	.343	.185	2426376.	0.0000	0.00	28305
28312	Y	ST	0.0	0.0	.878	.301	3956665.	0.0000	0.00	28313
28314	Y	ST	5.0	0.0	.886	.303	3959734.	0.0000	0.00	28315
28316	Y	ST	10.0	0.0	.884	.302	3939559.	0.0000	0.00	28320
28321	Y	ST	12.0	0.0	.878	.301	3913926.	0.0000	0.00	28322
28323	Y	ST	13.0	0.0	.860	.298	3863673.	0.0000	0.00	28400
28401	Y	ST	14.0	0.0	.827	.292	3779496.	0.0000	0.00	28402
28403	Y	ST	15.0	0.0	.859	.298	3837643.	0.0000	0.00	28404
28408	Y	ST	16.0	0.0	.857	.298	3842021.	0.0000	0.00	28409
28410	Y	ST	0.0	0.0	.882	.302	3836732.	0.0000	0.00	28411
24022	N	US	15.0	10.0	.850	.296	3840159.	.0246	1.31	24023
24100	N	US	15.0	10.0	.814	.290	3732983.	.0501	2.62	24104
24105	N	US	15.0	10.0	.813	.289	3714780.	.1002	5.24	24108
24109	N	US	15.0	10.0	.779	.283	3625374.	.1534	7.86	24110
24117	N	US	15.0	10.0	.765	.260	3598067.	.0982	4.98	24118
24201	N	US	15.0	10.0	.609	.248	3211200.	.0990	4.46	24202
24209	N	US	15.0	10.0	.480	.220	2846350.	.0984	3.93	24210
24217	N	US	15.0	10.0	.340	.184	2396118.	.0986	3.30	24219
24302	N	US	7.5	10.0	.340	.184	2396387.	.0493	1.65	24304
24306	N	US	7.5	10.0	.341	.184	2394970.	.1966	6.60	24307
24314	N	US	15.0	10.0	.123	.110	1504089.	.0994	1.96	24316
24323	N	US	15.0	10.0	.054	.073	994952.	.0992	1.30	24400
25022	N	US	10.0	10.0	.881	.302	3844899.	.0245	1.34	25023

TABLE 11.- Continued.

(b) Concluded.

A FRAME	TRIP	TYPE	AO	A1	Q	M	RE	K	FREQ	B FRAME
25102	N	US	10.0	10.0	.881	.302	3831527.	.0489	2.68	25103
25104	N	US	10.0	10.0	.880	.302	3816708.	.0978	5.36	25108
25109	N	US	10.0	10.0	.879	.302	3810775.	.1468	8.04	25110
25117	N	US	10.0	5.0	.884	.303	3829075.	.0244	1.34	
25118	N	US	10.0	5.0	.879	.302	3803407.	.0489	2.68	
25119	N	US	10.0	5.0	.863	.303	3805390.	.0975	5.36	
25121	N	US	10.0	5.0	.881	.302	3813088.	.1465	8.04	
25122	N	US	10.0	5.0	.884	.303	3819823.	.1462	8.04	
25123	N	US	10.0	5.0	.885	.303	3816827.	.1947	10.72	
29023	Y	US	15.0	10.0	.820	.291	3697799.	.0248	1.31	29100
29101	Y	US	15.0	10.0	.805	.288	3639654.	.0500	2.62	29102
29106	Y	US	15.0	10.0	.806	.288	3646183.	.1001	5.24	29107
29115	Y	US	15.0	10.0	.340	.184	2418131.	.0494	1.65	29116
29117	Y	US	15.0	10.0	.341	.184	2418248.	.0987	3.30	29118
29119	Y	US	15.0	10.0	.341	.184	2417060.	.1481	4.95	29121
29205	N	US	5.0	10.0	.876	.301	3947215.	.0098	.53	29206
29207	N	US	5.0	10.0	.877	.301	3918856.	.0496	2.68	29210
29211	N	US	5.0	10.0	.877	.301	3902857.	.0991	5.36	29212
29213	N	US	5.0	10.0	.879	.301	3896095.	.1483	8.04	29214
29215	N	US	5.0	10.0	.879	.301	3891313.	.1481	8.04	
29223	N	US	13.5	2.0	.876	.301	3611877.	.1965	10.72	29300
29304	N	US	14.5	2.0	.870	.300	3777473.	.1967	10.72	29306
29309	N	US	16.5	2.0	.852	.296	3722411.	.1986	10.72	29310
29317	N	US	15.0	10.0	.013	.035	472349.	.1021	.65	29318
30019	N	US	15.0	10.0	.865	.298	3856941.	.0097	.52	30021
30020	N	US	15.0	10.0	.864	.298	3828146.	.0096	.52	30021
30105	N	US	10.0	10.0	.880	.301	3844592.	.0097	.53	30106
30110	N	US	15.0	5.0	.877	.301	3817844.	.0097	.53	30111
30119	N	US	10.0	5.0	.874	.300	3819252.	.0097	.53	30120
30201	N	US	11.0	5.0	.877	.301	3814196.	.0099	.54	30202
30206	N	US	14.0	2.0	.876	.301	3818960.	.0097	.53	30208
30215	N	US	7.5	10.0	.338	.183	2415733.	.0099	.33	30216
31102	N	US	10.0	10.0	.877	.302	3680208.	.0247	1.34	31103
31104	N	US	10.0	10.0	.878	.302	3859857.	.0492	2.68	31105
31110	N	US	10.0	10.0	.880	.302	3841535.	.1471	8.04	31111
31112	N	US	10.0	10.0	.880	.302	3832051.	.1469	8.04	31111
31119	N	US	5.0	10.0	.884	.303	3856266.	.0245	1.34	31120
31121	N	US	5.0	10.0	.880	.302	3826984.	.0489	2.68	31122
31123	N	US	5.0	10.0	.884	.303	3823741.	.0975	5.36	31200
31201	N	US	5.0	10.0	.883	.303	3816623.	.1463	8.04	31202
31209	N	US	15.0	10.0	.341	.184	2421425.	.0987	3.30	31210
31215	N	US	7.5	10.0	.341	.184	2425489.	.0494	1.65	31216
31217	N	US	7.5	10.0	.341	.185	2423083.	.1972	6.60	31218
31302	N	US	14.5	2.0	.852	.297	3765532.	.1990	10.72	31304
31310	N	US	14.5	2.0	.854	.298	3731989.	.1485	8.04	31312
25204	N	US	15.0	5.0	.877	.301	3973275.	.0249	1.34	
25205	N	US	15.0	5.0	.878	.301	3952662.	.0497	2.68	
25208	N	US	15.0	5.0	.878	.301	3950602.	.0994	5.36	
25209	N	US	15.0	5.0	.857	.298	3887313.	.1506	8.04	
25210	N	US	15.0	5.0	.852	.297	3865306.	.2013	10.72	
25214	N	US	11.0	5.0	.880	.302	3926436.	.0495	2.68	25215
25216	N	US	11.0	5.0	.883	.302	3909711.	.0986	5.36	25217
25301	N	US	5.0	5.0	.884	.302	3903998.	.0984	5.36	25302
25303	N	US	5.0	5.0	.865	.303	3878688.	.1962	10.72	25304
25311	N	US	5.0	10.1	.881	.302	3852707.	.0982	5.36	25312
25319	N	US	5.5	10.0	.881	.302	3833693.	.0980	5.36	25320

TABLE 11.- Continued.

(c) Wortmann FX-098 airfoil.

A FRAME	TRIP	TYPE	AO	A1	Q	M	RE	K	FREQ	B FRAME
17208	Y	ST	0.0	0.0	.877	.301	3975279.	0.0000	0.00	17209
17212	Y	ST	5.0	0.0	.880	.301	3928557.	0.0000	0.00	17213
17220	Y	ST	10.0	0.0	.879	.302	3911481.	0.0000	0.00	17221
17303	Y	ST	12.0	0.0	.847	.296	3802285.	0.0000	0.00	17304
17305	Y	ST	13.0	0.0	.870	.300	3835772.	0.0000	0.00	17306
17310	Y	ST	14.0	0.0	.866	.299	3820036.	0.0000	0.00	17311
17312	Y	ST	15.0	0.0	.866	.299	3805980.	0.0000	0.00	17313
17314	Y	ST	16.0	0.0	.828	.292	3710084.	0.0000	0.00	17315
18019	Y	ST	0.0	0.0	.341	.184	2398709.	0.0000	0.00	18020
18102	Y	ST	5.0	0.0	.343	.185	2400750.	0.0000	0.00	18103
18106	Y	ST	10.0	0.0	.339	.184	2378846.	0.0000	0.00	18107
18108	Y	ST	12.0	0.0	.343	.185	2388927.	0.0000	0.00	18109
18115	Y	ST	13.0	0.0	.346	.185	2394744.	0.0000	0.00	18116
18117	Y	ST	14.0	0.0	.345	.185	2388872.	0.0000	0.00	18118
18119	Y	ST	15.0	0.0	.341	.184	2374587.	0.0000	0.00	18120
18121	Y	ST	16.0	0.0	.340	.184	2368089.	0.0000	0.00	18122
18123	Y	ST	19.9	0.0	.342	.184	2370588.	0.0000	0.00	18200
18206	Y	ST	0.0	0.0	.341	.134	2379635.	0.0000	0.00	18207
18215	N	ST	-5.0	0.0	.122	.110	1500031.	0.0000	0.00	18216
18217	N	ST	-2.0	0.0	.123	.110	1502458.	0.0000	0.00	
18218	N	ST	0.0	0.0	.121	.109	1487692.	0.0000	0.00	18219
18220	N	ST	2.0	0.0	.122	.110	1494149.	0.0000	0.00	
18221	N	ST	4.0	0.0	.121	.109	1486754.	0.0000	0.00	
18304	N	ST	8.0	0.0	.121	.109	1480425.	0.0000	0.00	
18305	N	ST	10.0	0.0	.122	.110	1483466.	0.0000	0.00	18306
18307	N	ST	12.0	0.0	.122	.109	1476483.	0.0000	0.00	18308
18312	N	ST	13.0	0.0	.121	.109	1466753.	0.0000	0.00	18313
18319	N	ST	13.5	0.0	.123	.109	1469738.	0.0000	0.00	18320
18321	N	ST	14.0	0.0	.124	.110	1474082.	0.0000	0.00	18322
18323	N	ST	15.0	0.0	.122	.110	1463922.	0.0000	0.00	18400
18401	N	ST	16.0	0.0	.122	.109	1461183.	0.0000	0.00	18402
18410	N	ST	18.0	0.0	.124	.111	1459953.	0.0000	0.00	18412
18411	N	ST	20.0	0.0	.123	.110	1447617.	0.0000	0.00	18412
18413	N	ST	25.0	0.0	.123	.109	1445110.	0.0000	0.00	
18414	N	ST	20.0	0.0	.122	.110	1439675.	0.0000	0.00	
18421	N	ST	16.0	0.0	.123	.109	1445948.	0.0000	0.00	
18422	N	ST	14.0	0.0	.122	.110	1438216.	0.0000	0.00	
18423	N	ST	13.0	0.0	.122	.109	1439933.	0.0000	0.00	
18500	N	ST	11.0	0.0	.122	.110	1437504.	0.0000	0.00	
18501	N	ST	5.0	0.0	.122	.109	1436482.	0.0000	0.00	
18502	N	ST	0.0	0.0	.122	.110	1439616.	0.0000	0.00	
19020	N	ST	-5.0	0.0	.342	.185	2454849.	0.0000	0.00	19021
19022	N	ST	-2.0	0.0	.342	.184	2447610.	0.0000	0.00	
19023	N	ST	0.0	0.0	.340	.185	2441467.	0.0000	0.00	19100
19101	N	ST	2.0	0.0	.341	.185	2443653.	0.0000	0.00	
19110	N	ST	4.0	0.0	.340	.185	2399877.	0.0000	0.00	
19116	N	ST	8.0	0.0	.341	.185	2378719.	0.0000	0.00	
19117	N	ST	10.0	0.0	.340	.185	2372613.	0.0000	0.00	19118
19119	N	ST	12.0	0.0	.343	.185	2379520.	0.0000	0.00	19120
19121	N	ST	13.0	0.0	.338	.183	2355087.	0.0000	0.00	19122
19123	N	ST	13.5	0.0	.343	.185	2370521.	0.0000	0.00	19200
19204	N	ST	14.0	0.0	.340	.185	2361633.	0.0000	0.00	19205
19206	N	ST	15.0	0.0	.342	.185	2364851.	0.0000	0.00	19207
19208	N	ST	16.0	0.0	.342	.185	2361273.	0.0000	0.00	19209
19213	N	ST	18.0	0.0	.341	.185	2365586.	0.0000	0.00	
19214	N	ST	20.0	0.0	.340	.185	2358408.	0.0000	0.00	19215
19216	N	ST	25.0	0.0	.341	.184	2351317.	0.0000	0.00	
19217	N	ST	20.0	0.0	.340	.185	2348131.	0.0000	0.00	
19221	N	ST	16.0	0.0	.341	.185	2359002.	0.0000	0.00	
19222	N	ST	14.0	0.0	.343	.186	2364589.	0.0000	0.00	

A FRAME	TRIP	TYPE	AO	A1	Q	M	RE	K	FREQ	B FRAME
19223	N	ST	13.0	0.0	.340	.185	2353097.	0.0000	0.00	
19300	N	ST	11.0	0.0	.341	.185	2354186.	0.0000	0.00	
19305	N	ST	5.0	0.0	.340	.185	2357348.	0.0000	0.00	
19308	N	ST	0.0	0.0	.340	.185	2354786.	0.0000	0.00	
19314	N	ST	-5.0	0.0	.614	.250	3151118.	0.0000	0.00	19315
19316	N	ST	-2.0	0.0	.611	.250	3138172.	0.0000	0.00	
19317	N	ST	0.0	0.0	.612	.250	3137611.	0.0000	0.00	19318
19401	N	ST	2.0	0.0	.616	.251	3300956.	0.0000	0.00	
19402	N	ST	4.0	0.0	.616	.251	3297074.	0.0000	0.00	
19405	N	ST	8.0	0.0	.617	.251	3287867.	0.0000	0.00	
19406	N	ST	10.0	0.0	.614	.250	3275608.	0.0000	0.00	19407
19411	N	ST	12.0	0.0	.617	.251	3278455.	0.0000	0.00	19412
19413	N	ST	13.0	0.0	.618	.251	3268218.	0.0000	0.00	19414
19415	N	ST	13.5	0.0	.620	.251	3264994.	0.0000	0.00	19416
19423	N	ST	14.0	0.0	.613	.250	3235583.	0.0000	0.00	19500
19504	N	ST	15.0	0.0	.613	.250	3233310.	0.0000	0.00	19505
19506	N	ST	16.0	0.0	.613	.250	3228546.	0.0000	0.00	19507
19508	N	ST	18.0	0.0	.602	.248	3194789.	0.0000	0.00	
20019	N	ST	25.0	0.0	.610	.249	3162267.	0.0000	0.00	
20020	N	ST	20.0	0.0	.612	.250	3158666.	0.0000	0.00	
20021	N	ST	16.0	0.0	.614	.250	3163174.	0.0000	0.00	
20022	N	ST	14.0	0.0	.614	.250	3163970.	0.0000	0.00	
20103	N	ST	13.0	0.0	.610	.249	3155282.	0.0000	0.00	
20104	N	ST	11.0	0.0	.609	.249	3150506.	0.0000	0.00	
20109	N	ST	5.0	0.0	.613	.250	3157103.	0.0000	0.00	
20112	N	ST	0.0	0.0	.615	.250	3152218.	0.0000	0.00	
20118	N	ST	-5.0	0.0	.883	.304	3774892.	0.0000	0.00	20119
20122	N	ST	-2.0	0.0	.883	.303	3776701.	0.0000	0.00	
20123	N	ST	0.0	0.0	.877	.302	3758789.	0.0000	0.00	20200
20203	N	ST	2.0	0.0	.879	.303	3748627.	0.0000	0.00	
20204	N	ST	4.0	0.0	.876	.302	3741653.	0.0000	0.00	
20210	N	ST	8.0	0.0	.878	.303	3768915.	0.0000	0.00	
20211	N	ST	10.0	0.0	.880	.302	3764181.	0.0000	0.00	20212
20213	N	ST	12.0	0.0	.860	.299	3709078.	0.0000	0.00	20214
20222	N	ST	13.0	0.0	.821	.291	3820534.	0.0000	0.00	20223
20300	N	ST	13.5	0.0	.841	.295	3848559.	0.0000	0.00	20301
20302	N	ST	14.0	0.0	.875	.301	3916076.	0.0000	0.00	20303
20307	N	ST	15.0	0.0	.866	.299	3903574.	0.0000	0.00	20308
20309	N	ST	16.0	0.0	.877	.302	3913381.	0.0000	0.00	20310
20311	N	ST	18.0	0.0	.835	.294	3811625.	0.0000	0.00	
20312	N	ST	20.0	0.0	.737	.275	3577136.	0.0000	0.00	20313
20317	N	ST	25.0	0.0	.668	.261	3411407.	0.0000	0.00	
20318	N	ST	20.0	0.0	.740	.275	3578432.	0.0000	0.00	
20319	N	ST	16.0	0.0	.881	.302	3892367.	0.0000	0.00	
20320	N	ST	14.0	0.0	.882	.302	3888966.	0.0000	0.00	
20321	N	ST	13.0	0.0	.867	.300	3850481.	0.0000	0.00	
20322	N	ST	11.0	0.0	.879	.302	3875469.	0.0000	0.00	
16019	N	UN	15.0	10.0	.013	.036	488137.	.1007	.66	16022
16105	N	UN	15.0	10.0	.056	.074	986067.	.0972	1.30	16106
16114	N	UN	15.0	10.0	.123	.110	1463255.	.0932	1.96	16115
16200	N	UN	15.0	10.0	.343	.185	2429922.	.0983	3.30	16201
16213	N	UN	6.5	10.0	.340	.184	2502119.	.0500	1.65	16217
16215	N	UN	6.5	10.0	.340	.184	2494598.	.1999	6.60	16216
16300	N	UN	15.0	10.0	.481	.220	2890556.	.0988	3.93	16301
16308	N	UN	15.0	10.0	.612	.249	3229332.	.0988	4.46	16309
17100	Y	UN	15.0	10.0	.340	.184	2457108.	.0497	1.65	17102
17103	Y	UN	15.0	10.0	.341	.184	2452721.	.0992	3.30	17108
17109	Y	UN	15.0	10.0	.342	.184	2452926.	.1486	4.95	17110
17117	Y	UN	15.0	10.0	.830	.293	3772247.	.0248	1.31	17118
17119	Y	UN	15.0	10.0	.823	.291	3724643.	.0497	2.62	17123

TABLE 11.- Continued.

(c) Concluded.

A FRAME	TRIP	TYPE	AO	A1	Q	M	RE	K	FREQ	B FRAME
17200	Y	UN	15.0	10.0	.814	.290	3702477.	.0999	5.24	17201
21100	N	UN	15.0	10.0	.823	.291	3718613.	.0099	.52	21102
21107	N	UN	10.0	10.0	.867	.299	3792469.	.0098	.53	
21200	N	UN	10.0	5.0	.875	.301	3932117.	.0098	.53	21201
21208	N	UN	3.3	10.0	.882	.302	3898549.	.0097	.53	21209
21219	N	UN	6.5	10.0	.339	.184	2455459.	.0098	.33	21220
22023	N	UN	15.0	10.0	.827	.293	3727983.	.0247	1.31	22100
22103	N	UN	15.0	10.0	.837	.294	3749080.	.0492	2.62	22104
22201	N	UN	15.0	10.0	.785	.285	3554419.	.1008	5.24	22202
22206	N	UN	15.0	10.0	.754	.279	3477029.	.1542	7.86	22207
22208	N	UN	15.0	10.0	.763	.281	3483672.	.0969	4.98	22209
22216	N	UN	10.0	10.0	.875	.302	3732111.	.0243	1.34	
22217	N	UN	10.0	10.0	.875	.302	3720266.	.0485	2.68	
22218	N	UN	10.0	10.0	.862	.300	3694571.	.0977	5.36	
22219	N	UN	10.0	10.0	.835	.294	3618609.	.1490	8.04	
22307	N	UN	10.0	5.0	.875	.301	3954387.	.0246	1.34	22223
22308	N	UN	10.0	5.0	.880	.303	3857324.	.0491	2.68	22300
22309	N	UN	10.0	5.0	.881	.303	3853461.	.0980	5.36	22301
22311	N	UN	10.0	5.0	.877	.302	3849798.	.1475	8.04	22302
22312	N	UN	10.0	5.0	.882	.303	3849072.	.1957	10.72	22303
23021	N	UN	15.0	5.0	.858	.298	3792196.	.0248	1.34	
23022	N	UN	15.0	5.0	.851	.297	3750472.	.0497	2.68	
23023	N	UN	15.0	5.0	.840	.295	3716891.	.1000	5.36	
23100	N	UN	15.0	5.0	.822	.292	3670934.	.1516	8.04	
23107	N	UN	5.0	5.0	.867	.300	3802836.	.0986	5.36	23108
23109	N	UN	5.0	5.0	.867	.300	3769174.	.1970	10.72	23110
23117	N	UN	5.0	10.0	.869	.300	3803440.	.0985	5.36	23118
23201	N	UN	3.8	10.0	.866	.299	3948210.	.1003	5.36	23202
23206	N	UN	3.3	10.0	.866	.299	3924045.	.0500	2.68	23207
23208	N	UN	3.3	10.0	.871	.300	3914485.	.0996	5.36	23210
23211	N	UN	3.3	10.0	.870	.300	3896319.	.1492	8.04	23212
23219	N	UN	12.0	2.0	.864	.299	3865609.	.1994	10.72	23220
23305	N	UN	14.0	2.0	.858	.298	3831711.	.1995	10.72	23306
23310	N	UN	16.0	2.0	.839	.294	3768762.	.2014	10.72	23311
21112	N	UN	15.0	5.0	.873	.301	3940131.	.0099	.53	
23101	N	UN	15.0	5.0	.800	.287	3617353.	.2049	10.72	

TABLE 11.- Continued.

(d) Sikorsky SC-1095 airfoil.

A FRAME	TRIP	TYPE	AO	A1	Q	M	RE	K	FREQ	B FRAME
34022	Y	ST	0.0	0.0	.878	.301	3985083.	0.0000	0.00	34023
34100	Y	ST	5.0	0.0	.880	.301	3976998.	0.0000	0.00	34101
34102	Y	ST	10.0	0.0	.884	.30[illegible]	3969476.	0.0000	0.00	34103
34107	Y	ST	12.0	0.0	.879	.302	3961576.	0.0000	0.00	34108
34109	Y	ST	13.0	0.0	.883	.302	3946692.	0.0000	0.00	34110
34111	Y	ST	14.0	0.0	.856	.297	3869254.	0.0000	0.00	34112
34113	Y	ST	16.0	0.0	.806	.287	3735399.	0.0000	0.00	34114
34115	Y	ST	0.0	0.0	.880	.301	3902976.	0.0000	0.00	34116
34200	Y	ST	0.0	0.0	.341	.184	2464109.	0.0000	0.00	34201
34202	Y	ST	5.0	0.0	.342	.184	2463733.	0.0000	0.00	34203
34204	Y	ST	10.0	0.0	.342	.184	2455124.	0.0000	0.00	34205
34208	Y	ST	13.0	0.0	.342	.184	2449358.	0.0000	0.00	34209
34210	Y	ST	14.0	0.0	.342	.184	2447969.	0.0000	0.00	34211
34212	Y	ST	16.0	0.0	.341	.184	2441097.	0.0000	0.00	34213
34214	Y	ST	0.0	0.0	.341	.184	2444858.	0.0000	0.00	34215
35021	N	ST	-5.0	0.0	.880	.301	3835776.	0.0000	0.00	35022
35023	N	ST	-2.0	0.0	.878	.301	3819752.	0.0000	0.00	
35100	N	ST	[illegible]	0.0	.877	.301	3816485.	0.0000	0.00	35101
35102	N	ST	[illegible]	0.0	.880	.301	3819991.	0.0000	0.00	
35103	N	ST	[illegible]	0.0	.877	.301	3811571.	0.0000	0.00	35104
35111	N	ST	8.0	0.0	.881	.302	4009328.	0.0000	0.00	
35112	N	ST	10.0	0.0	.879	.302	3991392.	0.0000	0.00	35113
35114	N	ST	12.0	0.0	.877	.301	3[illegible]60357.	0.0000	0.00	35115
35116	N	ST	13.0	0.0	.845	.295	3867672.	0.0000	0.00	35117
35118	N	ST	13.5	0.0	.836	.293	3835999.	0.0000	0.00	35119
35123	N	ST	14.0	0.0	.879	.302	3927789.	0.0000	0.00	
35200	N	ST	16.0	0.0	.832	.293	3808814.	0.0000	0.00	35201
35206	N	ST	14.0	0.0	.874	.301	3893325.	0.0000	0.00	
35207	N	ST	13.0	0.0	.822	.291	3760893.	0.0000	0.00	
35208	N	ST	12.5	0.0	.845	.295	3802021.	0.0000	0.00	
35213	N	ST	5.0	0.0	.878	.302	3894699.	0.0000	0.00	
35214	N	ST	0.0	0.0	.883	.302	3894747.	0.0000	0.00	
35220	N	ST	-5.0	0.0	.610	.249	3240465.	0.0000	0.00	
35221	N	ST	-2.0	0.0	.611	.249	3231739.	0.0000	0.00	
35222	N	ST	0.0	0.0	.613	.250	3233853.	0.0000	0.00	
35223	N	ST	2.0	0.0	.612	.249	3228312.	0.0000	0.00	
35300	N	ST	5.0	0.0	.613	.250	3228749.	0.0000	0.00	
35305	N	ST	8.0	0.0	.612	.249	3194450.	0.0000	0.00	
35306	N	ST	10.0	0.0	.614	.249	3194632.	0.0000	0.00	
35307	N	ST	12.0	0.0	.610	.249	3176162.	0.0000	0.00	
35308	N	ST	13.0	0.0	.609	.248	3167812.	0.0000	0.00	
35309	N	ST	13.5	0.0	.605	.247	3151475.	0.0000	0.00	
35310	N	ST	14.1	0.0	.615	.250	3175031.	0.0000	0.00	
35313	N	ST	16.0	0.0	.614	.249	3171847.	0.0000	0.00	
35314	N	ST	18.0	0.0	.611	.249	3155127.	0.0000	0.00	
35315	N	ST	20.0	0.0	.609	.248	3132360.	0.0000	0.00	
35316	N	ST	25.0	0.0	.612	.250	3135933.	0.0000	0.00	
35317	N	ST	14.0	0.0	.611	.249	3142583.	0.0000	0.00	
35318	N	ST	13.0	0.0	.612	.250	3143100.	0.0000	0.00	
35319	N	ST	12.5	0.0	.611	.249	3139723.	0.0000	0.00	
35400	N	ST	5.0	0.0	.614	.249	3166450.	0.0000	0.00	
35401	N	ST	0.0	0.0	.611	.249	3153505.	0.0000	0.00	
36019	N	ST	-5.0	0.0	.342	.184	2509809.	0.0000	0.00	
36020	N	ST	0.0	0.0	.341	.185	2503010.	0.0000	0.00	36021
36022	N	ST	5.0	0.0	.341	.185	2493947.	0.0000	0.00	36023
36106	N	ST	10.0	0.0	.341	.185	2467697.	0.0000	0.00	36107
36108	N	ST	12.0	0.0	.341	.185	2461702.	0.0000	0.00	36109
36110	N	ST	13.5	0.0	.340	.184	2452406.	0.0000	0.00	36111
36112	N	ST	14.0	0.0	.341	.185	2447787.	0.0000	0.00	36113
36117	N	ST	15.0	0.0	.338	.183	2429196.	0.0000	0.00	
36118	N	ST	16.0	0.0	.340	.184	2432059.	0.0000	0.00	36119
36120	N	ST	20.0	0.0	.341	.185	2424852.	0.0000	0.00	
36202	N	ST	-5.0	0.0	.123	.110	1457009.	0.0000	0.00	
36203	N	ST	0.0	0.0	.124	.111	1461763.	0.0000	0.00	
36204	N	ST	5.0	0.0	.123	.110	1455304.	0.0000	0.00	
36209	N	ST	10.0	0.0	.122	.110	1429342.	0.0000	0.00	
36210	N	ST	12.0	0.0	.121	.109	1420840.	0.0000	0.00	
36211	N	ST	13.5	0.0	.122	.110	1428033.	0.0000	0.00	
36212	N	ST	14.0	0.0	.124	.110	1430614.	0.0000	0.00	
36213	N	ST	15.0	0.0	.122	.110	1421260.	0.0000	0.00	
36216	N	ST	15.5	0.0	.123	.110	1425215.	0.0000	0.00	
36217	N	ST	16.0	0.0	.121	.109	1413387.	0.0000	0.00	
36218	N	ST	20.0	0.0	.120	.109	1408711.	0.0000	0.00	
33022	N	UN	15.0	10.0	.054	.073	975044.	.0987	1.30	33023
33106	N	UN	15.0	10.0	.124	.110	1462074.	.0979	1.96	33107
33110	N	UN	15.0	10.0	.339	.183	2400379.	.0990	3.30	33111
33118	N	UN	6.2	10.0	.334	.182	2390916.	.0499	1.65	33120
33121	N	UN	6.2	10.0	.340	.184	2409037.	.1975	6.60	33122
33205	N	UN	15.0	10.0	.479	.219	2837984.	.0985	3.93	33206
33207	N	UN	15.0	10.0	.612	.249	3185055.	.0984	4.46	33208
33215	N	UN	15.0	10.0	.762	.279	3744973.	.1002	4.98	33216
33217	N	UN	15.0	10.0	.855	.297	3920520.	.0247	1.31	33218
33222	N	UN	15.0	10.0	.852	.296	3886915.	.0494	2.62	33223
33300	N	UN	15.0	10.0	.832	.292	3816743.	.0997	5.24	33303
34306	Y	UN	15.0	10.0	.828	.292	3875513.	.0503	2.62	34307
34308	Y	UN	15.0	10.0	.807	.288	3800453.	.1017	5.24	34309
34318	Y	UN	15.0	10.0	.340	.184	2482077.	.0500	1.65	34319
34321	Y	UN	15.0	10.0	.341	.184	2476494.	.0998	3.30	34322
34323	Y	UN	15.0	10.0	.341	.184	2472265.	.1495	4.95	34400
34409	N	UN	15.0	10.0	.762	.279	3601340.	.1557	7.86	34410
34418	N	UN	4.4	10.0	.881	.302	3864557.	.0983	5.36	34419
37023	N	UN	10.0	10.0	.866	.300	3936295.	.0252	1.35	37100
37101	N	UN	10.0	10.0	.876	.301	3928667.	.0496	2.68	37102
37107	N	UN	10.0	10.0	.880	.302	3915346.	.0987	5.36	37108
37109	N	UN	10.0	10.0	.879	.302	3894279.	.1480	8.04	37113
37119	N	UN	4.1	10.0	.879	.302	3866563.	.0492	2.68	37120
37121	N	UN	4.1	10.0	.886	.303	3859634.	.0978	5.36	37122
37123	N	UN	4.1	10.0	.879	.302	3836077.	.1471	8.04	37201
37207	N	UN	10.0	5.0	.879	.302	3784178.	.0244	1.34	
37208	N	UN	10.0	5.0	.871	.301	3750400.	.0489	2.68	
37210	N	UN	10.0	5.0	.879	.302	3760364.	.0972	5.36	
37213	N	UN	10.0	5.0	.885	.303	3780389.	.1454	8.04	
37215	N	UN	10.0	5.0	.883	.303	3763997.	.1939	10.72	
37219	N	UN	11.0	5.0	.871	.301	3752512.	.0489	2.68	37220
37221	N	UN	11.0	5.0	.878	.302	3752961.	.0972	5.36	37222
37304	N	UN	12.0	8.0	.878	.301	4001117.	.0499	2.68	
37305	N	UN	12.0	8.0	.878	.301	3984111.	.0997	5.36	
37306	N	UN	12.0	8.0	.876	.301	3969804.	.1266	6.81	
38021	N	UN	15.0	5.0	.879	.302	3954977.	.0248	1.34	
38022	N	UN	15.0	5.0	.865	.299	3893850.	.0499	2.68	
38102	N	UN	15.0	5.0	.840	.294	3784856.	.1008	5.36	
38103	N	UN	15.0	5.0	.830	.293	3747172.	.1519	8.04	
38104	N	UN	15.0	5.0	.808	.289	3688250.	.2053	10.72	
38119	N	UN	14.0	2.0	.870	.300	3853545.	.1980	10.72	38121
38201	N	UN	12.3	2.0	.876	.301	3876423.	.1975	10.72	38204
38216	N	UN	6.2	10.0	.339	.183	2468863.	.0100	.33	38217
38300	N	UN	15.0	10.0	.862	.298	3951336.	.0102	.54	38302
38306	N	UN	10.0	10.0	.869	.299	3931609.	.0099	.53	38307
39021	N	UN	4.1	10.0	.875	.300	3811898.	.0097	.53	39022
39104	N	UN	15.0	5.0	.856	.297	3926571.	.0100	.53	

TABLE 11.- Continued.

(d) Concluded.

A FRAME	TRIP	TYPE	AO	A1	Q	M	RE	K	FREQ	B FRAME
39110	N	UN	11.0	5.0	.869	.299	3896687.	.0099	.53	
39115	N	UN	14.0	2.0	.865	.298	3838622.	.0100	.54	
38110	N	UN	16.0	2.0	.832	.293	3754517.	.2023	10.72	38111
39107	N	UN	10.0	5.0	.876	.300	3939495.	.0098	.53	

TABLE 11.- Continued.

(e) Hughes HH-02 airfoil.

A FRAME	TRIP	TYPE	AO	A1	Q	M	RE	K	FREQ	B FRAME
40018	N	ST	-5.0	0.0	.122	.110	1508746.	0.0000	0.00	
40019	N	ST	0.0	0.0	.121	.109	1502749.	0.0000	0.00	
40020	N	ST	5.0	0.0	.123	.110	1511661.	0.0000	0.00	
40101	N	ST	10.0	0.0	.123	.110	1511504.	0.0000	0.00	
40102	N	ST	12.0	0.0	.120	.109	1490668.	0.0000	0.00	
40103	N	ST	14.0	0.0	.125	.111	1514773.	0.0000	0.00	
40104	N	ST	14.5	0.0	.123	.109	1502336.	0.0000	0.00	
40105	N	ST	15.0	0.0	.122	.110	1499223.	0.0000	0.00	
40106	N	ST	15.5	0.0	.121	.109	1494155.	0.0000	0.00	
40107	N	ST	16.0	0.0	.121	.109	1487366.	0.0000	0.00	
40108	N	ST	20.0	0.0	.122	.110	1497097.	0.0000	0.00	
40114	N	ST	-5.0	0.0	.342	.185	2477234.	0.0000	0.00	
40115	N	ST	0.0	0.0	.341	.185	2465667.	0.0000	0.00	40116
40117	N	ST	4.9	0.0	.341	.165	2469822.	0.0000	0.00	40118
40201	N	ST	10.0	0.0	.341	.185	2478173.	0.0000	0.00	40202
40203	N	ST	12.0	0.0	.343	.185	2430399.	0.0000	0.00	40204
40205	N	ST	14.0	0.0	.341	.185	2474050.	0.0000	0.00	40206
40207	N	ST	14.5	0.0	.344	.186	2483787.	0.0000	0.00	40208
40212	N	ST	15.0	0.0	.340	.185	2474314.	0.0000	0.00	
40213	N	ST	16.0	0.0	.340	.185	2473125.	0.0000	0.00	40214
40215	N	ST	20.0	0.0	.342	.185	2473995.	0.0000	0.00	
40222	N	ST	8.0	0.0	.879	.302	4129994.	0.0000	0.00	
40223	N	ST	10.0	0.0	.874	.301	4103323.	0.0000	0.00	40300
40301	N	ST	12.0	0.0	.875	.300	4065502.	0.0000	0.00	40302
40303	N	ST	13.0	0.0	.869	.299	4051531.	0.0000	0.00	40304
40308	N	ST	13.5	0.0	.878	.301	4059676.	0.0000	0.00	40309
40310	N	ST	14.0	0.0	.878	.301	4041789.	0.0000	0.00	40311
40312	N	ST	14.5	0.0	.883	.302	4039947.	0.0000	0.00	40313
40314	N	ST	15.0	0.0	.884	.303	4032069.	0.0000	0.00	40315
40319	N	ST	18.0	0.0	.806	.288	3854130.	0.0000	0.00	40320
40321	N	ST	20.0	0.0	.715	.270	3619314.	0.0000	0.00	
40322	N	ST	14.0	0.0	.881	.301	4009498.	0.0000	0.00	
40323	N	ST	13.0	0.0	.869	.299	3950164.	0.0000	0.00	
40400	N	ST	12.5	0.0	.871	.300	3981021.	0.0000	0.00	
40406	N	ST	5.0	0.0	.877	.301	4024289.	0.0000	0.00	
40407	N	ST	0.0	0.0	.878	.301	4023056.	0.0000	0.00	
41019	N	ST	-5.0	0.0	.874	.300	4148783.	0.0000	0.00	41020
41021	N	ST	-2.0	0.0	.874	.300	4123880.	0.0000	0.00	
41100	N	ST	0.0	0.0	.872	.300	4107145.	0.0000	0.00	41101
41102	N	ST	2.0	0.0	.875	.300	4097393.	0.0000	0.00	.
41103	N	ST	5.0	0.0	.877	.301	4090950.	0.0000	0.00	41104
41110	N	ST	-5.0	0.0	.610	.248	3409824.	0.0000	0.00	
41111	N	ST	-2.0	0.0	.610	.248	3397141.	0.0000	0.00	
41112	N	ST	0.0	0.0	.610	.248	3393868.	0.0000	0.00	
41113	N	ST	2.0	0.0	.611	.248	3391537.	0.0000	0.00	
41114	N	ST	5.0	0.0	.609	.248	3381054.	0.0000	0.00	
41119	N	ST	8.0	0.0	.610	.248	3361029.	0.0000	0.00	
41120	N	ST	10.0	0.0	.609	.248	3342575.	0.0000	0.00	
41121	N	ST	12.0	0.0	.609	.248	3337152.	0.0000	0.00	
41122	N	ST	13.0	0.0	.612	.249	3337682.	0.0000	0.00	
41123	N	ST	13.5	0.0	.614	.249	3341019.	0.0000	0.00	
41200	N	ST	14.0	0.0	.611	.249	3329347.	0.0000	0.00	
41201	N	ST	14.5	0.0	.610	.248	3321682.	0.0000	0.00	
41202	N	ST	15.0	0.0	.609	.248	3315976.	0.0000	0.00	
41205	N	ST	18.0	0.0	.608	.248	3317238.	0.0000	0.00	
41206	N	ST	20.0	0.0	.608	.248	3306068.	0.0000	0.00	
41207	N	ST	14.0	0.0	.614	.249	3321536.	0.0000	0.00	
41208	N	ST	13.0	0.0	.609	.248	3310470.	0.0000	0.00	
41209	N	ST	12.5	0.0	.613	.249	3319411.	0.0000	0.00	
41214	N	ST	5.0	0.0	.613	.249	3342074.	0.0000	0.00	

A FRAME	TRIP	TYPE	AO	A1	Q	M	RE	K	FREQ	B FRAME
41215	N	ST	0.0	0.0	.611	.249	3331668.	0.0000	0.00	
41221	Y	ST	0.0	0.0	.875	.299	4054062.	0.0000	0.00	41222
41223	Y	ST	5.0	0.0	.874	.300	4025612.	0.0000	0.00	41300
41301	Y	ST	10.0	0.0	.877	.300	4012119.	0.0000	0.00	41302
41303	Y	ST	12.0	0.0	.873	.300	3995297.	0.0000	0.00	41304
41305	Y	ST	13.0	0.0	.858	.296	3950234.	0.0000	0.00	41306
41307	Y	ST	13.5	0.0	.879	.300	3987094.	0.0000	0.00	41308
41312	Y	ST	14.0	0.0	.876	.300	3990589.	0.0000	0.00	41313
41314	Y	ST	16.0	0.0	.811	.287	3822102.	0.0000	0.00	41315
41401	Y	ST	0.0	0.0	.336	.182	2505262.	0.0000	0.00	41402
41403	Y	ST	5.0	0.0	.340	.184	2516822.	0.0000	0.00	41404
41405	Y	ST	10.0	0.0	.339	.183	2509654.	0.0000	0.00	41406
41407	Y	ST	12.0	0.0	.336	.182	2495906.	0.0000	0.00	41408
41409	Y	ST	13.0	0.0	.337	.183	2499130.	0.0000	0.00	41410
41411	Y	ST	13.5	0.0	.333	.182	2498901.	0.0000	0.00	41412
41413	Y	ST	14.0	0.0	.334	.181	2488812.	0.0000	0.00	41414
41415	Y	ST	14.5	0.0	.339	.183	2503241.	0.0000	0.00	41416
41417	Y	ST	16.0	0.0	.338	.182	2496014.	0.0000	0.00	41418
41419	Y	ST	0.0	0.0	.338	.182	2495914.	0.0000	0.00	
42019	Y	US	15.0	10.0	.836	.292	3955253.	.0252	1.31	42020
42021	Y	US	15.0	10.0	.821	.289	3684045.	.0508	2.62	42022
42100	Y	US	15.0	10.0	.788	.283	3796236.	.1035	5.24	42101
42108	Y	US	15.0	10.0	.339	.183	2530006.	.0506	1.65	42109
42110	Y	US	15.0	10.0	.338	.183	2526566.	.1013	3.30	42112
42113	Y	US	15.0	10.0	.340	.183	2532492.	.1516	4.95	42114
42121	N	US	15.0	10.0	.054	.072	1027532.	.1011	1.30	42122
42206	N	US	15.0	10.0	.823	.290	3980979.	.0256	1.31	42207
42208	N	US	15.0	10.0	.834	.292	3977572.	.0507	2.62	42209
42210	N	US	15.0	10.0	.813	.288	3911977.	.1025	5.24	42211
42212	N	US	15.0	10.0	.786	.283	3830288.	.1561	7.85	42213
42217	N	US	15.0	10.0	.786	.283	3833375.	.1564	7.86	
42218	N	US	15.0	10.0	.759	.278	3756013.	.1008	4.98	42219
42302	N	US	15.0	10.0	.339	.183	2526332.	.1011	3.30	42303
42309	N	US	15.0	10.0	.476	.218	2981460.	.1011	3.93	42310
42313	N	US	15.0	10.0	.604	.246	3327957.	.1013	4.46	42314
42321	N	US	15.0	10.0	.120	.108	1510607.	.1013	1.96	42322
43019	N	US	10.0	10.0	.858	.297	3898111.	.0101	.54	43020
43106	N	US	10.0	10.0	.870	.301	3930420.	.0249	1.34	43107
43108	N	US	10.0	10.0	.876	.302	3927336.	.0496	2.68	43109
43114	N	US	10.0	10.0	.861	.299	3899487.	.1502	8.04	
43117	N	US	10.0	10.0	.849	.297	3886604.	.1514	8.04	43118
43202	N	US	3.8	10.0	.874	.301	3968134.	.0249	1.34	43203
43112	N	US	10.0	10.0	.876	.302	3945527.	.0993	5.36	43113
43204	N	US	3.8	10.0	.877	.302	3962955.	.0497	2.68	43205
43206	N	US	3.8	10.0	.876	.302	3955351.	.0994	5.36	43208
43209	N	US	3.8	10.0	.878	.302	3955884.	.1469	8.04	43210
43215	N	US	3.8	10.0	.876	.302	4060507.	.0101	.54	43216
43219	N	US	4.0	10.0	.879	.303	4045704.	.0999	5.36	43221
43303	N	US	15.0	5.0	.845	.296	3918196.	.0254	1.34	
43304	N	US	15.0	5.0	.821	.292	3841831.	.0515	2.68	
43305	N	US	15.0	5.0	.817	.291	3822850.	.1030	5.36	
43309	N	US	15.0	5.0	.805	.289	3776817.	.2073	10.72	
43314	N	US	11.0	5.0	.876	.302	3934345.	.0248	1.34	
43315	N	US	11.0	5.0	.877	.302	3922072.	.0489	2.65	
43316	N	US	11.0	5.0	.875	.302	3909299.	.0990	5.36	
44019	N	US	10.0	5.0	.869	.301	3960458.	.0101	.54	44020
44021	N	US	10.0	5.0	.876	.302	3950518.	.0248	1.34	44022
44023	N	US	10.0	5.0	.876	.302	3943793.	.0496	2.69	44100
44104	N	US	10.0	5.0	.881	.303	3996291.	.0993	5.36	44105
44106	N	US	10.0	5.0	.880	.303	3991389.	.1490	8.04	44107

TABLE 11.- Continued.

(e) Concluded.

A FRAME	TRIP	TYPE	AO	A1	Q	M	RE	K	FREQ	B FRAME
44112	N	US	10.0	5.0	.880	.303	4003278.	.1989	10.72	44113
44118	N	US	10.0	5.0	.880	.302	4037690.	.0999	5.36	
44119	N	US	10.0	5.0	.876	.302	4019097.	.0250	1.34	
44120	N	US	10.0	5.0	.878	.302	4007236.	.1997	10.72	
44202	N	US	14.0	2.0	.875	.301	4004232.	.1001	5.36	44203
44204	N	US	14.0	2.0	.872	.301	3987136.	.2002	10.72	44205
44209	N	US	17.5	2.0	.773	.282	3756572.	.2132	10.72	
44212	N	US	15.5	2.0	.854	.297	3961107.	.0102	.54	
44214	N	US	15.5	2.0	.851	.297	3917470.	.0253	1.34	
44215	N	US	15.5	2.0	.849	.296	3904494.	.0506	2.68	
44216	N	US	15.5	2.0	.829	.293	3854681.	.1024	5.36	
44217	N	US	15.5	2.0	.820	.291	3826794.	.1545	8.04	
44218	N	US	15.5	2.0	.824	.292	3832243.	.2054	10.72	
44221	N	US	12.5	2.0	.871	.301	3956605.	.0101	.54	
44222	N	US	12.5	2.0	.877	.302	3946321.	.0248	1.34	
44223	N	US	12.5	2.0	.871	.301	3926090.	.0498	2.68	
44300	N	US	12.5	2.0	.874	.301	3929775.	.0994	5.36	
44303	N	US	12.5	2.0	.877	.302	3952217.	.1490	8.04	
44304	N	US	12.5	2.0	.878	.302	3945918.	.1984	10.72	
43308	N	US	15.0	5.0	.813	.290	3809287.	.1549	8.04	

TABLE 11.- Continued.

(f) Vertol VR-7 airfoil.

A FRAME	TRIP	TYPE	AO	A1	Q	M	RE	K	FREQ	B FRAME
46018	N	ST	-5.0	0.0	.121	.108	1551001.	0.0000	0.00	
46019	N	ST	0.0	0.0	.121	.108	1546271.	0.0000	0.00	
46020	N	ST	5.0	0.0	.123	.109	1557517.	0.0000	0.00	
46101	N	ST	10.0	0.0	.118	.107	1512690.	0.0000	0.00	
46102	N	ST	12.0	0.0	.122	.109	1540066.	0.0000	0.00	
46103	N	ST	12.5	0.0	.123	.109	1547844.	0.0000	0.00	
46104	N	ST	13.0	0.0	.123	.109	1543789.	0.0000	0.00	
46105	N	ST	13.5	0.0	.123	.109	1542255.	0.0000	0.00	
46106	N	ST	14.0	0.0	.122	.109	1535872.	0.0000	0.00	
46107	N	ST	15.0	0.0	.122	.109	1537932.	0.0000	0.00	
46108	N	ST	17.0	0.0	.123	.109	1541148.	0.0000	0.00	
46109	N	ST	20.0	0.0	.122	.109	1534206.	0.0000	0.00	
46110	N	ST	25.0	0.0	.120	.108	1523001.	0.0000	0.00	
46116	N	ST	-5.0	0.0	.341	.184	2550698.	0.0000	0.00	
46117	N	ST	0.0	0.0	.342	.183	2552563.	0.0000	0.00	46118
46119	N	ST	5.0	0.0	.341	.183	2546269.	0.0000	0.00	46120
46203	N	ST	10.0	0.0	.343	.184	2562110.	0.0000	0.00	46204
46205	N	ST	12.0	0.0	.341	.183	2551368.	0.0000	0.00	46206
46207	N	ST	12.5	0.0	.342	.183	2553262.	0.0000	0.00	46208
46209	N	ST	13.0	0.0	.342	.184	2553793.	0.0000	0.00	46210
46211	N	ST	13.5	0.0	.341	.183	2550511.	0.0000	0.00	46212
46217	N	ST	14.0	0.0	.342	.183	2637541.	0.0000	0.00	46218
46219	N	ST	15.0	0.0	.341	.183	2630320.	0.0000	0.00	46220
46221	N	ST	17.0	0.0	.340	.183	2624424.	0.0000	0.00	46222
46223	N	ST	20.0	0.0	.340	.183	2622591.	0.0000	0.00	46300
46301	N	ST	25.0	0.0	.340	.183	2614669.	0.0000	0.00	
46307	N	ST	-5.0	0.0	.612	.248	3482182.	0.0000	0.00	
46308	N	ST	-2.0	0.0	.613	.249	3476509.	0.0000	0.00	
46309	N	ST	0.0	0.0	.612	.248	3469801.	0.0000	0.00	
46310	N	ST	2.0	0.0	.611	.248	3461144.	0.0000	0.00	
46311	N	ST	5.0	0.0	.614	.248	3462655.	0.0000	0.00	
46317	N	ST	8.0	0.0	.615	.249	3457898.	0.0000	0.00	
46318	N	ST	10.0	0.0	.611	.248	3435015.	0.0000	0.00	
46319	N	ST	12.0	0.0	.613	.248	3433344.	0.0000	0.00	
46320	N	ST	12.5	0.0	.615	.249	3429825.	0.0000	0.00	
46321	N	ST	13.0	0.0	.612	.248	3419429.	0.0000	0.00	
46322	N	ST	13.5	0.0	.610	.248	3409796.	0.0000	0.00	
46323	N	ST	14.0	0.0	.613	.249	3417715.	0.0000	0.00	
46400	N	ST	15.0	0.0	.613	.249	3413348.	0.0000	0.00	
46403	N	ST	17.0	0.0	.616	.249	3427697.	0.0000	0.00	
46404	N	ST	20.0	0.0	.615	.249	3412222.	0.0000	0.00	
46405	N	ST	25.0	0.0	.614	.248	3396768.	0.0000	0.00	
46406	N	ST	13.0	0.0	.613	.249	3398737.	0.0000	0.00	
46407	N	ST	12.0	0.0	.610	.248	3391942.	0.0000	0.00	
46412	N	ST	0.0	0.0	.614	.248	3394265.	0.0000	0.00	
46418	N	ST	-5.0	0.0	.877	.300	3996105.	0.0000	0.00	46419
46420	N	ST	-2.0	0.0	.878	.301	3986471.	0.0000	0.00	
46423	N	ST	2.0	0.0	.875	.300	3966864.	0.0000	0.00	
46500	N	ST	5.0	0.0	.877	.300	3965878.	0.0000	0.00	46501
46508	N	ST	8.0	0.0	.878	.300	4161706.	0.0000	0.00	
46509	N	ST	10.0	0.0	.870	.298	4126333.	0.0000	0.00	46510
46511	N	ST	12.0	0.0	.876	.299	4119351.	0.0000	0.00	46512
46513	N	ST	12.5	0.0	.874	.299	4099803.	0.0000	0.00	46514
46515	N	ST	13.0	0.0	.867	.298	4070743.	0.0000	0.00	46516
46517	N	ST	13.5	0.0	.879	.300	4087558.	0.0000	0.00	46518
46519	N	ST	14.0	0.0	.878	.300	4077474.	0.0000	0.00	46520
46600	N	ST	15.0	0.0	.873	.299	4089463.	0.0000	0.00	46601
46602	N	ST	17.0	0.0	.878	.300	4078318.	0.0000	0.00	46603
46604	N	ST	20.0	0.0	.831	.291	3955770.	0.0000	0.00	
46608	N	ST	25.0	0.0	.690	.265	3626593.	0.0000	0.00	

A FRAME	TRIP	TYPE	AO	A1	Q	M	RE	K	FREQ	B FRAME
46609	N	ST	13.0	0.0	.876	.299	4071175.	0.0000	0.00	
46610	N	ST	12.0	0.0	.872	.299	4055190.	0.0000	0.00	
46615	N	ST	0.0	0.0	.881	.300	4097411.	0.0000	0.00	
46621	Y	ST	0.0	0.0	.340	.183	2522757.	0.0000	0.00	46622
46623	Y	ST	5.0	0.0	.340	.183	2514978.	0.0000	0.00	46700
46701	Y	ST	10.0	0.0	.340	.183	2513421.	0.0000	0.00	46702
46703	Y	ST	12.0	0.0	.341	.183	2515138.	0.0000	0.00	46704
46705	Y	ST	13.0	0.0	.340	.183	2506104.	0.0000	0.00	46706
46707	Y	ST	14.0	0.0	.338	.182	2501582.	0.0000	0.00	46708
46712	Y	ST	15.0	0.0	.340	.183	2518275.	0.0000	0.00	46713
46714	Y	ST	16.0	0.0	.341	.184	2516975.	0.0000	0.00	46715
46716	Y	ST	20.0	0.0	.343	.184	2517610.	0.0000	0.00	46717
46718	Y	ST	0.0	0.0	.342	.183	2519323.	0.0000	0.00	46719
46802	Y	ST	0.0	0.0	.881	.300	4204772.	0.0000	0.00	46803
46804	Y	ST	5.0	0.0	.881	.300	4185103.	0.0000	0.00	46805
46806	Y	ST	10.0	0.0	.886	.301	4170536.	0.0000	0.00	46807
46808	Y	ST	12.0	0.0	.882	.300	4148330.	0.0000	0.00	46809
46810	Y	ST	13.0	0.0	.883	.301	4139718.	0.0000	0.00	46811
46815	Y	ST	14.0	0.0	.881	.300	4137342.	0.0000	0.00	46816
46817	Y	ST	15.0	0.0	.877	.300	4108330.	0.0000	0.00	46818
46819	Y	ST	16.0	0.0	.877	.299	4091352.	0.0000	0.00	46820
46821	Y	ST	20.0	0.0	.806	.287	3893404.	0.0000	0.00	46822
46823	Y	ST	0.0	0.0	.881	.300	4085157.	0.0000	0.00	46900
45019	N	UN	15.0	10.0	.873	.300	4062142.	.0247	1.31	45020
45021	N	UN	15.0	10.0	.830	.292	3937973.	.0505	2.62	45022
45023	N	UN	15.0	10.0	.835	.293	3931111.	.1005	5.24	45100
45101	N	UN	15.0	10.0	.793	.285	3824874.	.1549	7.86	45102
45109	N	UN	10.0	10.0	.873	.301	4033486.	.0101	.54	45110
45111	N	UN	10.0	10.0	.875	.301	4010614.	.0251	1.34	45112
45113	N	UN	10.0	10.0	.878	.301	4010372.	.0500	2.68	
45117	N	UN	10.0	10.0	.875	.301	4019136.	.1003	5.36	48118
45119	N	UN	10.0	10.0	.879	.302	4015256.	.1498	8.04	45120
45203	N	UN	15.0	5.0	.869	.300	4019028.	.0102	.54	45204
45205	N	UN	15.0	5.0	.876	.301	4008473.	.0250	1.34	45206
45207	N	UN	15.0	5.0	.877	.301	4005939.	.0500	2.68	45208
45209	N	UN	15.0	5.0	.871	.300	3966080.	.1002	5.36	45210
45211	N	UN	15.0	5.0	.860	.298	3957187.	.1513	8.04	45212
45213	N	UN	15.0	5.0	.841	.295	3908733.	.2041	10.72	45214
45221	N	UN	10.0	5.0	.878	.302	4054475.	.0251	1.34	45222
45223	N	UN	10.0	5.0	.877	.301	4032781.	.0501	2.68	
45300	N	UN	10.0	5.0	.878	.301	4031948.	.1001	5.36	45301
45302	N	UN	10.0	5.0	.879	.302	4030474.	.1500	8.04	
45303	N	UN	10.0	5.0	.878	.301	4025973.	.2002	10.72	45304
47020	Y	UN	15.0	10.0	.859	.299	4059175.	.0249	1.31	47021
47100	Y	UN	15.0	10.0	.820	.292	3928981.	.1014	5.24	47101
47110	Y	UN	15.0	10.0	.338	.184	2577907.	.0508	1.65	47111
47112	Y	UN	15.0	10.0	.342	.185	2586091.	.1008	3.30	47113
47114	Y	UN	15.0	10.0	.342	.185	2580642.	.1512	4.95	47115
47123	N	UN	15.0	10.0	.054	.073	1030887.	.1007	1.30	47200
47206	N	UN	15.0	10.0	.123	.110	1553432.	.1006	1.96	47207
47213	N	UN	15.0	10.0	.340	.185	2606965.	.1016	3.30	47214
47217	N	UN	15.0	10.0	.479	.221	3036397.	.1008	3.93	47218
47301	N	UN	15.0	10.0	.610	.250	3408483.	.1009	4.46	47302
47305	N	UN	15.0	10.0	.760	.281	3783711.	.1003	4.98	47306
54019	N	UN	10.0	10.0	.340	.183	2632968.	.0258	.83	54020
54022	N	UN	10.0	10.0	.340	.183	2616265.	.0511	1.65	54023
54101	N	UN	10.0	10.0	.339	.183	2607326.	.1021	3.30	54102
54110	N	UN	10.0	10.0	.341	.184	2597940.	.1526	4.95	54111
54113	N	UN	10.0	10.0	.341	.184	2588267.	.2030	6.60	54114
54116	N	UN	10.0	10.0	.341	.184	2581336.	.2535	8.25	54117

TABLE 11.- Continued.

(f) Concluded.

A FRAME	TRIP	TYPE	A0	A1	Q	M	RE	K	FREQ	B FRAME
54216	N	UN	15.0	10.0	.340	.184	2547606.	.1514	4.95	54217
48019	N	UN	4.1	10.0	.874	.299	4215503.	.0103	.54	48020
48023	N	UN	4.1	10.0	.880	.300	4189985.	.0255	1.34	48100
48101	N	UN	4.1	10.0	.877	.299	4160141.	.0509	2.68	48102
48103	N	UN	4.1	10.0	.879	.300	4154411.	.1016	5.36	48104
48116	N	UN	13.0	2.0	.878	.299	4094662.	.0253	1.34	48117
48118	N	UN	13.0	2.0	.878	.299	4059323.	.0504	2.68	48119
48122	N	UN	13.0	2.0	.876	.299	4057706.	.1010	5.36	48123
48209	N	UN	16.0	2.0	.870	.298	4059728.	.2028	10.72	48211
48215	N	UN	14.0	2.0	.877	.300	4057579.	.0504	2.68	
48216	N	UN	14.0	2.0	.879	.300	4047826.	.1005	5.36	
48217	N	UN	14.0	2.0	.879	.300	4039080.	.2009	10.72	48218
48300	N	UN	12.5	2.0	.878	.300	4033369.	.0101	.54	
48301	N	UN	12.5	2.0	.878	.300	4011900.	.0251	1.34	
48302	N	UN	12.5	2.0	.881	.301	4009055.	.0500	2.68	
48303	N	UN	12.5	2.0	.874	.299	3986169.	.1004	5.36	
48304	N	UN	12.5	2.0	.873	.299	3980450.	.1505	8.04	
48308	N	UN	12.5	2.0	.875	.300	3998448.	.2007	10.72	48309
49110	N	UN	15.0	10.0	.339	.184	2634248.	.0257	.83	49111
49117	N	UN	15.0	10.0	.342	.185	2619356.	.0507	1.65	49118
49120	N	UN	15.0	10.0	.340	.185	2599912.	.1014	3.30	49121
49203	N	UN	15.0	10.0	.341	.185	2592737.	.1518	4.95	49204
49206	N	UN	15.0	10.0	.341	.165	2584616.	.2020	6.60	49207
49216	N	UN	4.7	10.0	.340	.184	2560438.	.0254	.83	49217
49300	N	UN	4.7	10.0	.339	.184	2535655.	.1009	3.30	49301
49307	N	UN	4.7	10.0	.342	.185	2548693.	.2005	6.60	49308
49310	N	UN	4.7	10.0	.343	.185	2543519.	.2503	8.25	49311
49023	N	UN	15.0	10.0	.338	.184	2543127.	.0101	.33	49100
50116	N	UN	4.7	10.0	.339	.183	2531156.	.0101	.33	50117
57018	N	UN	15.0	10.0	.340	.184	2555187.	.1516	4.95	57019
58018	N	UN	15.0	10.0	.338	.183	2437793.	.1495	4.95	58019
58102	N	UN	15.0	10.0	.014	.037	496703.	.0983	.65	58103
58111	N	UN	15.0	10.0	.121	.109	1528745.	.1010	1.96	58112
58120	N	UN	15.0	10.0	.340	.184	2536174.	.1511	4.95	
58121	N	UN	15.0	10.0	.340	.184	2532230.	.1007	3.30	
47022	Y	UN	15.0	10.0	.841	.296	3990015.	.0501	2.62	47023
48200	N	UN	13.0	2.0	.884	.301	4062447.	.2006	10.72	48201

TABLE 11.- Continued.

(g) NLR-1 airfoil.

A FRAME	TRIP	TYPE	AO	A1	Q	M	RE	K	FREQ	B FRAME
61018	N	ST	-5.0	0.0	.122	.109	1524150.	0.0000	0.00	
61019	N	ST	0.0	0.0	.123	.110	1534313.	0.0000	0.00	
61020	N	ST	5.0	0.0	.122	.110	1529480.	0.0000	0.00	
61101	N	ST	10.0	0.0	.125	.111	1537127.	0.0000	0.00	
61102	N	ST	12.0	0.0	.122	.109	1517792.	0.0000	0.00	
61103	N	ST	14.0	0.0	.122	.110	1522421.	0.0000	0.00	
61104	N	ST	15.0	0.0	.122	.110	1517668.	0.0000	0.00	
61105	N	ST	14.6	0.0	.122	.110	1511515.	0.0000	0.00	
61106	N	ST	16.5	0.0	.121	.109	1502456.	0.0000	0.00	
61107	N	ST	18.0	0.0	.123	.110	1511233.	0.0000	0.00	
61108	N	ST	20.0	0.0	.122	.110	1509433.	0.0000	0.00	
61114	N	ST	-5.0	0.0	.341	.185	2466730.	0.0000	0.00	
61115	N	ST	0.0	0.0	.342	.185	2469459.	0.0000	0.00	61116
61117	N	ST	5.0	0.0	.341	.184	2461681.	0.0000	0.00	61118
61201	N	ST	10.0	0.0	.341	.184	2434057.	0.0000	0.00	61202
61203	N	ST	12.0	0.0	.345	.185	2440090.	0.0000	0.00	61204
61205	N	ST	14.0	0.0	.344	.186	2430259.	0.0000	0.00	61206
61208	N	ST	15.4	0.0	.338	.184	2407482.	0.0000	0.00	
61212	N	ST	16.5	0.0	.342	.185	2420407.	0.0000	0.00	
61213	N	ST	18.0	0.0	.341	.184	2413757.	0.0000	0.00	61214
61215	N	ST	20.0	0.0	.342	.184	2407546.	0.0000	0.00	
61221	N	ST	-5.0	0.0	.612	.250	3195467.	0.0000	0.00	
61222	N	ST	-2.0	0.0	.614	.250	3197744.	0.0000	0.00	
61223	N	ST	0.0	0.0	.613	.250	3194392.	0.0000	0.00	
61300	N	ST	2.0	0.0	.612	.250	3191078.	0.0000	0.00	
61301	N	ST	5.0	0.0	.612	.250	3189268.	0.0000	0.00	
61306	N	ST	8.0	0.0	.616	.251	3401455.	0.0000	0.00	
61307	N	ST	10.0	0.0	.619	.251	3402068.	0.0000	0.00	
61308	N	ST	12.0	0.0	.613	.249	3391325.	0.0000	0.00	
61309	N	ST	12.5	0.0	.614	.250	3381216.	0.0000	0.00	
61310	N	ST	13.0	0.0	.610	.249	3364760.	0.0000	0.00	
61311	N	ST	14.0	0.0	.619	.251	3385628.	0.0000	0.00	
61312	N	ST	15.0	0.0	.611	.249	3361196.	0.0000	0.00	
61315	N	ST	16.0	0.0	.611	.249	3363498.	0.0000	0.00	
61316	N	ST	20.0	0.0	.612	.250	3357544.	0.0000	0.00	
61317	N	ST	25.0	0.0	.612	.250	3344638.	0.0000	0.00	
61318	N	ST	14.0	0.0	.612	.250	3349019.	0.0000	0.00	
61319	N	ST	12.5	0.0	.614	.250	3357487.	0.0000	0.00	
61400	N	ST	5.0	0.0	.613	.249	3372794.	0.0000	0.00	
61401	N	ST	0.0	0.0	.612	.250	3364756.	0.0000	0.00	
61407	N	ST	-5.0	0.0	.876	.301	3981952.	0.0000	0.00	61408
61409	N	ST	-2.0	0.0	.878	.302	3970720.	0.0000	0.00	
61410	N	ST	0.0	0.0	.877	.302	3963168.	0.0000	0.00	61411
61412	N	ST	2.0	0.0	.877	.302	3954548.	0.0000	0.00	
61413	N	ST	5.0	0.0	.879	.303	3954345.	0.0000	0.00	61414
61421	N	ST	8.0	0.0	.878	.302	3953659.	0.0000	0.00	
61422	N	ST	10.0	0.0	.869	.300	3921408.	0.0000	0.00	61423
61500	N	ST	12.0	0.0	.872	.301	3911370.	0.0000	0.00	61501
61502	N	ST	12.5	0.0	.879	.302	3915401.	0.0000	0.00	61503
61508	N	ST	12.5	0.0	.882	.302	4029504.	0.0000	0.00	61509
61510	N	ST	13.0	0.0	.882	.302	4003007.	0.0000	0.00	61511
61512	N	ST	14.0	0.0	.879	.302	3962342.	0.0000	0.00	
61513	N	ST	16.0	0.0	.877	.302	3963711.	0.0000	0.00	61514
61519	N	ST	20.0	0.0	.736	.275	3622389.	0.0000	0.00	61520
61521	N	ST	25.0	0.0	.677	.263	3459893.	0.0000	0.00	
61522	N	ST	14.0	0.0	.880	.302	3939697.	0.0000	0.00	
61523	N	ST	12.5	0.0	.870	.300	3913953.	0.0000	0.00	
61605	N	ST	5.0	0.0	.879	.302	3966363.	0.0000	0.00	
61606	N	ST	0.0	0.0	.880	.302	3963830.	0.0000	0.00	
64221	Y	ST	0.0	0.0	.341	.185	2352861.	0.0000	0.00	64222

A FRAME	TRIP	TYPE	AO	A1	Q	M	RE	K	FREQ	B FRAME
64223	Y	ST	5.0	0.0	.339	.184	2345411.	0.0000	0.00	64300
64301	Y	ST	10.0	0.0	.342	.185	2349991.	0.0000	0.00	64302
64303	Y	ST	12.0	0.0	.341	.185	2346533.	0.0000	0.00	64304
64305	Y	ST	13.0	0.0	.341	.185	2344262.	0.0000	0.00	64306
64307	Y	ST	14.0	0.0	.349	.187	2370314.	0.0000	0.00	64308
64309	Y	ST	16.0	0.0	.342	.185	2345780.	0.0000	0.00	64310
64311	Y	ST	0.0	0.0	.344	.186	2355621.	0.0000	0.00	64312
65019	Y	ST	-11.0	0.0	.875	.301	3814433.	0.0000	0.00	
65020	Y	ST	-9.0	0.0	.876	.301	3804399.	0.0000	0.00	
65021	Y	ST	-7.0	0.0	.875	.301	3798094.	0.0000	0.00	
65022	Y	ST	-6.0	0.0	.874	.301	3790531.	0.0000	0.00	
65023	Y	ST	-5.0	0.0	.876	.301	3792112.	0.0000	0.00	
65100	Y	ST	0.0	0.0	.875	.301	3786607.	0.0000	0.00	
65101	Y	ST	5.0	0.0	.878	.302	3783080.	0.0000	0.00	65102
65103	Y	ST	10.0	0.0	.875	.301	3764580.	0.0000	0.00	65104
65107	Y	ST	11.8	0.0	.842	.295	3697279.	0.0000	0.00	65108
65109	Y	ST	13.0	0.0	.858	.298	3722261.	0.0000	0.00	65110
65112	Y	ST	14.0	0.0	.839	.294	3665290.	0.0000	0.00	65111
65113	Y	ST	16.0	0.0	.800	.288	3574574.	0.0000	0.00	65114
65115	Y	ST	0.0	0.0	.879	.302	3745601.	0.0000	0.00	
62020	N	US	15.0	10.0	.054	.073	968160.	.0985	1.30	62021
62104	N	US	15.0	10.0	.121	.109	1446202.	.0987	1.96	62105
62112	N	US	15.0	10.0	.340	.184	3401.	.1003	3.30	62113
62114	N	US	15.0	10.0	.396	.199	2698892.	.1002	3.57	62115
62121	N	US	10.0	10.0	.398	.200	2557024.	.1712	6.25	
62201	N	US	15.0	5.0	.398	.200	2540409.	.2826	10.35	
62202	N	US	15.0	5.0	.396	.199	2534183.	.1710	6.25	
62208	N	US	15.0	10.0	.480	.220	2777505.	.0974	3.93	62209
62210	N	US	15.0	10.0	.612	.250	3113246.	.0972	4.46	62211
62218	N	US	15.0	10.0	.760	.280	3441981.	.0967	4.98	62219
62302	N	US	15.0	10.0	.838	.295	3859287.	.0248	1.31	62303
62304	N	US	15.0	10.0	.834	.294	3816841.	.0496	2.62	62305
62307	N	US	15.0	10.0	.835	.294	3810660.	.0991	5.24	62308
62309	N	US	15.0	10.0	.796	.287	3699269.	.1521	7.86	62310
62317	N	US	10.0	10.0	.872	.301	3725580.	.0098	.54	62318
62320	N	US	10.0	10.0	.874	.302	3704354.	.0243	1.34	62321
62322	N	US	10.0	10.0	.873	.301	3685360.	.0484	2.68	62323
62400	N	US	10.0	10.0	.878	.302	3685928.	.0965	5.36	62401
62403	N	US	10.0	10.0	.881	.303	3701055.	.1156	6.43	62404
62405	N	US	10.0	10.0	.866	.300	3656985.	.1457	8.04	62406
63018	N	US	15.0	5.0	.855	.297	3912793.	.0102	.54	
63019	N	US	15.0	5.0	.862	.299	3885789.	.0250	1.34	
63020	N	US	15.0	5.0	.862	.299	3871332.	.0499	2.68	
63021	N	US	15.0	5.0	.850	.297	3836177.	.1004	5.36	
63100	N	US	15.0	5.0	.848	.296	3831403.	.1206	6.43	
63101	N	US	15.0	5.0	.839	.295	3800952.	.1515	8.04	
63102	N	US	15.0	5.0	.812	.289	3730364.	.2054	10.72	
63108	N	US	10.0	5.0	.881	.303	3797137.	.0244	1.34	63109
63112	N	US	10.0	5.0	.873	.301	3755339.	.0976	5.36	63113
63114	N	US	10.0	5.0	.876	.302	3748040.	.1946	10.72	63115
63122	N	US	12.0	8.0	.868	.300	3740346.	.1175	6.43	63123
63208	N	US	16.4	2.0	.789	.286	3674699.	.2081	10.72	63209
63213	N	US	17.0	2.0	.790	.286	3652598.	.0519	2.68	63214
63215	N	US	17.0	2.0	.780	.284	3610518.	.1867	9.60	63216
63220	N	US	15.0	2.0	.833	.294	3728964.	.0503	2.68	63221
63302	N	US	11.1	2.0	.866	.300	3768588.	.0493	2.68	63303
63304	N	US	11.1	2.0	.876	.302	3790896.	.1955	10.72	63305
63312	N	US	2.5	10.0	.874	.302	3763317.	.0098	.54	63313
63314	N	US	2.5	10.0	.877	.302	3741348.	.0243	1.34	63315
63318	N	US	2.5	10.0	.879	.303	3756218.	.0485	2.68	63319

TABLE 11.- Continued.

(g) Concluded.

A FRAME	TRIP	TYPE	A0	A1	G	M	RE	K	FREQ	B FRAME
63320	N	US	2.5	10.0	.878	.303	3739575.	.0969	5.36	63321
63323	N	US	2.7	10.0	.880	.303	3746774.	.0969	5.36	63400
64019	Y	US	15.0	10.0	.844	.296	3865490.	.0247	1.31	64020
64021	Y	US	15.0	10.0	.840	.295	3813567.	.0493	2.62	64022
64023	Y	US	15.0	10.0	.821	.292	3752005.	.0997	5.24	64100
64107	Y	US	15.0	10.0	.340	.185	2448919.	.0496	1.65	64108
64109	Y	US	15.0	10.0	.340	.184	2439010.	.0991	3.30	64110
64111	Y	US	15.0	10.0	.341	.185	2439626.	.1481	4.95	64112
64119	Y	US	2.5	10.0	.876	.302	3823417.	.0099	.54	64120
64121	Y	US	2.5	10.0	.875	.302	3785031.	.0244	1.34	64122
64202	Y	US	2.5	10.0	.879	.303	3794515.	.0487	2.68	64203
64204	Y	US	2.5	10.0	.878	.302	3774318.	.0974	5.36	64205
64212	Y	US	-2.0	10.0	.877	.302	3717936.	.0098	.54	
64213	Y	US	-2.0	10.0	.878	.303	3695424.	.0241	1.34	
64214	Y	US	-2.0	10.0	.878	.302	3685179.	.0482	2.68	
64215	Y	US	-2.0	10.0	.880	.303	3683703.	.0963	5.36	
65121	N	US	-2.0	10.0	.869	.300	3717371.	.0098	.54	
65122	N	US	-2.0	10.0	.873	.301	3700235.	.0243	1.34	
65123	N	US	-2.0	10.0	.874	.301	3694893.	.0485	2.68	
65200	N	US	-2.0	10.0	.877	.302	3694943.	.0968	5.36	
65207	N	US	15.0	10.0	.395	.199	2646668.	.0997	3.57	
65209	N	US	15.0	10.0	.828	.292	3779170.	.1019	5.36	
65223	N	US	7.0	5.0	.121	.109	1475396.	.0249	.49	
65300	N	US	7.0	5.0	.121	.109	1472656.	.1996	3.92	
65311	N	US	7.0	5.0	.879	.301	3862901.	.1969	10.72	
65309	N	US	7.0	5.0	.876	.301	3889117.	.0100	.54	
63222	N	US	15.0	2.0	.818	.291	3675798.	.2028	10.72	63223

TABLE 11.- Continued.

(h) NLR-7301.

A FRAME	TRIP	TYPE	AO	A1	Q	M	RE	K	FREQ	B FRAME
66019	N	ST	-5.0	0.0	.872	.300	4003817.	0.0000	0.00	66020
66021	N	ST	-2.0	0.0	.876	.300	3999020.	0.0000	0.00	
66022	N	ST	0.0	0.0	.874	.301	3992026.	0.0000	0.00	66023
66100	N	ST	2.0	0.0	.883	.302	3999963.	0.0000	0.00	
66101	N	ST	5.0	0.0	.881	.301	3987844.	0.0000	0.00	66103
66109	N	ST	8.0	0.0	.877	.300	3982368.	0.0000	0.00	
66110	N	ST	10.0	0.0	.876	.300	3968075.	0.0000	0.00	66111
66112	N	ST	12.0	0.0	.867	.299	3933468.	0.0000	0.00	66113
66114	N	ST	14.0	0.0	.772	.281	3704260.	0.0000	0.00	66115
66116	N	ST	16.0	0.0	.717	.270	3564317.	0.0000	0.00	66117
66118	N	ST	17.6	0.0	.701	.267	3518002.	0.0000	0.00	66119
66120	N	ST	18.3	0.0	.733	.274	3568933.	0.0000	0.00	66121
66122	N	ST	20.0	0.0	.737	.274	3591274.	0.0000	0.00	66123
66200	N	ST	17.0	0.0	.702	.267	3499749.	0.0000	0.00	
66201	N	ST	16.0	0.0	.709	.269	3515184.	0.0000	0.00	
66208	N	ST	5.0	0.0	.877	.300	3932765.	0.0000	0.00	
66209	N	ST	0.0	0.0	.875	.300.	3922572.	0.0000	0.00	
66214	N	ST	-5.0	0.0	.609	.248	3230711.	0.0000	0.00	
66215	N	ST	0.0	0.0	.609	.248	3274639.	0.0000	0.00	
66216	N	ST	5 0	0.0	.608	.248	3269675.	0.0000	0.00	
66221	N	ST	8.0	0.0	.608	.248	3271957.	0.0000	0.00	
66222	N	ST	10.0	0.0	.610	.248	3269436.	0.0000	0.00	
66223	N	ST	12.0	0.0	.606	.247	3251575.	0.0000	0.00	
66300	N	ST	14.0	0.0	.607	.248	3245841.	0.0000	0.00	
66301	N	ST	16.0	0.0	.608	.247	3236014.	0.0000	0.00	
66302	N	ST	17.2	0.0	.610	.248	3235988.	0.0000	0.00	
66303	N	ST	20.0	0.0	.612	.249	3234835.	0.0000	0.00	
66304	N	ST	25.0	0.0	.602	.247	3196460.	0.0000	0.00	
66305	N	ST	17.0	0.0	.608	.248	3218130.	0.0000	0.00	
66306	N	ST	15.0	0.0	.612	.249	3223516.	0.0000	0.00	
66307	N	ST	14.0	0.0	.612	.249	3229433.	0.0000	0.00	
66308	N	ST	12.0	0.0	.610	.248	3226538.	0.0000	0.00	
66313	N	ST	5.0	0.0	.608	.248	3256298.	0.0000	0.00	
66314	N	ST	0.0	0.0	.606	.247	3249961.	0.0000	0.00	
66320	N	ST	-5.0	0.0	.340	.184	2469188.	0.0000	0.00	
66321	N	ST	0.0	0.0	.339	.183	2461096.	0.0000	0.00	66322
66323	N	ST	5.0	0.0	.341	.184	2463521.	0.0000	0.00	66400
66405	N	ST	8.0	0.0	.339	.183	2464083.	0.0000	0.00	
66406	N	ST	10.0	0.0	.339	.183	2457696.	0.0000	0.00	66407
66408	N	ST	12.0	0.0	.340	.184	2459029.	0.0000	0.00	66409
66410	N	ST	14.0	0.0	.340	.184	2457291.	0.0000	0.00	66411
66412	N	ST	16.0	0.0	.339	.183	2452670.	0.0000	0.00	66413
66414	N	ST	17.4	0.0	.341	.184	2455643.	0.0000	0.00	66415
66421	N	ST	20.0	0.0	.339	.183	2455801.	0.0000	0.00	66422
66423	N	ST	25.0	0.0	.338	.183	2447905.	0.0000	0.00	66500
66500	N	ST	17.0	0.0	.339	.183	2450544.	0.0000	0.00	
66501	N	ST	15.0	0.0	.339	.183	2452240.	0.0000	0.00	
66502	N	ST	14.0	0.0	.337	.183	2448905.	0.0000	0.00	
66503	N	ST	13.0	0.0	.338	.183	2449911.	0.0000	0.00	
66504	N	ST	12.0	0.0	.339	.183	2451875.	0.0000	0.00	
66510	N	ST	5.0	0.0	.338	.183	2553873.	0.0000	0.00	
66511	N	ST	0.0	0.0	.339	.183	2555680.	0.0000	0.00	
66516	N	ST	-5.0	0.0	.121	.108	1534072.	0.0000	0.00	
66517	N	ST	0.0	0.0	.122	.109	1535757.	0.0000	0.00	
66518	N	ST	5.0	0.0	.121	.109	1534265.	0.0000	0.00	
66600	N	ST	10.0	0.0	.122	.109	1527646.	0.0000	0.00	
66601	N	ST	12.0	0.0	.120	.109	1519094.	0.0000	0.00	
66602	N	ST	14.0	0.0	.120	.109	1516730.	0.0000	0.00	
66603	N	ST	16.0	0.0	.121	.108	1516123.	0.0000	0.00	
66604	N	ST	16.5	0.0	.121	.109	1517915.	0.0000	0.00	
66605	N	ST	20.0	0.0	.122	.109	1517157.	0.0000	0.00	
66606	N	ST	25.0	0.0	.122	.109	1520439.	0.0000	0.00	
66607	N	ST	17.0	0.0	.122	.109	1519469.	0.0000	0.00	
66608	N	ST	15.0	0.0	.121	.108	1513500.	0.0000	0.00	
66609	N	ST	13.0	0.0	.121	.109	1513362.	0.0000	0.00	
66610	N	ST	12.0	0.0	.122	.109	1519732.	0.0000	0.00	
66611	N	ST	11.5	0.0	.122	.109	1517895.	0.0000	0.00	
66616	N	ST	5.0	0.0	.121	.109	1516191.	0.0000	0.00	
66617	N	ST	0.0	0.0	.124	.110	1528781.	0.0000	0.00	
66623	Y	ST	0.0	0.0	.337	.183	2468560.	0.0000	0.00	66700
66701	Y	ST	5.0	0.0	.338	.183	2463488.	0.0000	0.00	66702
66703	Y	ST	10.0	0.0	.338	.182	2456240.	0.0000	0.00	66704
66705	Y	ST	12.0	0.0	.338	.182	2456043.	0.0000	0.00	66706
66707	Y	ST	14.7	0.0	.338	.182	2454470.	0.0000	0.00	66708
66709	Y	ST	15.5	0.0	.343	.184	2472156.	0.0000	0.00	66710
66711	Y	ST	17.0	0.0	.337	.133	2459276.	0.0000	0.00	66712
66716	Y	ST	18.0	0.0	.338	.183	2456445.	0.0000	0.00	66717
66718	Y	ST	20.0	0.0	.338	.183	2453475.	0.0000	0.00	66719
66720	Y	ST	25.0	0.0	.337	.183	2446074.	0.0000	0.00	66721
66722	Y	ST	17.0	0.0	.343	.184	2464989.	0.0000	0.00	66723
66800	Y	ST	14.7	0.0	.339	.183	2452952.	0.0000	0.00	66801
66802	Y	ST	0.0	0.0	.341	.184	2459672.	0.0000	0.00	66803
66810	Y	ST	0.0	0.0	.871	.299	3970550.	0.0000	0.00	66811
66812	Y	ST	5.0	0.0	.873	.300	3962919.	0.0000	0.00	66813
66814	Y	ST	8.0	0.0	.875	.300	3952795.	0.0000	0.00	66815
66818	Y	ST	12.0	0.0	.845	.294	3862413.	0.0000	0.00	66819
66820	Y	ST	13.0	0.0	.820	.290	3795900.	0.0000	0.00	66821
66822	Y	ST	0.0	0.0	.874	.300	3915017.	0.0000	0.00	
67019	Y	US	15.0	10.0	.339	.183	2438650.	.0250	.83	67020
67021	Y	US	15.0	10.0	.340	.184	2433341.	.0992	3.30	67022
67023	Y	US	15.0	10.0	.340	.183	2428420.	.1985	6.60	67100
67108	Y	US	10.0	5.0	.880	.301	3808875.	.0245	1.34	67109
67110	Y	US	10.0	5.0	.862	.298	3754299.	.0494	2.68	67111
67112	Y	US	10.0	5.0	.860	.298	3743871.	.0988	5.36	67113
67120	N	US	15.0	10.0	.122	.110	1481685.	.0991	1.96	67121
67201	N	US	10.0	10.0	.122	.110	1463308.	.0992	1.96	67202
67208	N	US	10.0	10.0	.341	.184	2461921.	.0250	.83	67209
67210	N	US	10.0	10.0	.343	.185	2458942.	.0990	3.30	67211
67212	N	US	10.0	10.0	.341	.184	2452737.	.1983	6.60	67213
67218	N	US	15.0	10.0	.341	.184	2458480.	.0250	.83	67219
67220	N	US	15.0	10.0	.342	.184	2454782.	.0991	3.30	67221
67222	N	US	15.0	10.0	.342	.184	2453910.	.1981	6.60	67223
67305	N	US	15.0	10.0	.609	.248	3254400.	.0995	4.46	67306
67310	N	US	10.0	10.0	.613	.250	3264300.	.0991	4.46	67311
68019	N	US	15.0	5.0	.803	.287	3792076.	.0105	.54	68020
68100	N	US	15.0	5.0	.806	.288	3774246.	.0259	1.34	68101
68102	N	US	15.0	5.0	.796	.286	3726319.	.0521	2.68	68103
68104	N	US	15.0	5.0	.803	.287	3729996.	.1037	5.36	68105
68109	N	US	15.0	5.0	.822	.291	3787615.	.1537	8.04	68110
68111	N	US	15.0	5.0	.833	.293	3793358.	.2031	10.72	68112
68119	N	US	10.0	5.0	.853	.297	3813741.	.0101	.54	68120
68121	N	US	10.0	5.0	.860	.298	3792628.	.0248	1.34	68122
68123	N	US	10.0	5.0	.863	.299	3791082.	.0495	2.68	68200
68201	N	US	10.0	5.0	.872	.300	3805465.	.0985	5.36	68202
68203	N	US	10.0	5.0	.882	.302	3824398.	.1956	10.72	68204
68211	N	US	5.0	5.0	.869	.299	3842765.	.1981	10.72	68212
68219	N	US	12.0	2.0	.843	.295	3766519.	.0502	2.68	68220
68221	N	US	12.0	2.0	.834	.293	3725832.	.1007	5.36	68303
68304	N	US	12.0	2.0	.835	.293	3722222.	.2012	10.72	68305
69019	N	US	10.0	10.0	.871	.299	3949663.	.0101	.54	69020

TABLE 11.- Concluded.

(h) Concluded.

A FRAME	TRIP	TYPE	AO	A1	Q	M	RE	K	FREQ	B FRAME
69100	N	US	10.0	10.0	.873	.300	3918788.	.0249	1.34	69101
69102	N	US	10.0	10.0	.876	.300	3900063.	.0496	2.68	69103
69105	N	US	10.0	10.0	.877	.301	3904003.	.0991	5.36	69106
69107	N	US	10.0	10.0	.876	.300	3884160.	.1484	8.04	69108
69119	N	US	16.8	2.0	.727	.273	3492462.	.0270	1.34	69120
69121	N	US	16.8	2.0	.710	.270	3430737.	.0546	2.68	69122
69123	N	US	16.8	2.0	.700	.268	3396634.	.1100	5.36	69200
69201	N	US	16.8	2.0	.692	.267	3366783.	.2208	10.72	69202
69206	N	US	17.2	2.0	.734	.275	3460551.	.0268	1.34	69207
69208	N	US	17.2	2.0	.745	.277	3469110.	.0530	2.68	69209
69211	N	US	17.2	2.0	.709	.270	3370669.	.1086	5.36	69212
69213	N	US	17.2	2.0	.719	.272	3387722.	.1616	8.04	69214
69215	N	US	17.2	2.0	.755	.279	3459727.	.2098	10.72	69216
69221	N	US	17.5	2.0	.726	.273	3404711.	.0536	2.68	69222
69223	N	US	17.5	2.0	.694	.265	3286912.	.2205	10.72	69300
69304	N	US	18.5	2.0	.688	.266	3285767.	.0549	2.68	69305
69310	N	US	16.5	2.0	.671	.252	3218013.	.0554	2.68	69311
70019	N	US	9.4	10.0	.341	.185	2344007.	.0245	.83	70020
70021	N	US	9.4	10.0	.340	.185	2338519.	.0973	3.30	70022
70023	N	US	9.4	10.0	.340	.185	2336677.	.1948	6.60	70100
70107	N	US	5.7	10.0	.875	.301	3916444.	.0104	.56	70108
70109	N	US	5.7	10.0	.876	.301	3876178.	.0247	1.34	70110
70113	N	US	5.7	10.0	.872	.300	3861569.	.0495	2.68	70114
70115	N	US	5.7	10.0	.875	.301	3854654.	.0936	5.36	70116
70117	N	US	5.7	10.0	.874	.301	3843662.	.1479	8.04	70118

TABLE 12.- LIST OF STATIC DATA

Airfoil[a]	M_∞	First frame	Last frame	No. of frames	α_{min}	α_{max}	Figure	Airfoil[a]	M_∞	First frame	Last frame	No. of frames	α_{min}	α_{max}	Figure
N-0012	0.30	04019	04412	24	-5.0	20.0		FX-098T	0.30	17208	17314	8	0.0	20.0	
	.30	11018	11309	33	-5.0	30.0	9,12,16	FX-098T	.18	18019	18206	10	0.0	20.0	
	.30	12102	(quasi-steady)		-5.0	15.0	16	SC-1095	.30	35021	35214	17	-5.0	16.0	19
	.28	12109			-4.0	16.0		SC-1095	.25	35220	35401	20	-5.0	25.0	
	.28	13222			10.1	29.9		SC-1095	.18	36019	36120	10	-5.0	20.0	
	.27	12020			10.1	29.9		SC-1095	.11	36202	36218	11	-5.0	20.0	
	.26	12118			10.1	29.9		SC-1095T	.30	34022	34115	8	0.0	16.0	
	.25	12208			-3.0	17.0		SC-1095T	.18	34200	34214	7	0.0	16.0	
	.25	13303			-3.0	17.0		HH-02	.30	40222	41103	20	-5.0	20.0	20
	.23	12203			10.1	29.9		HH-02	.25	41110	41215	20	-5.0	20.0	
	.22	13308			-3.0	17.0		HH-02	.18	40114	40215	10	-5.0	20.0	
	.22	13310			-3.0	17.0		HH-02	.11	40018	40108	11	-5.0	20.0	
	.20	12300			10.1	29.9		HH-02T	.30	41221	41314	8	0.0	16.0	
	.18	12310			-3.0	17.0		HH-02T	.18	41401	41419	10	0.0	16.0	
	.17	12305			10.1	29.9		VR-7	.30	46418	46615	18	-5.0	25.0	11,21
	.11	13021			-3.0	17.0		VR-7	.25	46307	46412	19	-5.0	25.0	
	.11	13107			10.1	29.9		VR-7	.18	46116	46301	13	-5.0	25.0	
	.07	13120			-3.0	17.0		VR-7	.11	46018	46110	13	-5.0	25.0	
	.07	13115			10.1	29.9		VR-7T	.30	46802	46823	10	0.0	20.0	
	.04	13205			-5.0	15.0		VR-7T	.18	46621	46718	10	0.0	20.0	
	.04	13217			10.1	29.9		NLR-1	.30	61407	61606	19	-5.0	25.0	22
N-0012T	.29	13321			-3.0	17.0		NLR-1	.25	61221	61401	19	-5.0	25.0	
N-0012T	.18	13313			-3.0	17.0		NLR-1	.18	61114	61215	10	-5.0	20.0	
Ames-01	.30	26020	26307	23	-5.0	25.0	17	NLR-1	.11	61018	61108	11	-5.0	20.0	
Ames-01	.25	26313	27117	22	-5.0	25.0		NLR-1T	.30	65019	65115	13	-11.0	16.0	
Ames-01	.18	27123	27318	22	-5.0	25.0		NLR-1T	.18	64221	64311	8	0.0	16.0	
Ames-01	.11	27400	28120	21	-5.0	25.0		NLR-7301	.30	66019	66209	17	-5.0	20.0	23
Ames-01T	.30	28312	28410	9	0.0	16.0		NLR-7301	.25	66214	66314	17	-5.0	25.0	
Ames-01T	.19	28207	28304	10	0.0	20.0		NLR-7301	.18	66320	66511	18	-5.0	25.0	
FX-098	.30	20118	20322	21	-5.0	25.0	18	NLR-7301	.11	66516	66617	17	-5.0	25.0	
FX-098	.25	19314	20112	22	-5.0	25.0		NLR-7301T	.30	66810	66822	6	0.0	13.0	
FX-098	.18	19020	19308	23	-5.0	25.0		NLR-7301T	.18	66623	66802	13	0.0	25.0	
FX-098	.11	18215	18502	23	-5.0	25.0	10								

[a] T = trip.

TABLE 13.- MACH NUMBER SWEEP AT $\alpha = 15° + 10° \sin \omega t$, k = 0.10

M_∞[a]	NACA 0012	A-01	FX-098	SC-1095	HH-02	VR-7	NLR-1	NLR-7301
0.035	8102		16019			58102		
.07	8114	24323	16105	33022	42121	47123	62020	
.11	8214	24314	16114	33106	42321	47206 58111	62104	67120
.18	8220	24217 31209	16200	33110	42302	47213 58121	62112	67220
.18T	14021 14106	29117	17103	34321	42110	47112	64109	67021
.20							62114 65207	
.22	9202	24209	16300	33205	42309	47217	62208	
.25	9203	24201	16308	33207	42313	47301	62210	67305
.28	9208	24117	22208	33215	42218	47305	62218	
.29	9217 14220	24105	22201	33300	42210	45023	62307 65209	
.29T	14208 14210	29106	17200	34308	42100	47100	64023	

[a]T = trip.

TABLE 14.- FREQUENCY SWEEP AT $M_\infty = 0.29$, $\alpha = 15° + 10° \sin \omega t$

k[a]	NACA 0012	A-01	FX-098	SC-1095	HH-02	VR-7	NLR-1	NLR-7301
0.01	9210	30019 30020	21100	38300				
.025	9213 14218	24022	22023	33217	42206	45019	62302	
.025T	14117 14200	29023	17117		42019	47020	64019	
.05	9214 14219	24100	22103	33222	42208	45021	62304	
.05T	14119 14202	29101	17119	34306	42021	47022	64021	
.10	9217 14220	24105	22201	33300	42210	45023	62307 65209	
.10T	14208 14210	29106	17200	34308	42100	47100	64023	
.15	9218	24109	22206	34409	42212 42217	45101	62309	

[a]T = trip.

TABLE 15.- FREQUENCY SWEEP AT $M_\infty = 0.30$, $\alpha = 10° + 10° \sin \omega t$

k	NACA 0012	A-01	FX-098	SC-1095	HH-02	VR-7	NLR-1	NLR-7301
0.01	9221	30105	21107	38306	43019	45109	62317	69019
.025	9222	25022 31102	22216	37023	43106	45111	62320	69100
.05	9223	25102 31104	22217	37101	43108	45113	62322	69102
.10	9302	25104	22218	37107	43112	45117	62400	69105
.12							62403	
.15	9307	25109 31110 31112	22219	37109	43114 43117	45119	62405	69107

TABLE 16.- FREQUENCY SWEEP AT $M_\infty = 0.30$, $\alpha = 15° + 5° \sin \omega t$

k	NACA 0012	A-01	FX-098	SC-1095	HH-02	VR-7	NLR-1	NLR-7301
0.01	10113	30110	21112	39104		45203	63018	68019
.025	10114	25204	23021	38021	43303	45205	63019	68100
.05	10117	25205	23022	38022	43304	45207	63020	68102
.10	10118	25208	23023	38102	43305	45209	63021	68104
.12							63100	
.15	10120	25209	23100	38103	43308	45211	63101	68109
.20	10123	25210	23101	38104	43309	45213	63102	68111

TABLE 17.- FREQUENCY SWEEP AT $M_\infty = 0.30$, $\alpha = 10° + 5° \sin \omega t$

k	NACA 0012	A-01	FX-098	SC-1095	HH-02	VR-7	NLR-1	NLR-7301	NLR-7301T
0.01	10202	30119	21200	39107	44019			68119	
.025	7112 10203	25117	22307	37207	44021 44119	45221	63108	68121	67108
.05	7222 10204	25118	22308	37208	44023	45223		68123	67110
.075	10207								
.10	7113 10208	25119	22309	37210	44104 44118	45300	63112	68201	67112
.15	7300 10211	25121 25122	22311	37213	44106	45302			
.20	7114 10212	25123	22312	37215	44112 44120	45303	63114	68203	

TABLE 18.- STALL ONSET AT $M_\infty = 0.30$, $\alpha = \alpha_o + 10° \sin \omega t$, $k = 0.10$

NACA 0012, $\alpha_o = 3.8°$	A-01, $\alpha_o = 5.5°$	FX-098, $\alpha_o = 3.8°$	SC-1095, $\alpha_o = 4.4°$	HH-02, $\alpha_o = 4.0°$	VR-7, $\alpha_o = 4.6°$	NLR-1, $\alpha_o = 2.7°$	NLR-7301, $\alpha_o = 5.7°$
10305	25319	23201	34418	43219		63323	70115

TABLE 19.- STALL SUPPRESSION AT $M_\infty = 0.30$, $\alpha = \alpha_o + 10° \sin \omega t$

k	NACA 0012	A-01, $\alpha_o = 5.0°$	FX-098, $\alpha_o = 3.3°$	SC-1095, $\alpha_o = 4.1°$	HH-02, $\alpha_o = 3.8°$	VR-7, $\alpha_o = 4.1°$	NLR-1,[a] $\alpha_o = 2.5°$	NLR-7301, $\alpha_o = 5.7°$
0.01		29205	21208	39021	43215	48019	63312	70107
.025		31119			43202	48023	63314	70109
.05		{29207, 31121}	23206	37119	43204	48101	63318	70113
.10		{25311, 29211, 31123}	23208	37121	43206	48103	63320	70115
.15		{29213, 29215, 31201}	23211	37123	43209			70117

[a]See table 24.

TABLE 20.- STALL SUPPRESSION AT $M_\infty = 0.18$, $\alpha = \alpha_o + 10° \sin \omega t$

k	NACA 0012, $\alpha_o = 8.0°$	A-01, $\alpha_o = 7.5°$	FX-098, $\alpha_o = 6.5°$	SC-1095, $\alpha_o = 6.2°$	HH-02	VR-7, $\alpha_o = 4.7°$	NLR-1	NLR-7301, $\alpha_o = 9.4°$
0.01	9110	30215	21219			50116		
.025						49216		70019
.05	9112	{24302, 31215}	16213	33118				
.10						49300		70021
.20	9118	{24306, 31217}	16215	33121		49307		70023
.25						49310		

TABLE 21.- PITCH DAMPING STUDIES AT $M_\infty = 0.30$, $\alpha = \alpha_o + 2° \sin \omega t$

NACA 0012	A-01	FX-098	SC-1095	HH-02	VR-7	NLR-1	NLR-7301[a]
k = 0.01							
	$\alpha_o = 14.0°$ 30206		$\alpha_o = 14.0°$ 39115	$\alpha_o = 12.5°$ 44221	$\alpha_o = 12.5°$ 48300		
				$\alpha_o = 15.5°$ 44212			
k = 0.025							
				$\alpha_o = 12.5°$ 44222	$\alpha_o = 12.5°$ 48301		$\alpha_o = 16.8°$ 69119
				$\alpha_o = 15.5°$ 44214	$\alpha_o = 13.0°$ 48116		$\alpha_o = 17.2°$ 69206
k = 0.05							
				$\alpha_o = 12.5°$ 44223	$\alpha_o = 12.5°$ 48302	$\alpha_o = 11.1°$ 63302	$\alpha_o = 16.5°$ 69310
				$\alpha_o = 15.5°$ 44215	$\alpha_o = 13.0°$ 48118	$\alpha_o = 15.0°$ 63220	$\alpha_o = 16.8°$ 69121
					$\alpha_o = 14.0°$ 48215	$\alpha_o = 17.0°$ 63213	$\alpha_o = 17.2°$ 69208
							$\alpha_o = 17.5°$ 69221
							$\alpha_o = 18.5°$ 69304
k = 0.10							
				$\alpha_o = 12.5°$ 44300	$\alpha_o = 12.5°$ 48303		$\alpha_o = 16.8°$ 69123
				$\alpha_o = 14.0°$ 44202	$\alpha_o = 13.0°$ 48122		$\alpha_o = 17.2°$ 69211
				$\alpha_o = 15.5°$ 44216	$\alpha_o = 14.0°$ 48216		

Table 21.- Concluded.

NACA 0012	A-01	FX-098	SC-1095	HH-02	VR-7	NLR-1	NLR-7301[a]
				k = 0.15			
	$\alpha_o = 14.5°$ 31310			$\alpha_o = 12.5°$ 44303	$\alpha_o = 12.5°$ 48304		$\alpha_o = 17.2°$ 69213
				$\alpha_o = 15.5°$ 44217			
				k = 0.20			
	$\alpha_o = 13.5°$ 29223	$\alpha_o = 12.0°$ 23219	$\alpha_o = 12.3°$ 38201	$\alpha_o = 12.5°$ 44304	$\alpha_o = 12.5°$ 48308	$\alpha_o = 11.1°$ 63304	$\alpha_o = 16.8°$ 69201
	$\alpha_o = 14.5°$ 29304 31302	$\alpha_o = 14.0°$ 23305	$\alpha_o = 14.0°$ 38119	$\alpha_o = 14.0°$ 44204	$\alpha_o = 13.0°$ 48200	$\alpha_o = 15.0°$ 63222	$\alpha_o = 17.2°$ 69215
		$\alpha_o = 16.0°$ 23310	$\alpha_o = 16.0°$ 38110	$\alpha_o = 15.5°$ 42218	$\alpha_o = 14.0°$ 48217	$\alpha_o = 16.4°$ 63208	$\alpha_o = 17.5°$ 69223
	$\alpha_o = 16.5°$ 29309			$\alpha_o = 17.5°$ 44209	$\alpha_o = 16.0°$ 48209	$\alpha_o = 17.0°$ 63215	

[a]See table 24.

TABLE 22.- NO SEPARATION: $M_\infty = 0.30$, $\alpha = 5° + 5° \sin \omega t$

k	NACA 0012	A-01	FX-098	SC-1095	HH-02	VR-7	NLR-1[a]	NLR-7301[a]
0.01	10218							
.10	10221	25301	23107					
.20	10222	25303	23109					68211

[a]See table 24.

TABLE 23.- DYNAMIC BOUNDARY-LAYER TRIP DATA

M_∞	k	NACA 0012	A-01	FX-098	SC-1095	HH-02	VR-7	NLR-1	NLR-7301
0.18	0.05	14019 14104	29115	17100	34318	42108	47110	64107	67019
.18	.10	14021 14106	29117	17103	34321	42110	47112	64109	67021
.18	.15	14023 14108	29119	17109	34323	42113	47114	64111	
.18	.20								67023
.30	.025	14117 14200	29023	17117		42019	47020	64019[a]	(a)
.30	.05	14119 14202	29101	17119	34306	42021	47022	64021[a]	(a)
.30	.10	14208 14210	29106	17200	34308	42100	47100	64023[a]	(a)

[a]See table 24.

TABLE 24.- MISCELLANEOUS DYNAMIC DATA

Airfoil	Frame	M_∞	α_o	α_1	k	Remarks
N-0012	8019	0.035	10.0	10.0	0.10	Low Reynolds number, 0.5×10^6
	8021	.035	10.0	10.0	.15	
	8023	.035	10.0	10.0	.25	
	8104	.035	15.0	10.0	.15	
	8106	.035	15.0	14.0	.10	
	8116	.07	15.0	10.0	.15	Match reference 3
	8118	.07	15.0	10.0	.25	
	8123	.07	15.0	14.0	.10	Match reference 3
	8203	.07	10.0	10.0	.25	
	8210	.11	10.0	10.0	.25	
	8222	.18	15.0	10.0	.15	Match reference 3
	8306	.18	15.0	14.0	.10	Match reference 3
	9022	.18	15.0	6.0	.24	Match reference 3
	9101	.18	15.0	5.0	.29	
	9106	.18	10.0	10.0	.25	
	7108	.30	8.0	5.0	.025	Variable α_o
	7110		8.0		.10	
	7111		8.0		.20	
	7216		8.8		.05	
	7214		8.8		.10	
	7212		8.8		.15	
	7104		9.0		.025	
	7019		9.0		.05	
	7021		9.0		.10	
	7101		9.0		.15	
	7023		9.0		.20	
			10.0		See table 17	
	7117		11.0		.025	
	7118		11.0		.05	
	7119		11.0		.10	
	7120		11.0		.15	
	7121		11.0		.20	
	7200		12.0		.025	
	7202		12.0		.05	
	7205		12.0		.10	
	7305		12.0		.15	
	7207		12.0		.20	
			15.0		See table 16	
	10309		2.8	10.0	.10	
	10305		3.8			
	10303		5.0			
	9302		10.0			
	10022		12.0			
	9217	.29	15.0			
	14220	.29	15.0			
	10101	.27	20.0			
	10104	.30	12.0	8.0	.05	Match reference 17
	10105	.30	12.0	8.0	.10	Match reference 17
	10108	.30	12.0	8.0	.13	Match reference 17
	15218	.29	15.0	10.0	.10	Pressure orifices closed

TABLE 24.- Continued.

Airfoil	Frame	M_∞	α_o	α_1	k	Remarks
N-0012	Many	Variable	Variable	10.0	0.001	Quasi-static; see table 12
W-098	23117	0.30	5.0	10.0	.10	
Ames-01	30201		11.0	5.0	.01	
Ames-01	25214				.05	
Ames-01	25216				.10	
SC-1095	39110				.01	
	37219				.05	
	37221				.10	
	37304		12.0	8.0	.05	Match reference 18
	37305		12.0	8.0	.10	Match reference 18
	37306		12.0	8.0	.13	Match reference 18
HH-02	43314		11.0	5.0	.025	
HH-02	43315		11.0	5.0	.05	
HH-02	43316		11.0	5.0	.10	
VR-7	54019	.18	10.0	10.0	.025	
	54022		10.0		.05	
	54101		10.0		.10	
	54110		10.0		.15	
	54113		10.0		.20	
	54116		10.0		.25	
	49023		15.0		.01	
	49110				.025	
	49117				.05	
	49120				.10	
	58121				.10	
	49203				.15	
	54216				.15	
	57018				.15	
	58018				.15	
	58120				.15	
	49206				.20	
NLR-1	65223	.11	7.0	5.0	.025	No separation
	65300	.11	7.0	5.0	.20	No separation
	62114	.20	15.0	10.0	.10	
	65207	.20	15.0	10.0	.10	
	62121	.20	10.0	10.0	.17	Match reference 19
	62202	.20	15.0	5.0	.17	
	62201	.20	15.0	5.0	.28	
	62403	.30	10.0	10.0	.12	
	63100		15.0	5.0	.12	
	63122		12.0	8.0	.12	
	65309		7.0	5.0	.01	No separation
	65311		7.0	5.0	.20	No separation
	65121		-2.0	10.0	.01	Stall at negative α
	65122				.025	Stall at negative α
	65123				.05	Stall at negative α
	65200				.10	Stall at negative α
NLR-1T	64212				.01	Trip; stall at negative α
NLR-1T	64213				.025	Trip; stall at negative α
NLR-1T	64214				.05	Trip; stall at negative α

TABLE 24.- Concluded.

Airfoil	Frame	M_∞	α_o	α_1	k	Remarks
NLR-1T	64215	0.30	-2.0	10.0	0.10	Trip; stall at negative α
NLR-1T	64119	.30	2.5		.01	Trip; stall suppression
NLR-1T	64121	.30	2.5		.025	Trip; stall suppression
NLR-1T	64202	.30	2.5		.05	Trip; stall suppression
NLR-1T	64204	.30	2.5		.10	Trip; stall suppression
NLR-7	67201	.11	10.0		.10	
	67208	.18	10.0		.025	
	67210	.18	10.0		.10	
	67212	.18	10.0		.20	
	67218	.18	15.0		.025	
	67220	.18	15.0		.10	
	67222	.18	15.0		.20	
	67310	.25	10.0		.10	
	68219	.30	12.0	2.0	.05	No separation
	68221	.30	12.0	2.0	.10	No separation
	68304	.30	12.0	2.0	.20	No separation
NLR-7T	67108	.30	10.0	5.0	.025	Trip
NLR-7T	67110	.30	10.0	5.0	.05	Trip
NLR-7T	67112	.30	10.0	5.0	.10	Trip

TABLE 25.- TEST CASES FOR NUMERICAL ANALYSIS (ref. 1)

Case	Frame	Airfoil	α_0	α_1	k	Case	Frame	Airfoil	α_0	α_1	k
1	10222	NACA 0012	5	5	0.20	7	10212	NACA 0012	10	5	0.20
2	68211	NLR-7301	5			8	9302		10	10	.10
3	7111	NACA 0012	8			9	10113		15	5	.01
4	68203	NLR-7301	10				10114				.025
5	7023	NACA 0012	9				10117				.05
6	45221	VR-7	10		.025		10118				.10
	45223				.05		10120				.15
	45300				.10		10123				.20
	45302				.15	10	45203	VR-7			.01
	45303				.20		45205				.025
7	10202	NACA 0012			.01		45207				.05
	10203				.025		45209				.10
	10204				.05		45211				.15
	10208				.10		45213				.20
	10211				.15						

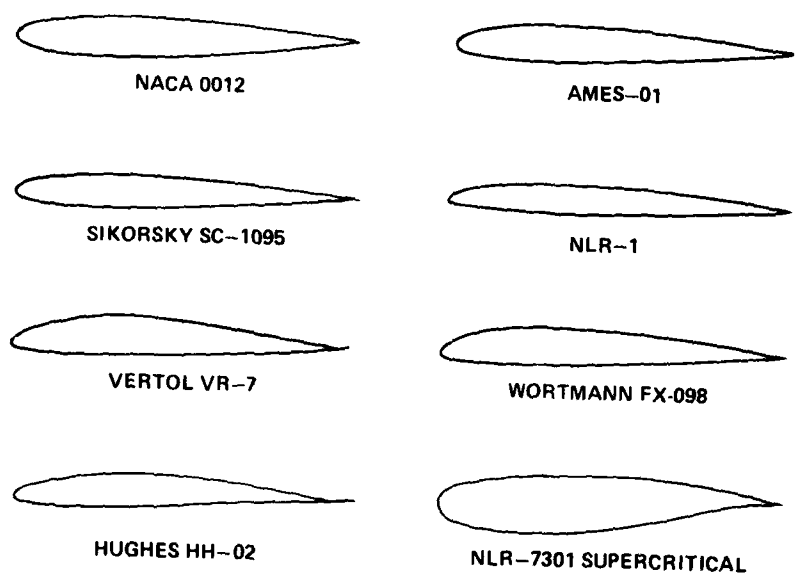

Figure 1.- Airfoils tested in the experiment.

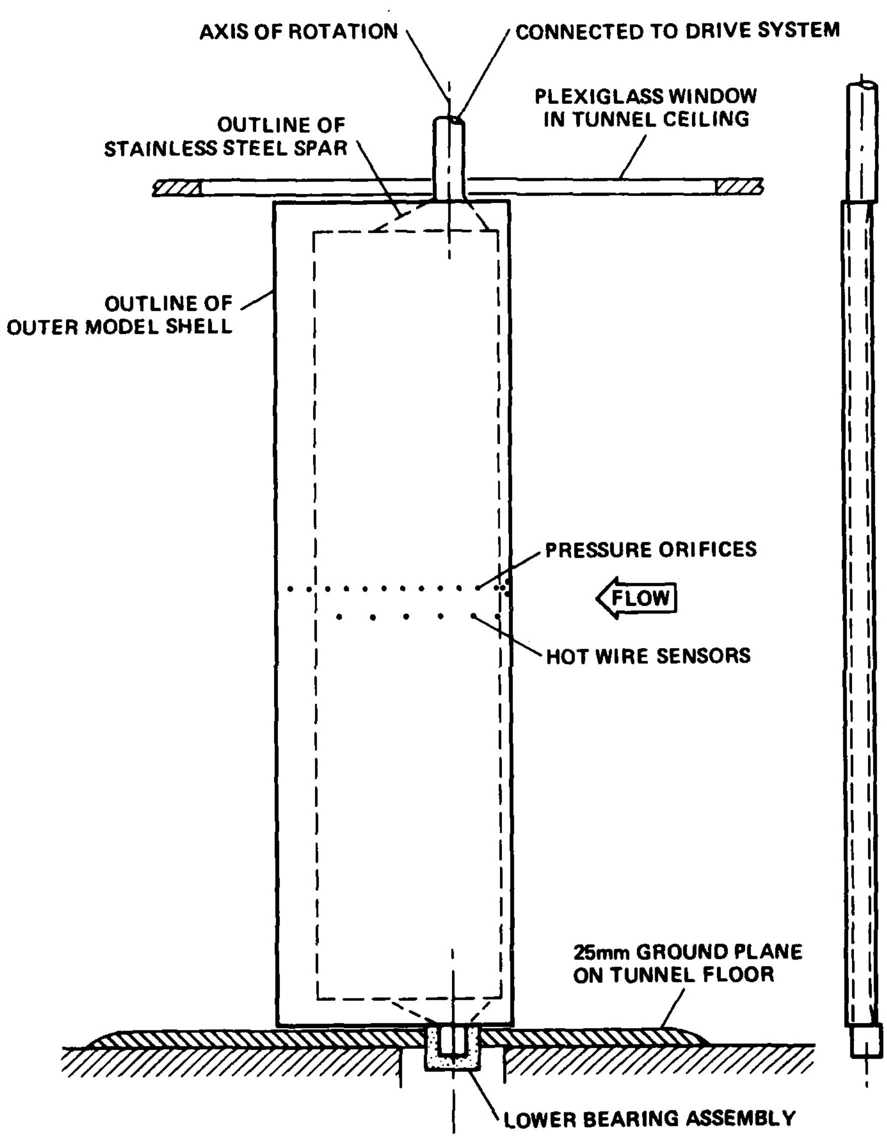

Figure 2.- Model installation in the test section.

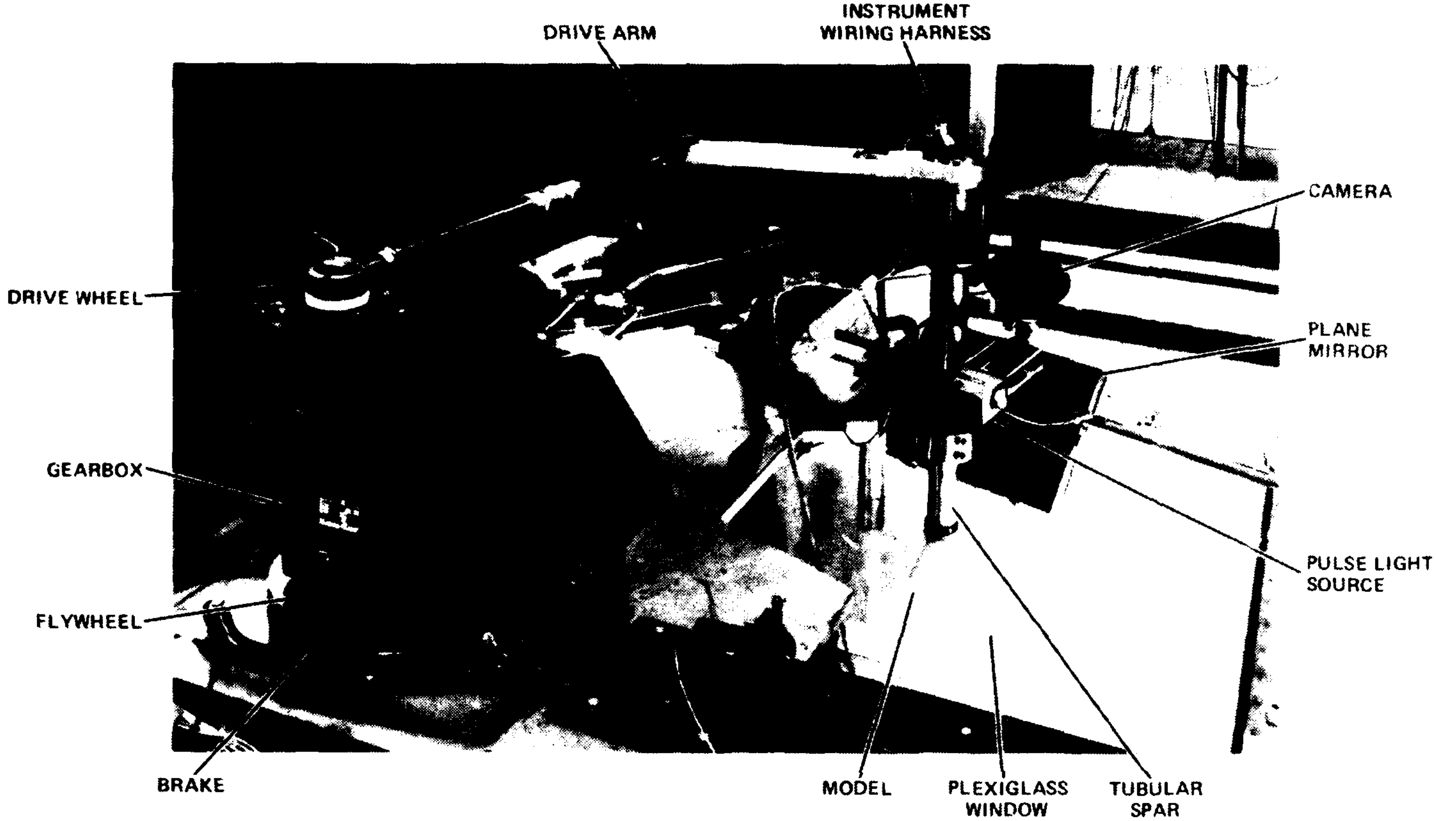

Figure 3.- Photograph of the oscillation mechanism.

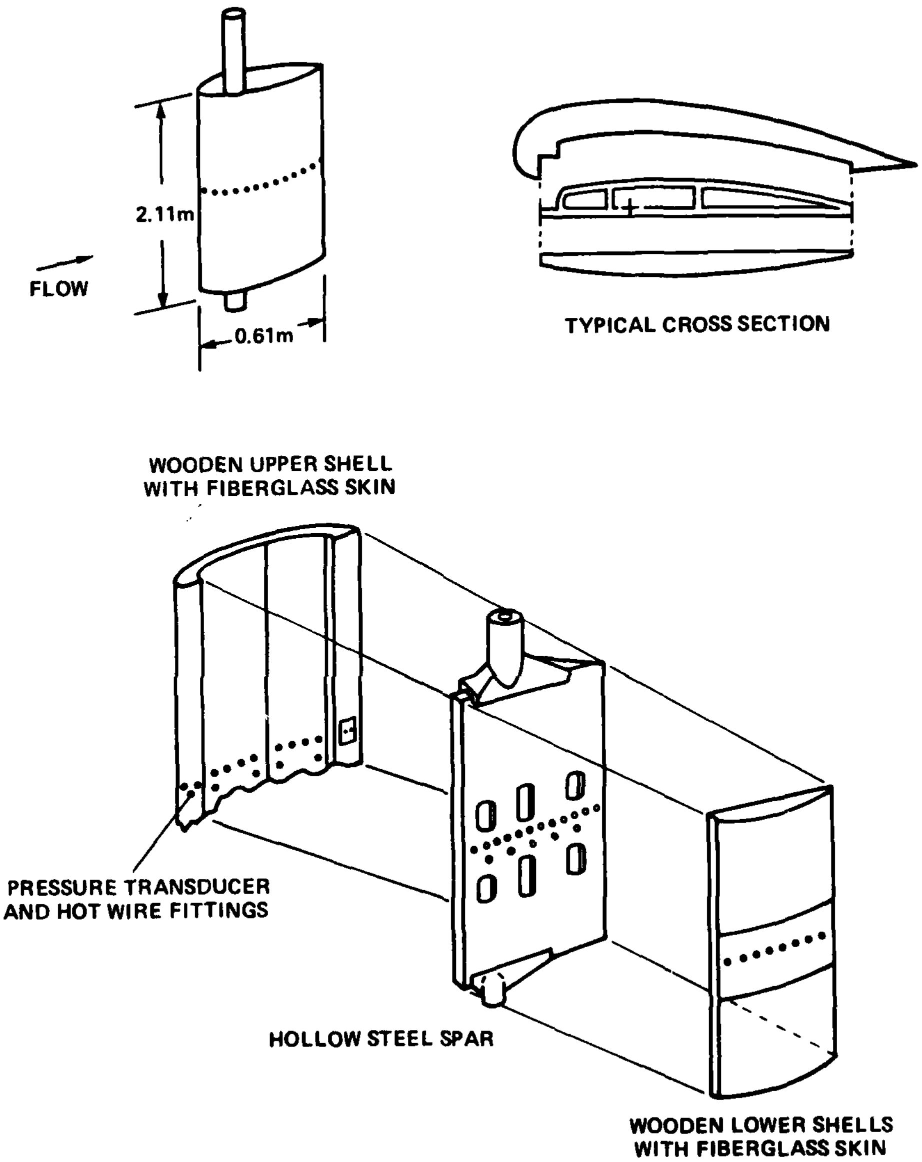

Figure 4.- Sketch of the wooden model shells surrounding the steel spar.

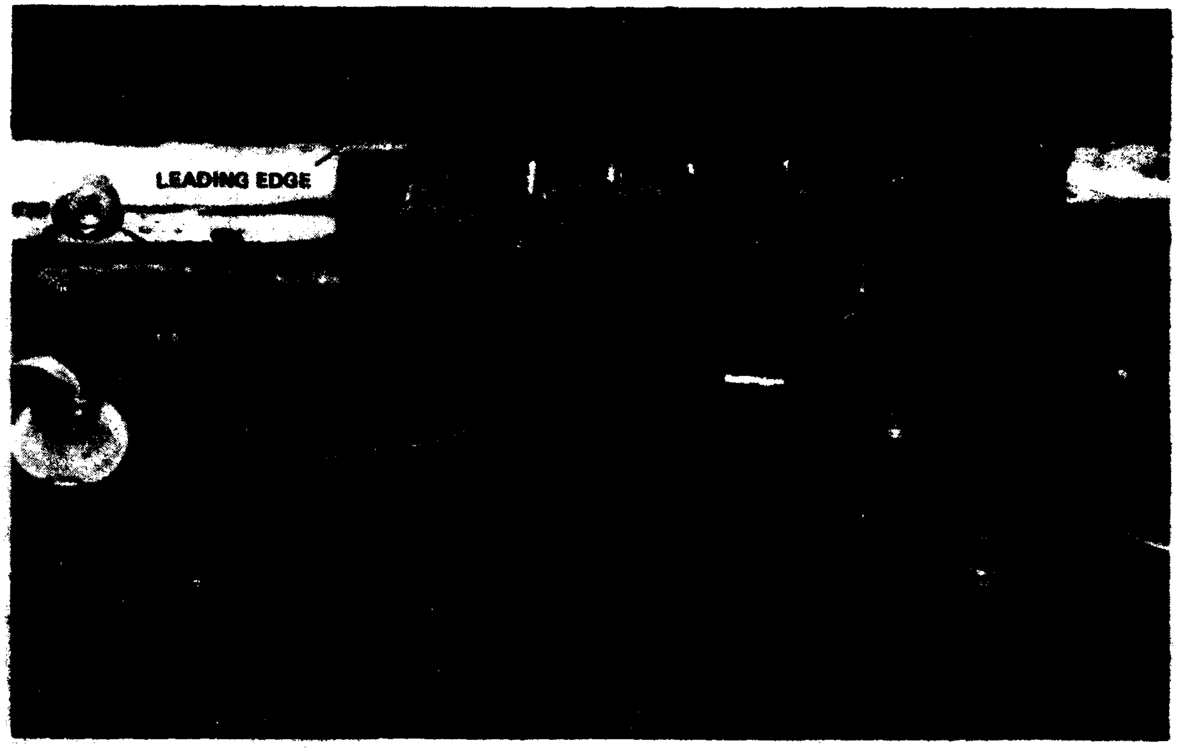

Figure 5.- Pressure transducer and hot-wire installation: view from inside the upper-surface shell.

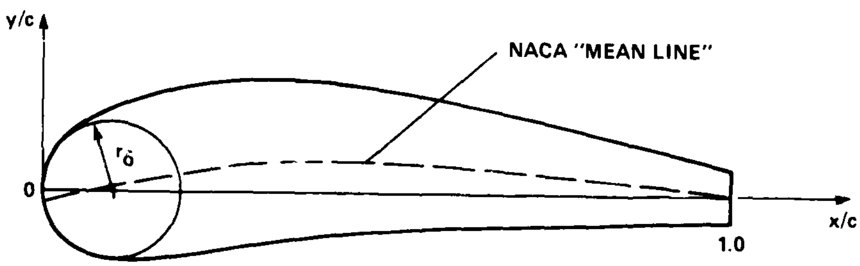

Figure 6.- Coordinate axes for the airfoils.

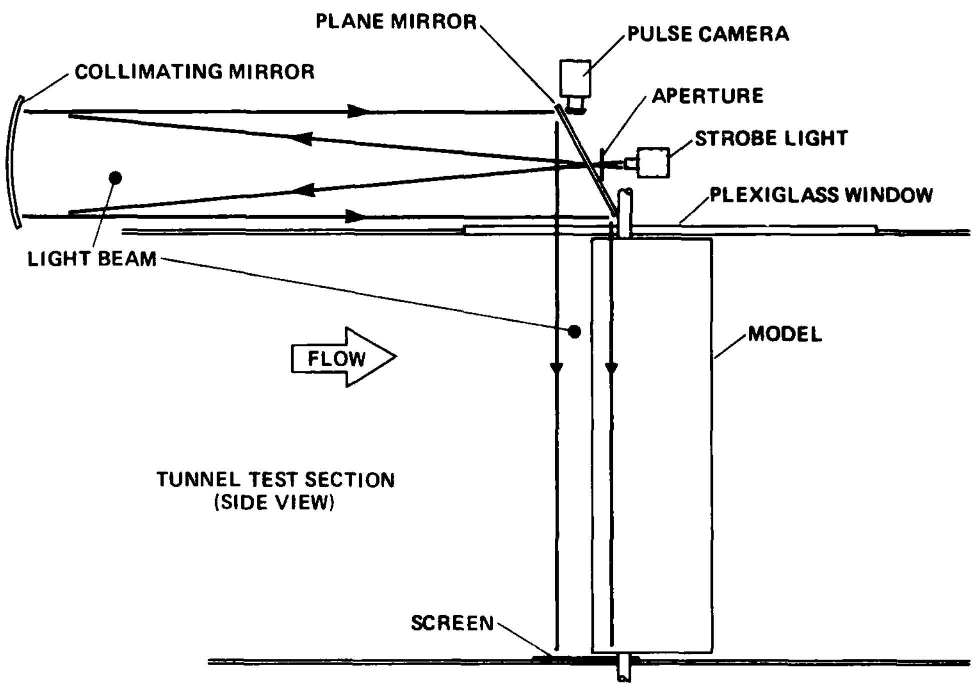

Figure 7.- Sketch of the shadowgraph system for visualizing the leading-edge region.

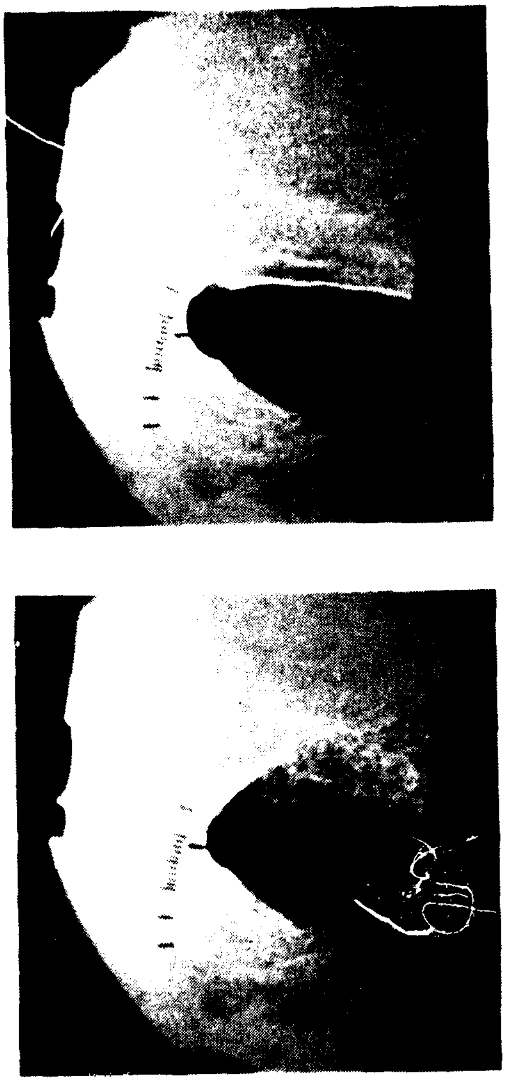

Figure 8.- Representative shadowgraphs before (upper) and during (lower) dynamic stall: Sikorsky SC-1095 airfoil, $M_\infty = 0.30$, $\alpha = 10° + 10° \sin \omega t$, $k = 0.10$.

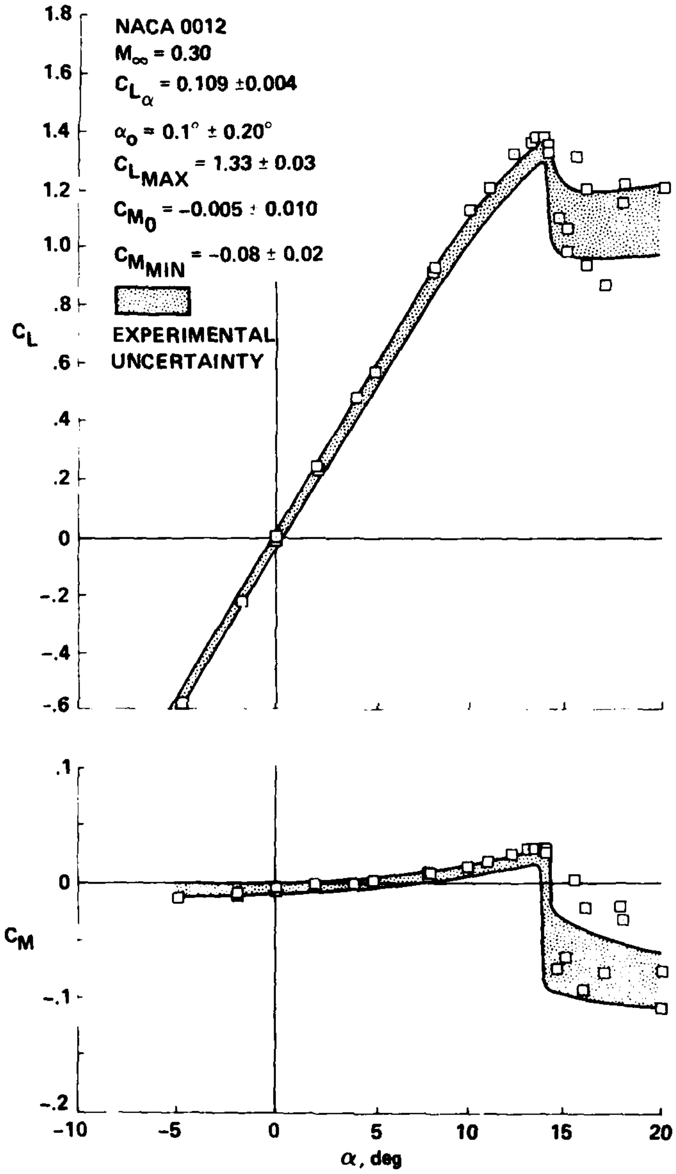

Figure 9.- Static lift and moment data on the NACA 0012 airfoil at $M_\infty = 0.3$; shaded bands represent uncertainty limits of data corrected for wind-tunnel-wall effects.

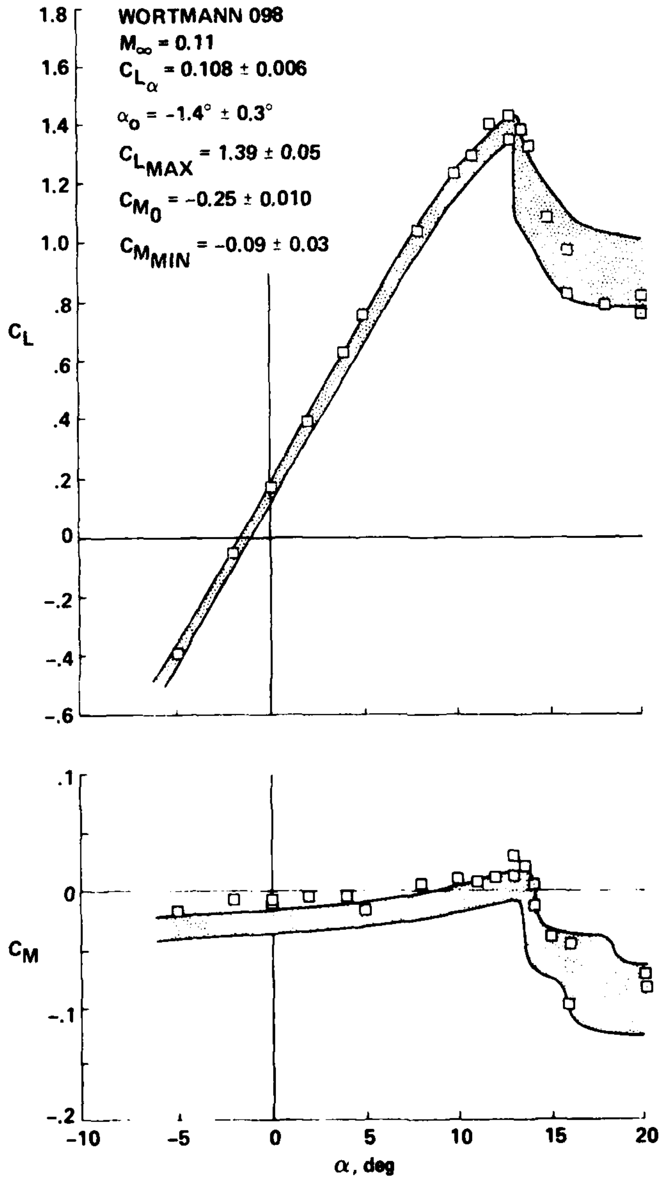

Figure 10.- Static lift and moment data on the Wortmann FX-098 airfoil at $M_\infty = 0.11$.

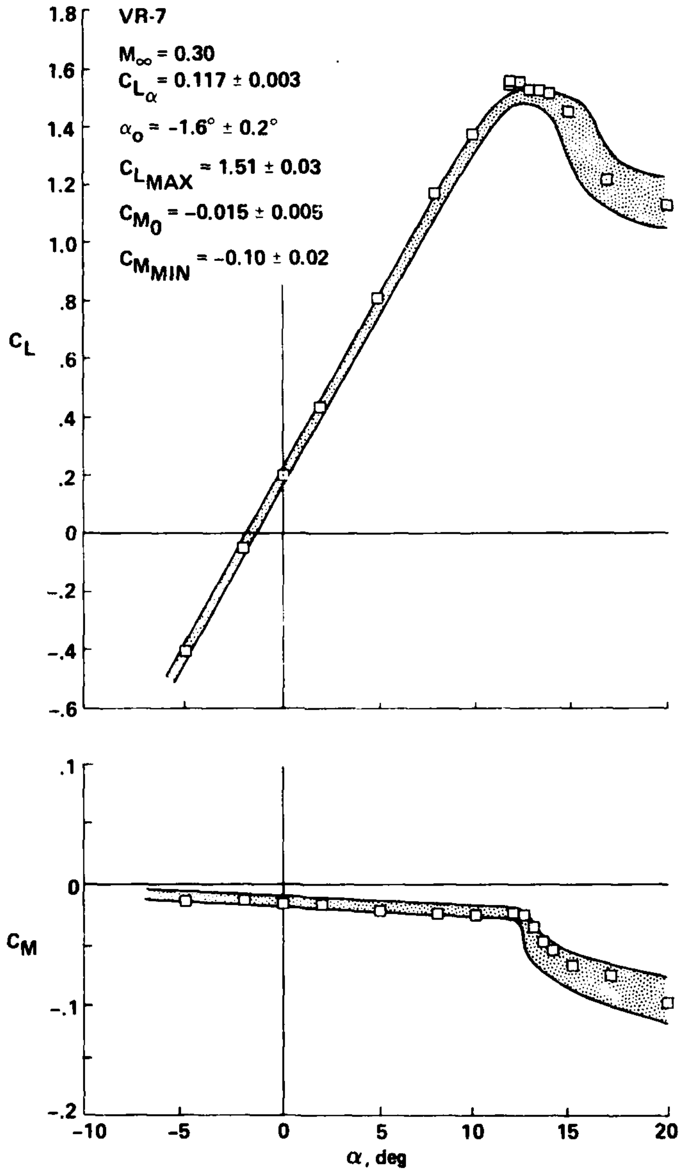

Figure 11.- Static lift and moment data on the Vertol VR-7 airfoil at $M_\infty = 0.30$.

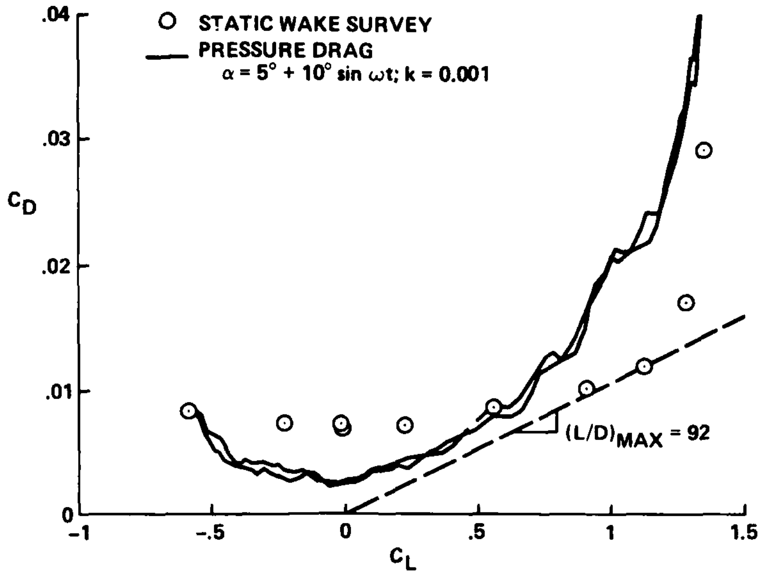

Figure 12.- Comparison of measured lift-drag polars for the NACA 0012 airfoil at $M_\infty = 0.30$, including wind-tunnel-wall corrections.

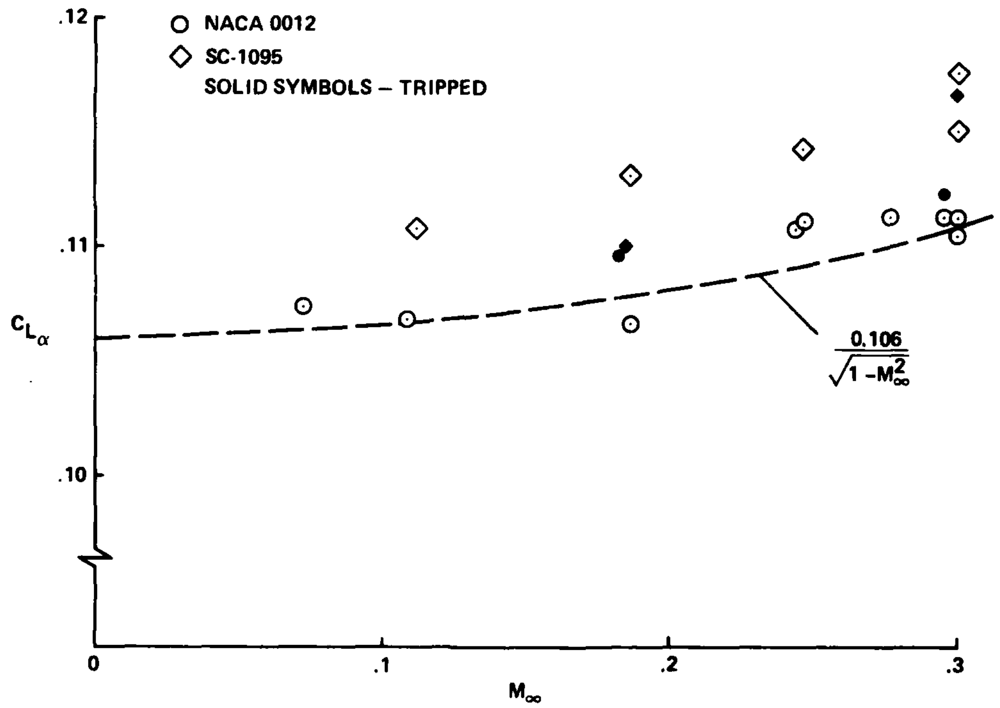

Figure 13.- Comparison of lift-curve slopes on the NACA 0012 and SC-1095 airfoils, including wind-tunnel-wall corrections.

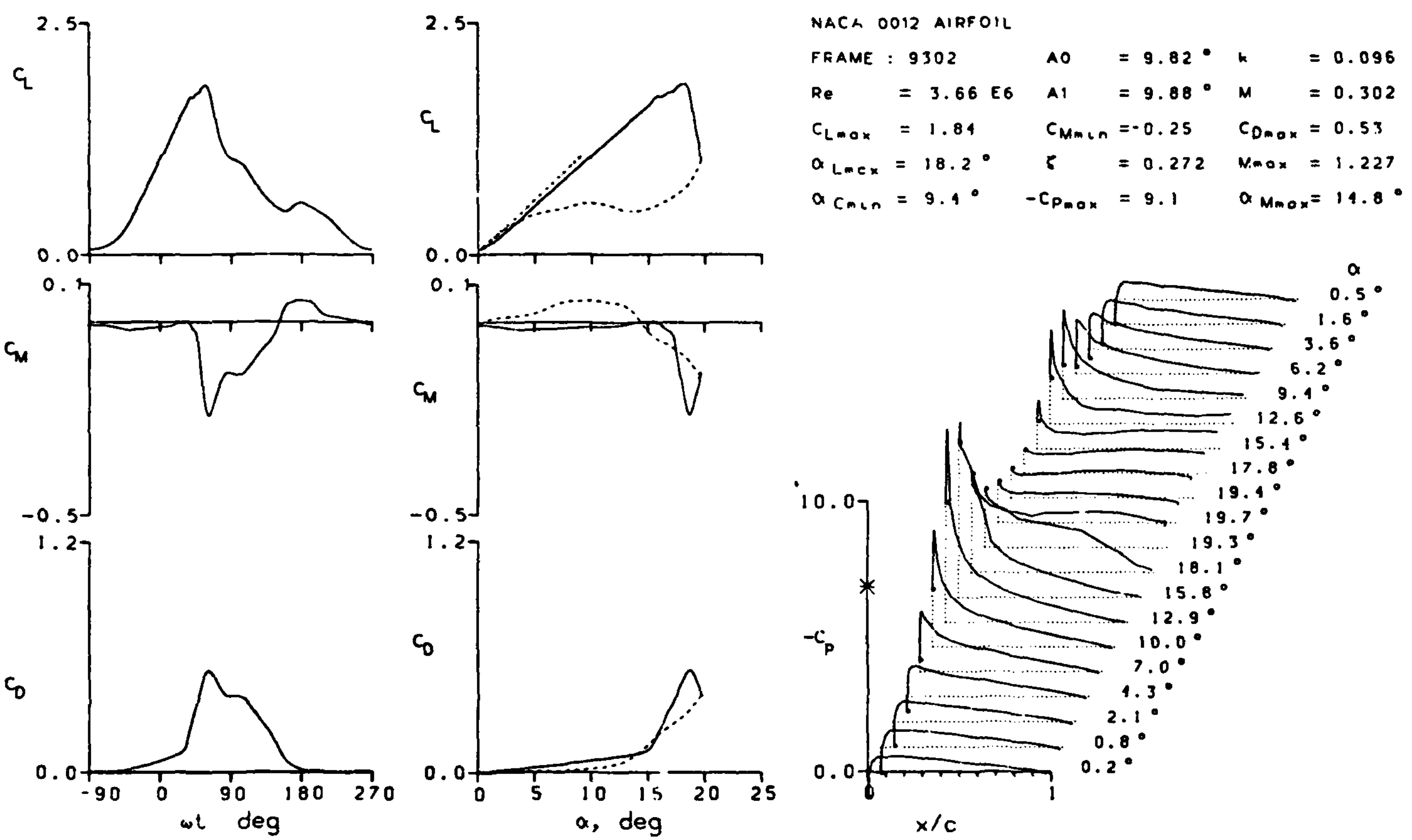

Figure 14.- Typical data presentation from volume 2; no wall corrections.

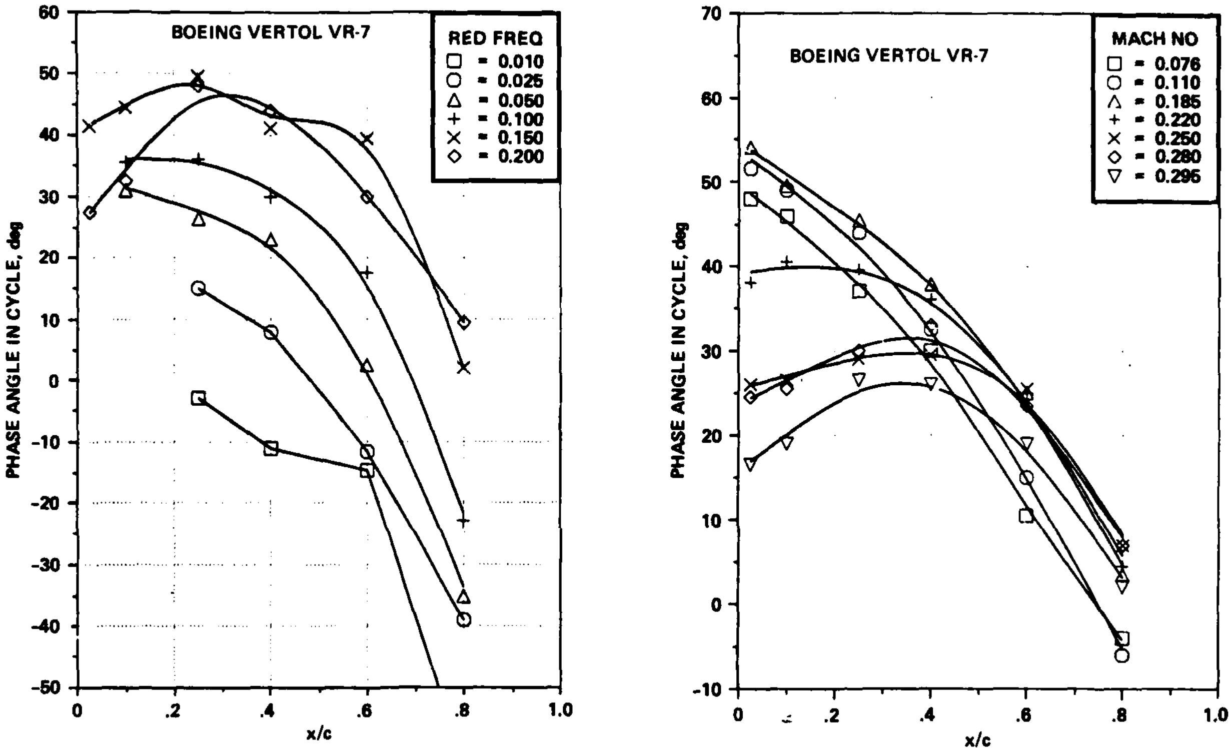

(a) Reduced frequency sweep: light stall.

(b) Mach number sweep: deep stall.

Figure 15.- Typical data presentation from volume 3.

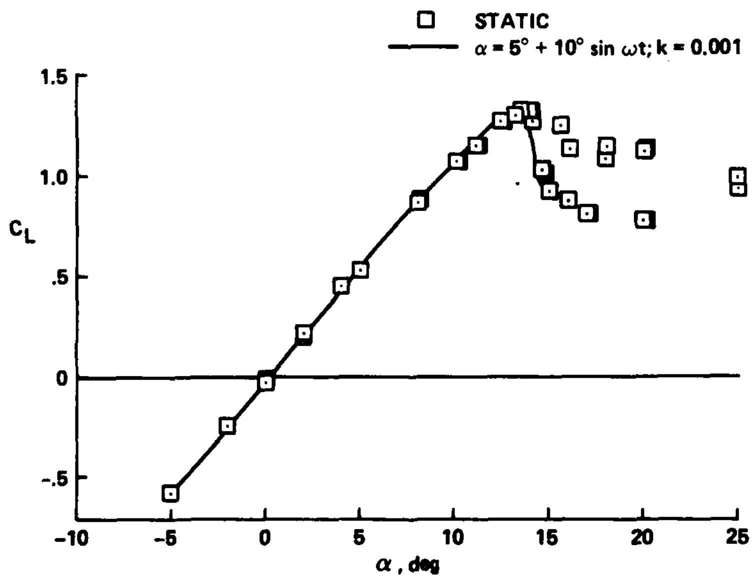

(a) C_L vs α.

Figure 16.- Static characteristics of the NACA 0012 airfoil at $M_\infty = 0.30$, including wind-tunnel-wall corrections.

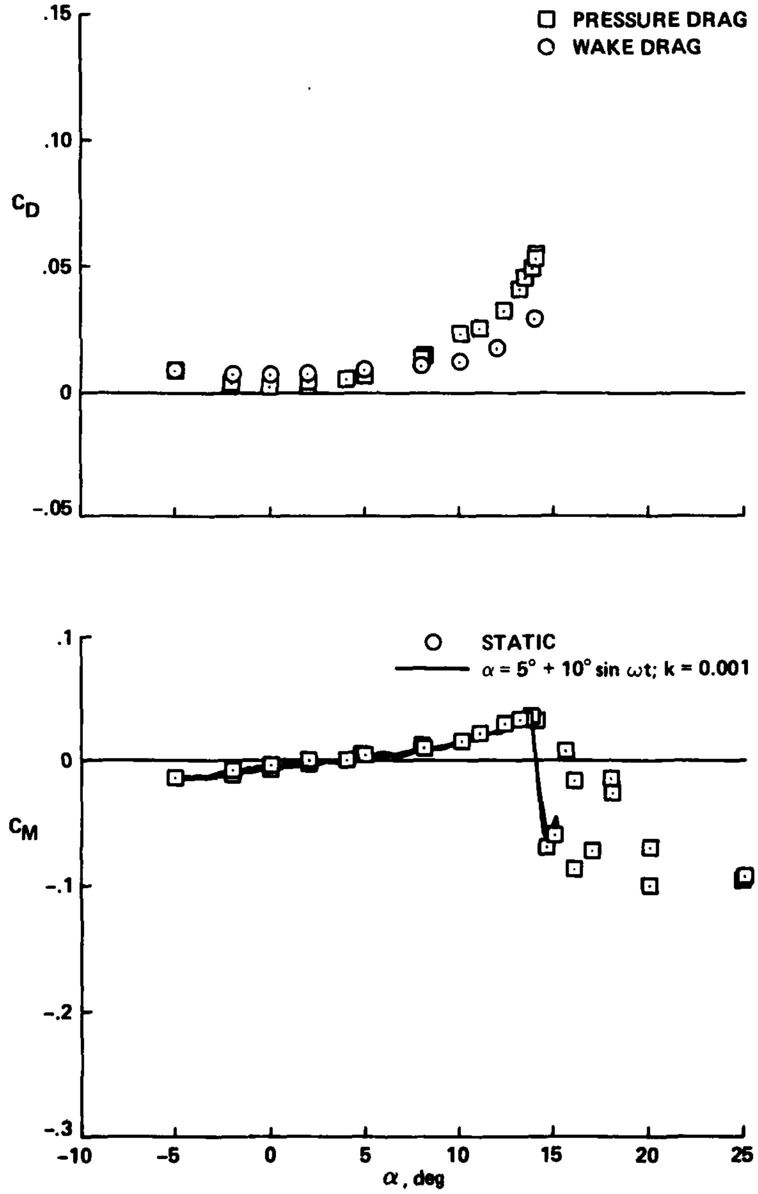

(b) C_D and C_M vs α.

Figure 16.- Concluded.

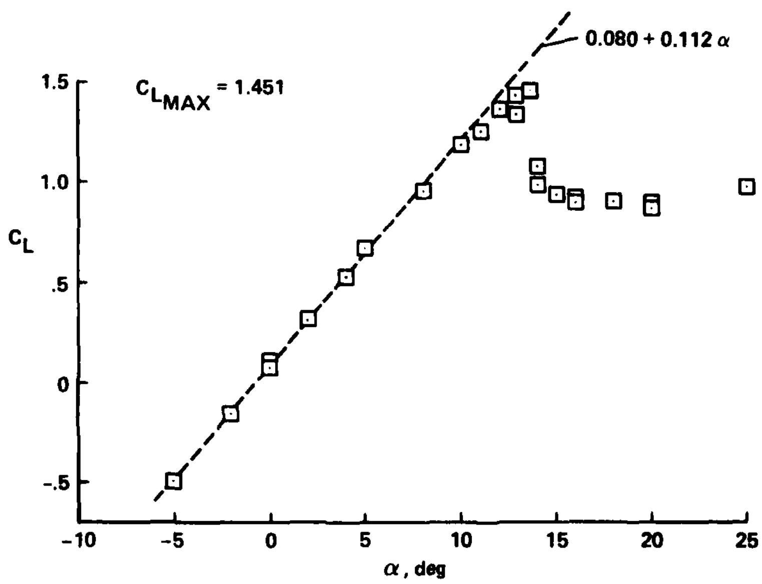

(a) C_L vs α.

Figure 17.- Static characteristics of the Ames A-01 airfoil at $M_\infty = 0.30$, including wind-tunnel-wall corrections.

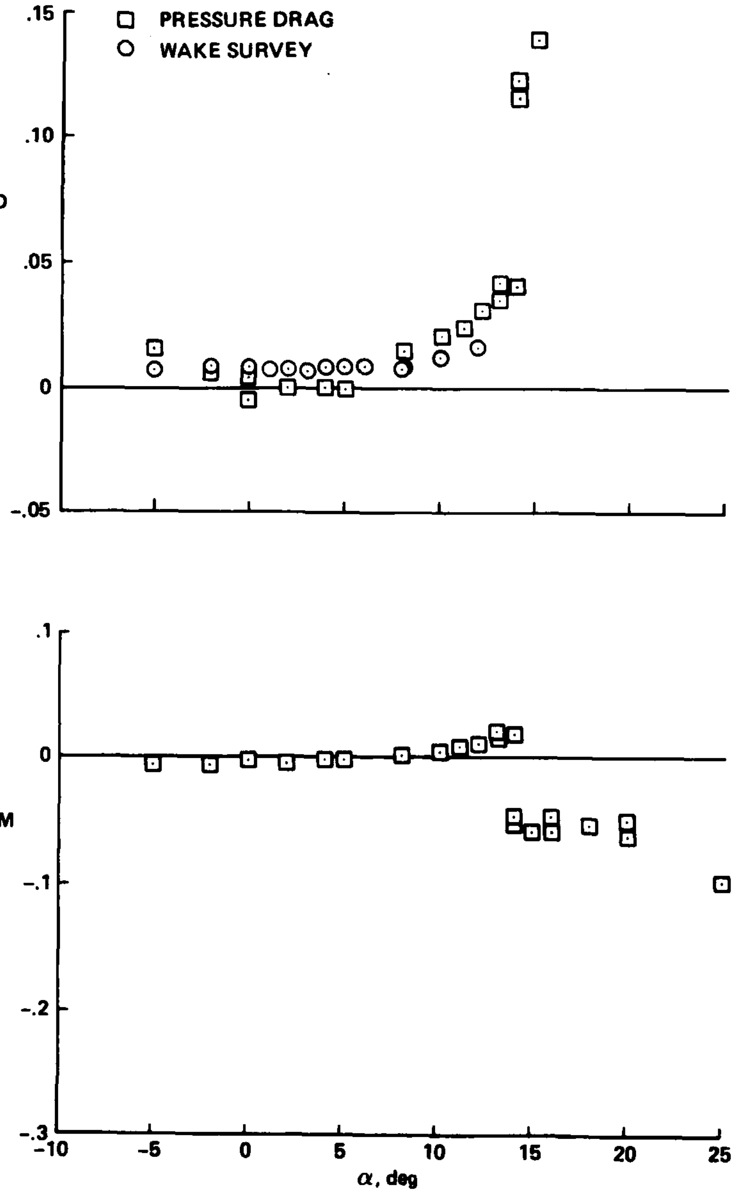

(b) C_D and C_M vs α.

Figure 17.- Concluded.

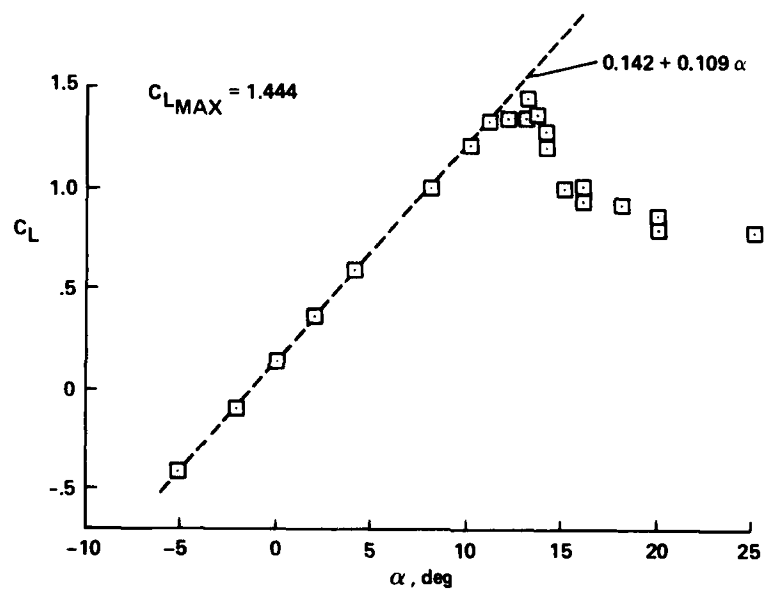

(a) C_L vs α.

Figure 18.- Static characteristics of the Wortmann FX-098 airfoil at $M_\infty = 0.30$, including wind-tunnel-wall corrections.

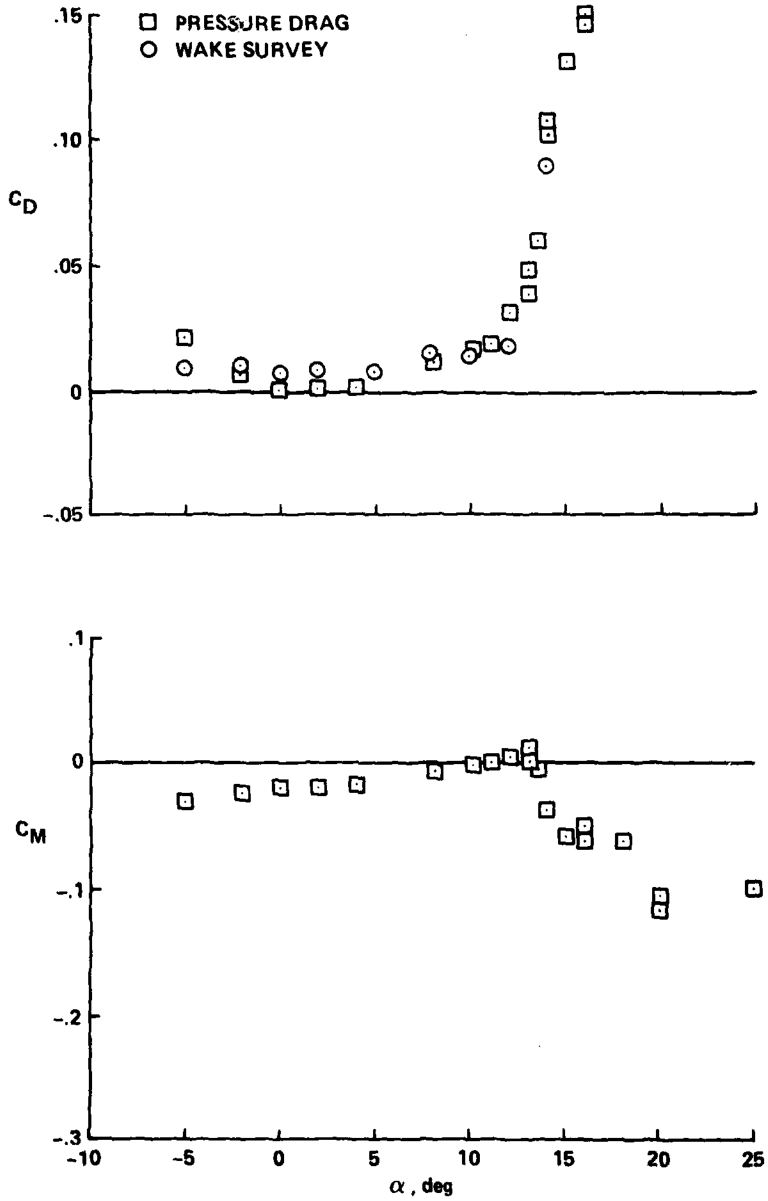

(b) C_D and C_M vs α.

Figure 18.- Concluded.

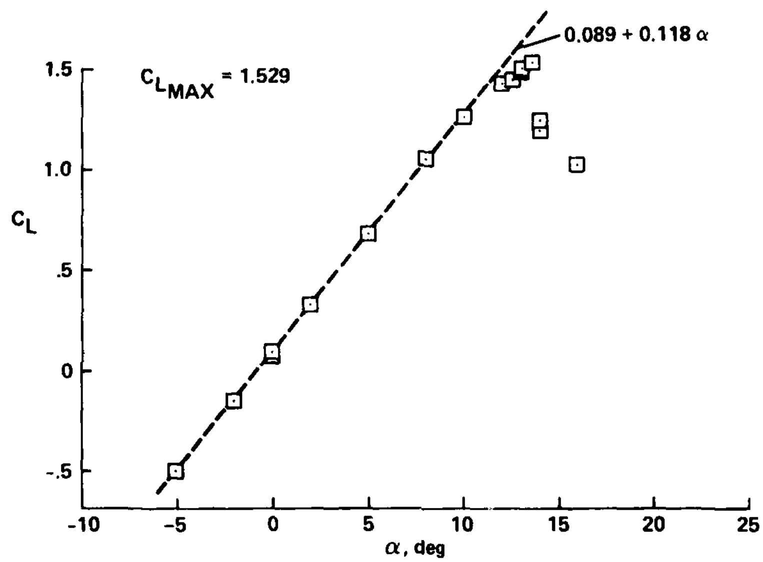

(a) C_L vs α.

Figure 19.- Static characteristics of the Sikorsky SC-1095 airfoil at $M_\infty = 0.30$, including wind-tunnel-wall corrections.

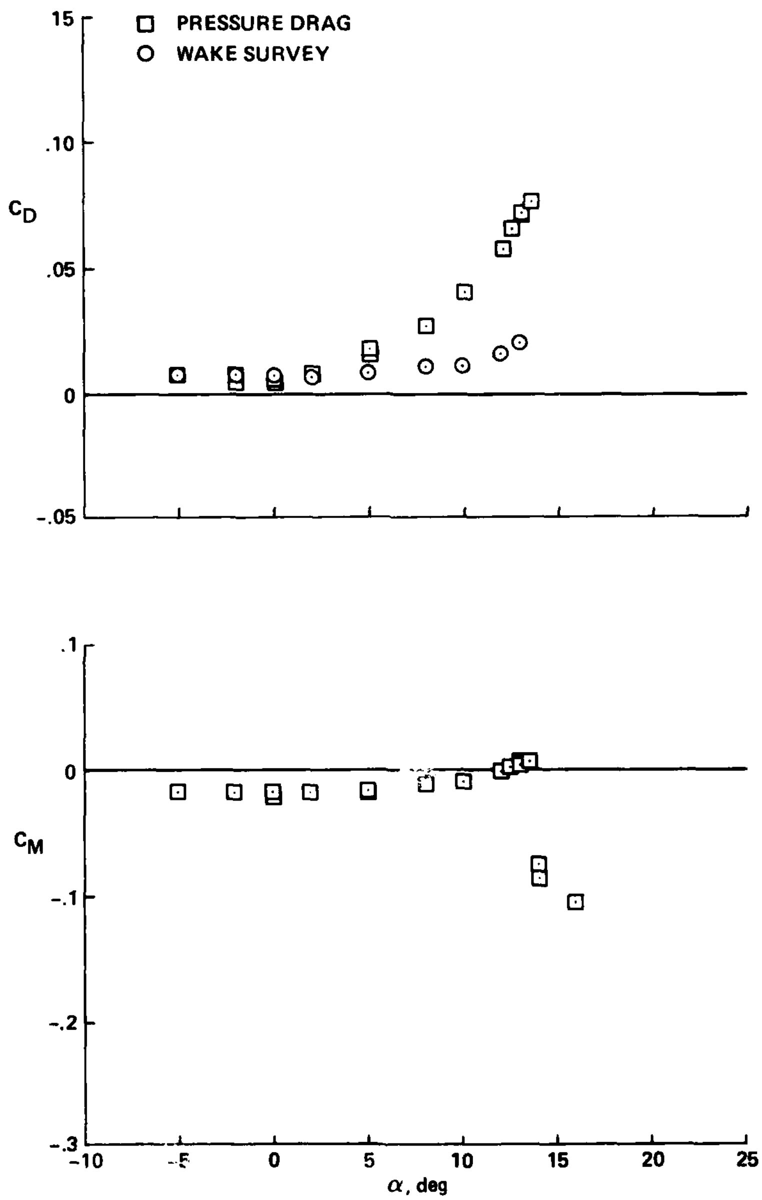

(b) C_D and C_M vs α.

Figure 19.- Concluded.

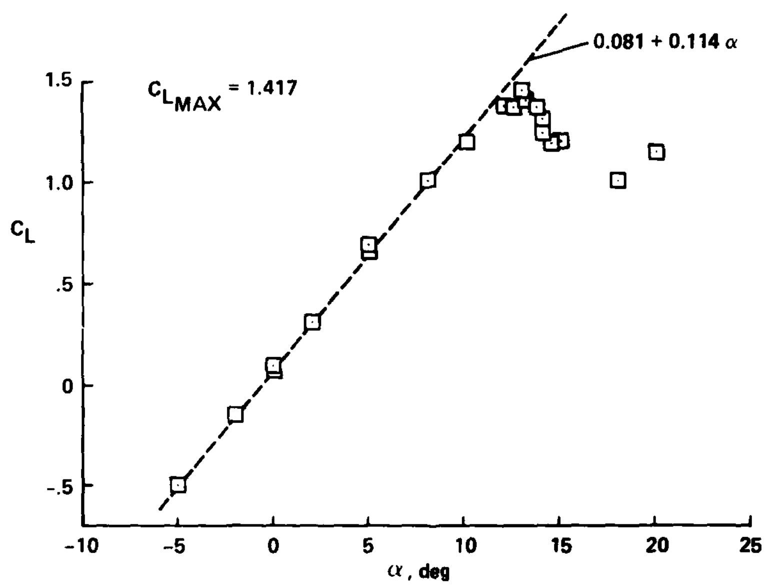

(a) C_L vs α.

Figure 20.- Static characteristics of the Hughes HH-02 airfoil at $M_\infty = 0.30$, including wind-tunnel-wall corrections.

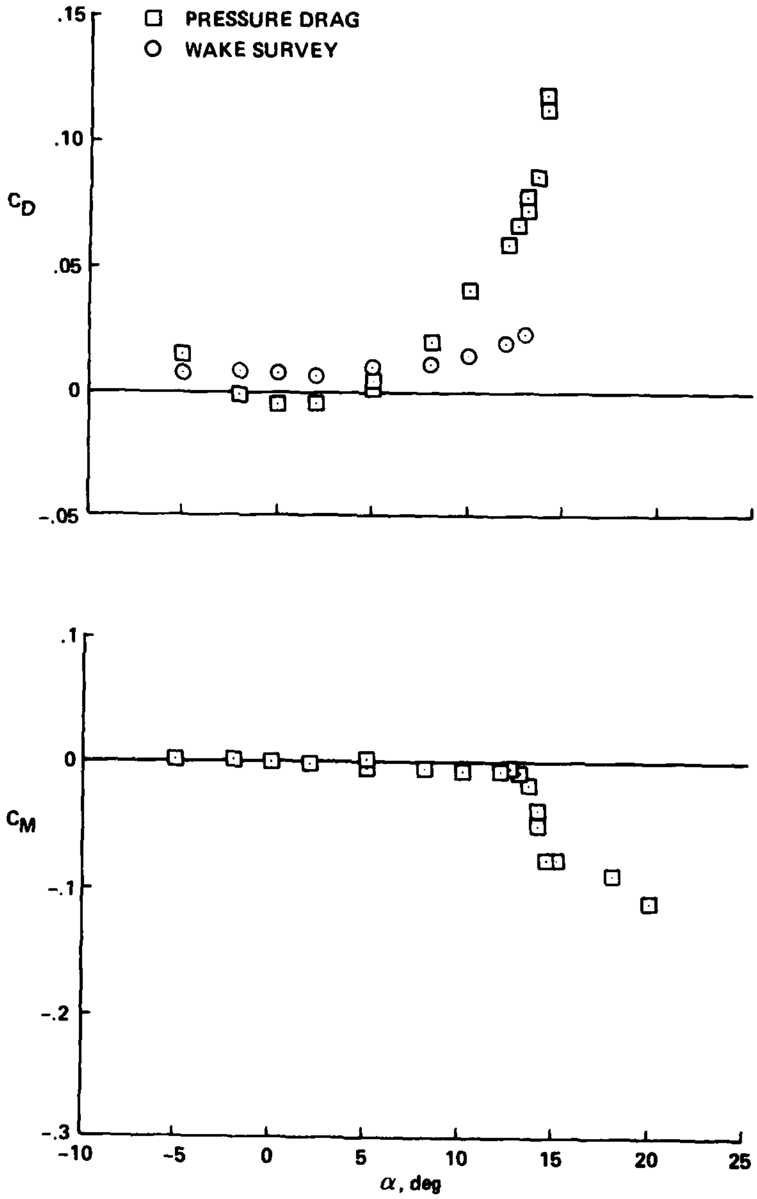

(b) C_D and C_M vs α.

Figure 20.- Concluded.

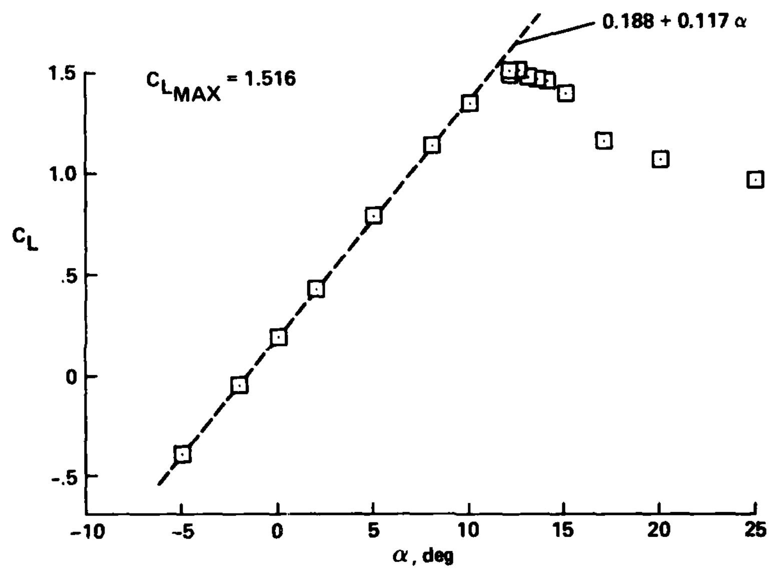

(a) C_L vs α.

Figure 21.- Static characteristics of the Vertol VR-7 airfoil at $M_\infty = 0.30$, including wind-tunnel-wall corrections.

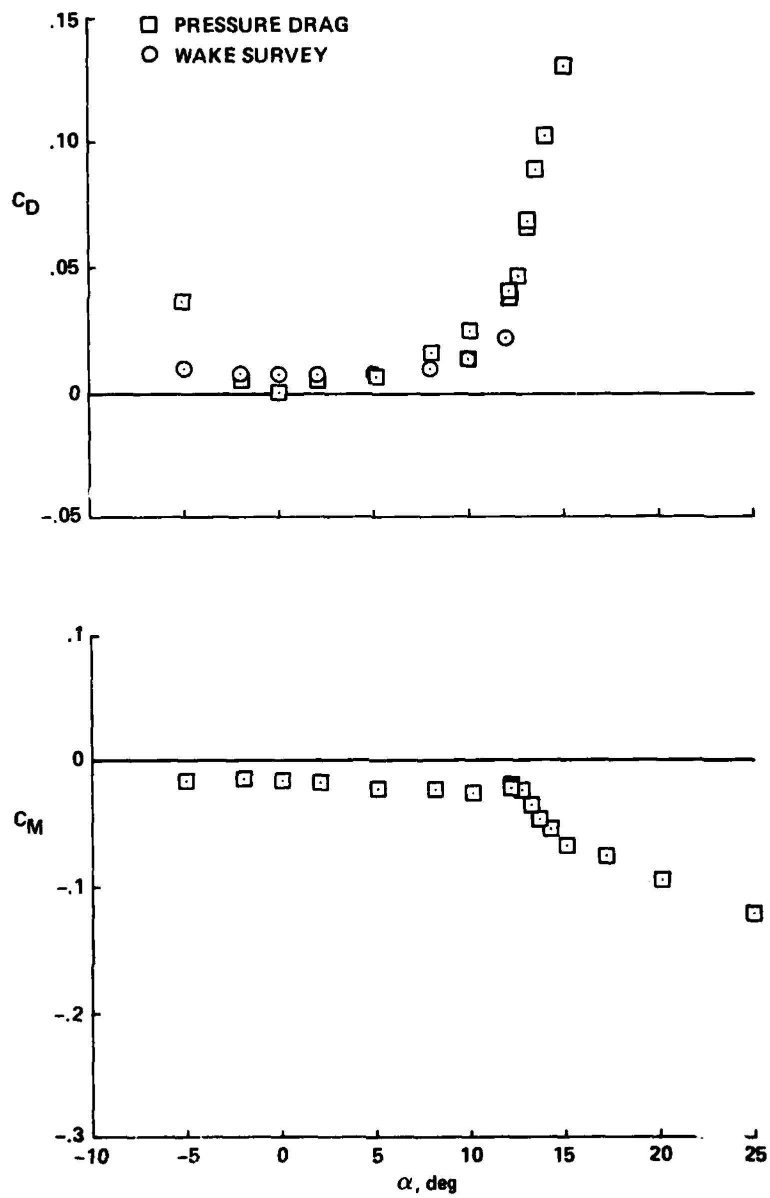

(b) C_D and C_M vs α.

Figure 21.- Concluded.

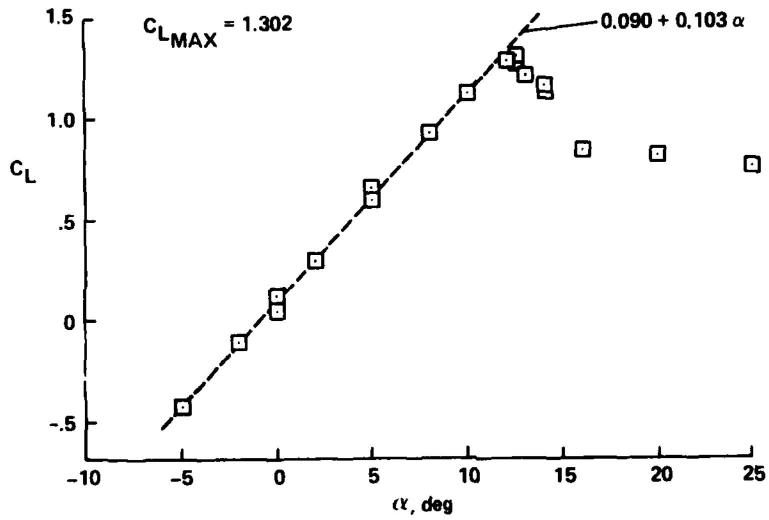

(a) C_L vs α.

Figure 22.- Static characteristics of the NLR-1 airfoil at $M_\infty = 0.30$, including wind-tunnel-wall corrections.

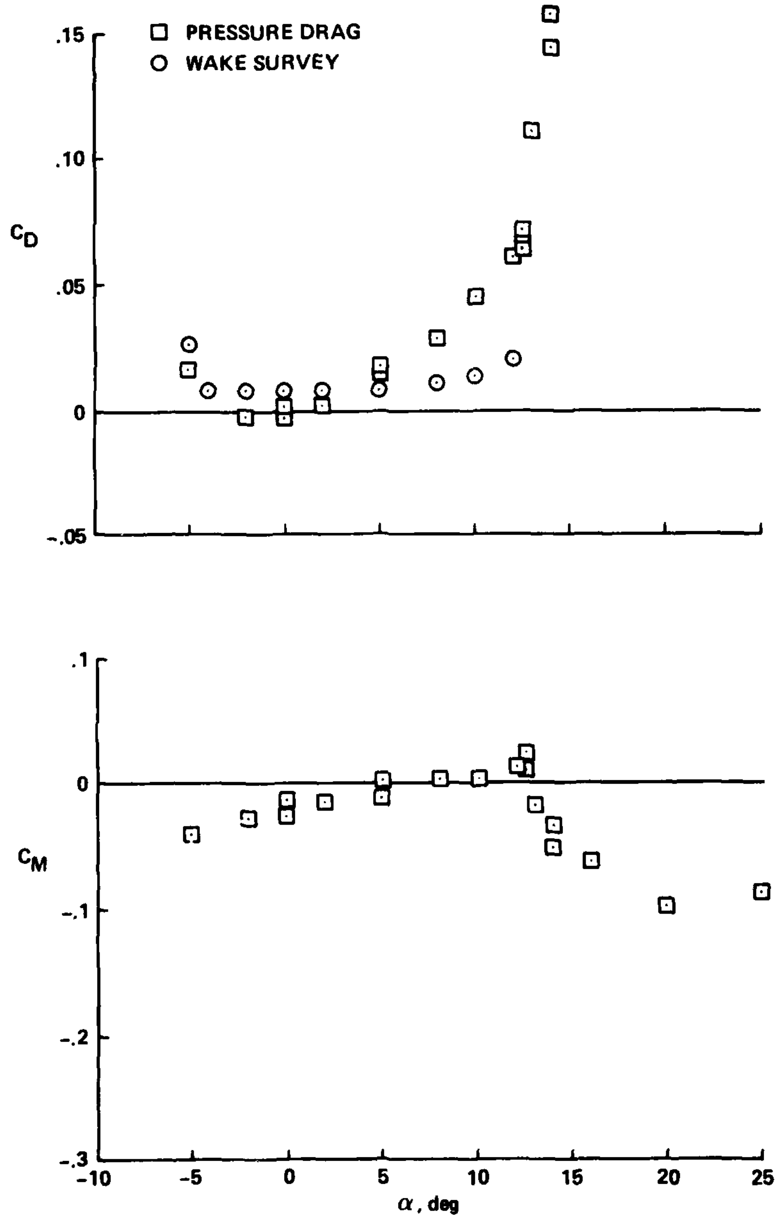

(b) C_D and C_M vs α.

Figure 22.- Concluded.

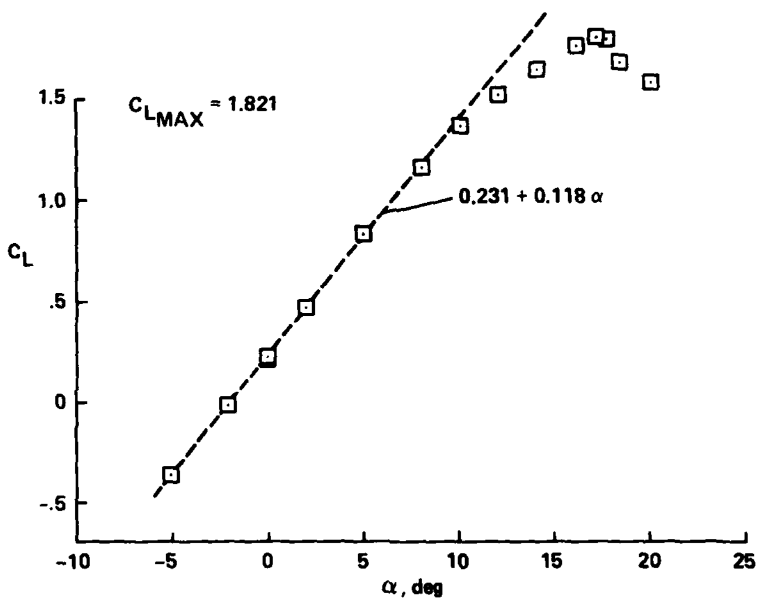

(a) C_L vs α.

Figure 23.- Static characteristics of the NLR-7301 airfoil at $M_\infty = 0.30$, including wind-tunnel-wall corrections.

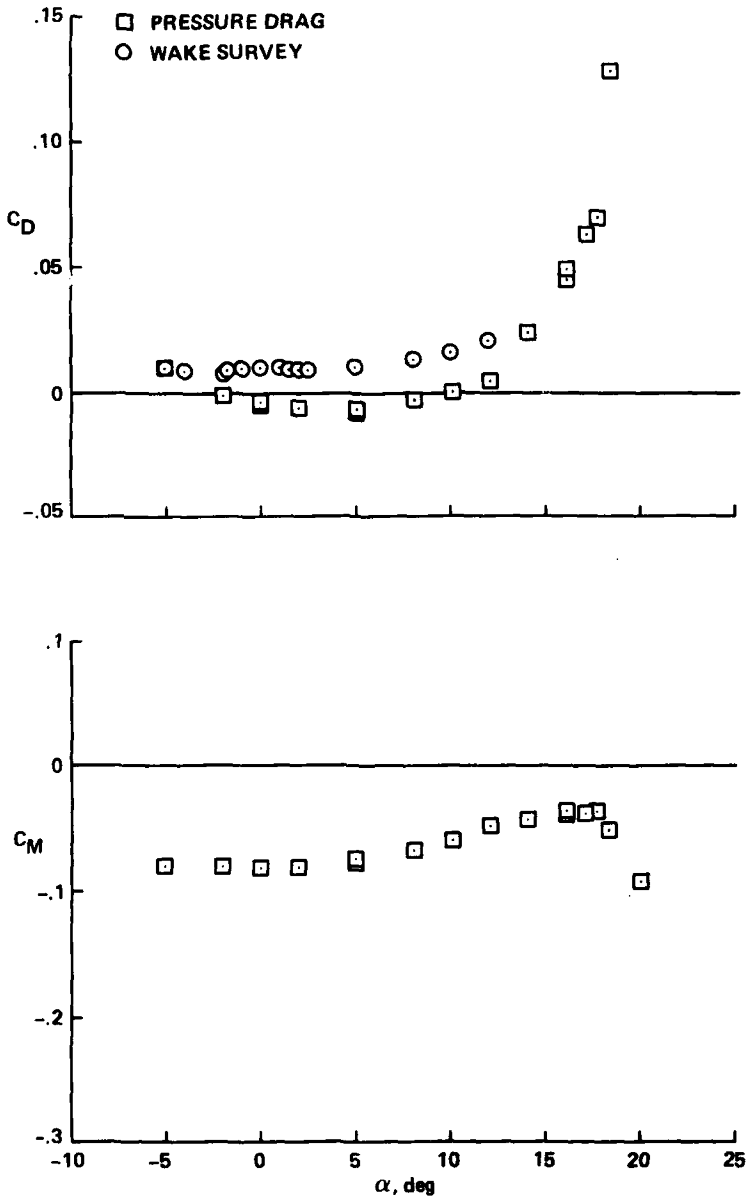

(b) C_D and C_M vs α.

Figure 23.- Concluded.

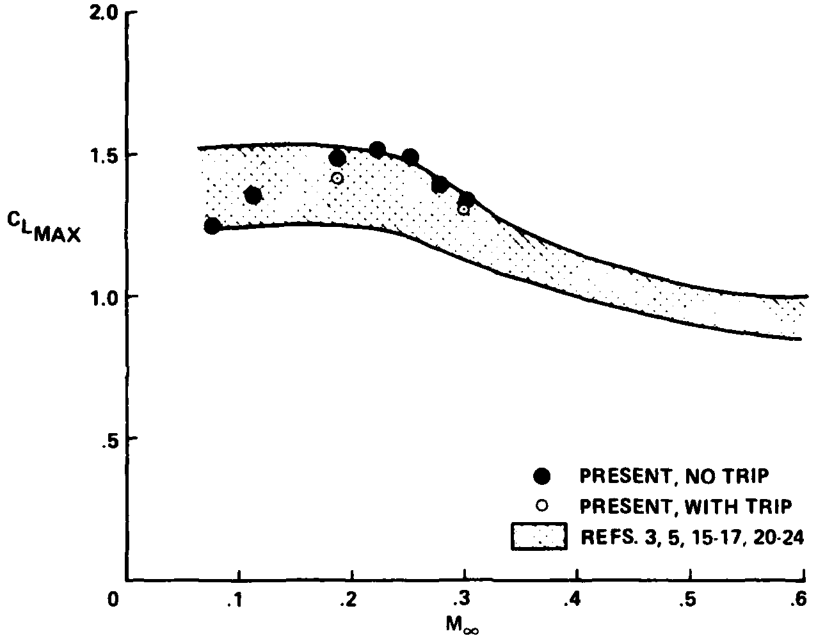

Figure 24.- Comparison of maximum static lift on the NACA 0012 airfoil.

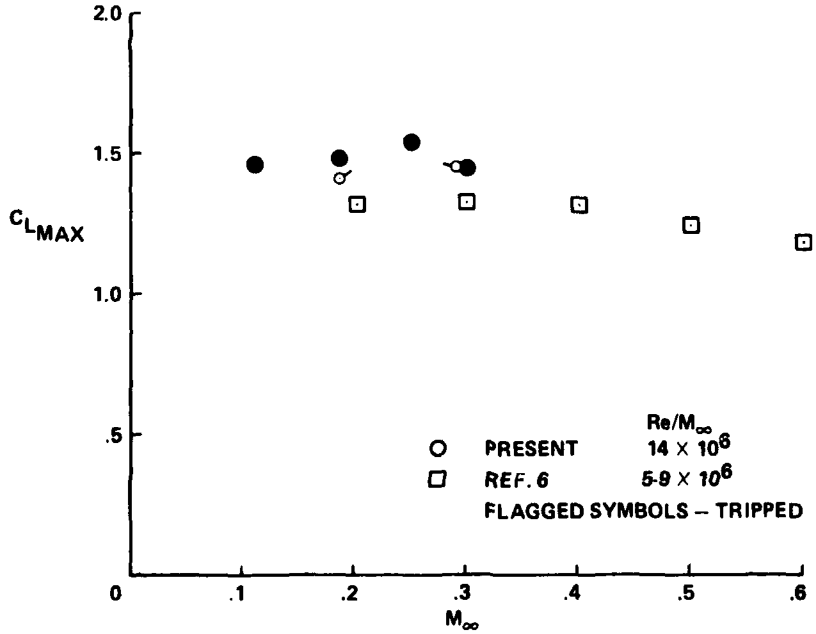

Figure 25.- Comparison of maximum static lift on the Ames A-01 airfoil.

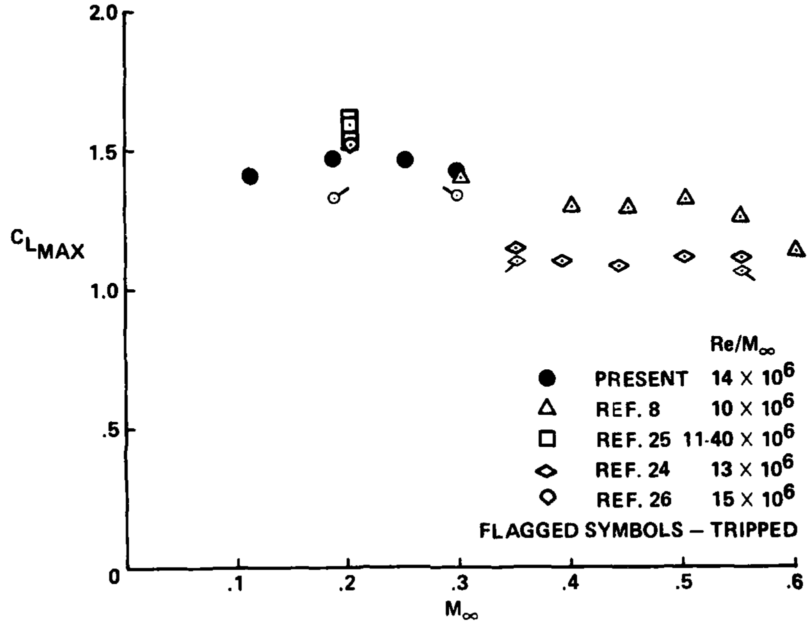

Figure 26.- Comparison of maximum static lift on the Wortmann FX-098 airfoil.

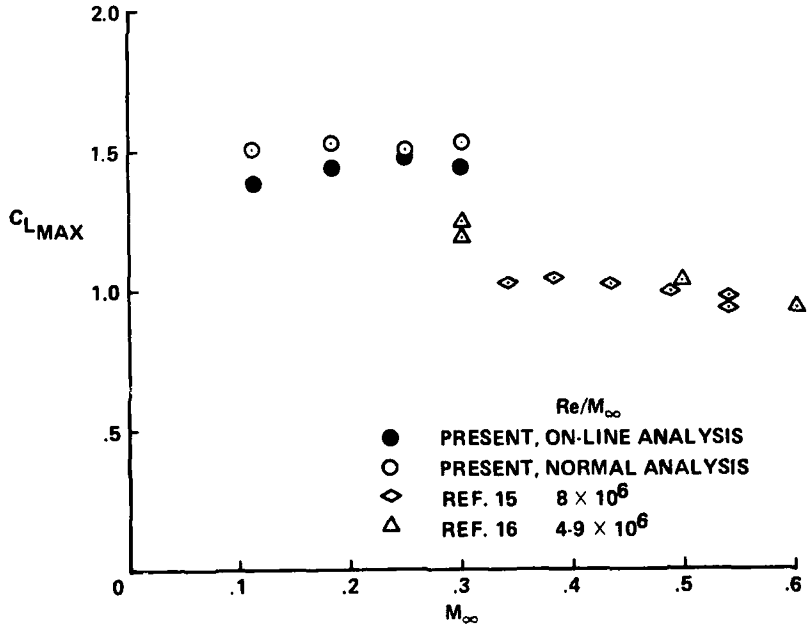

Figure 27.- Comparison of maximum static lift on the Sikorsky SC-1095 airfoil.

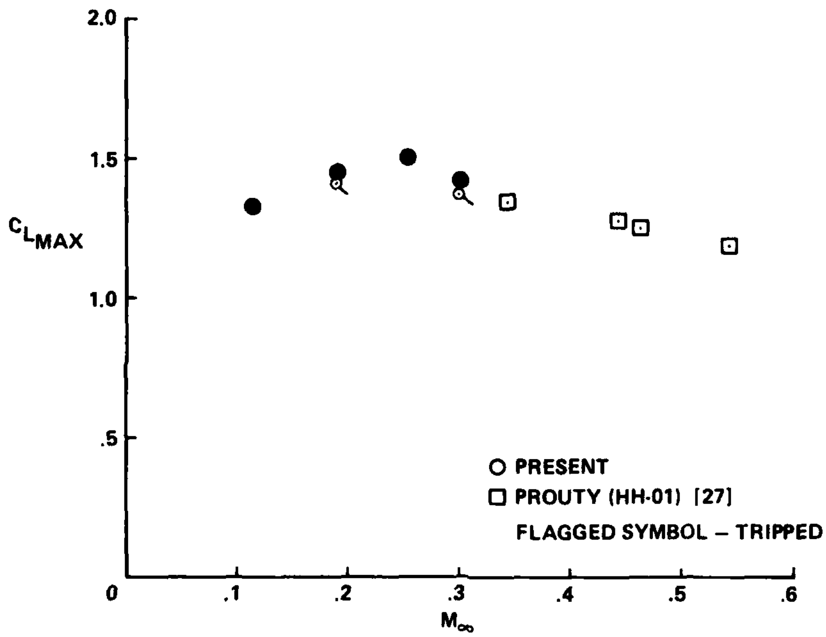

Figure 28.- Comparison of maximum static lift on the Hughes HH-02 airfoil.

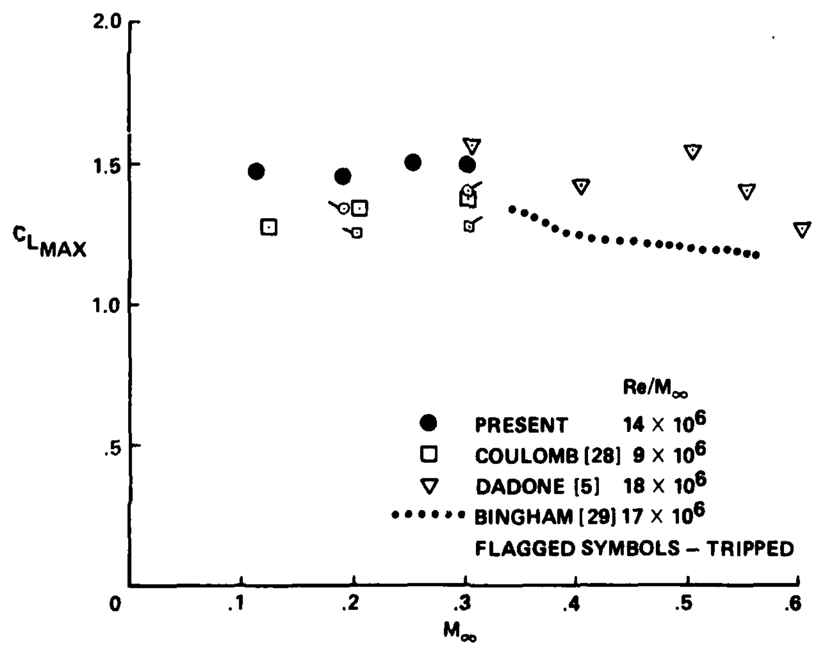

Figure 29.- Comparison of maximum static lift on the Vertol VR-7 airfoil.

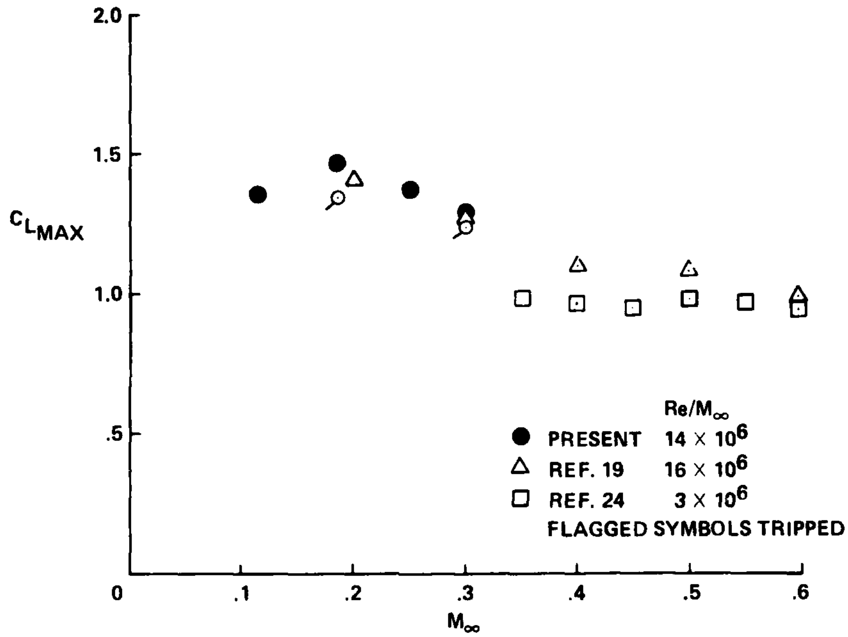

Figure 30.- Comparison of maximum static lift on the NLR-1 airfoil.

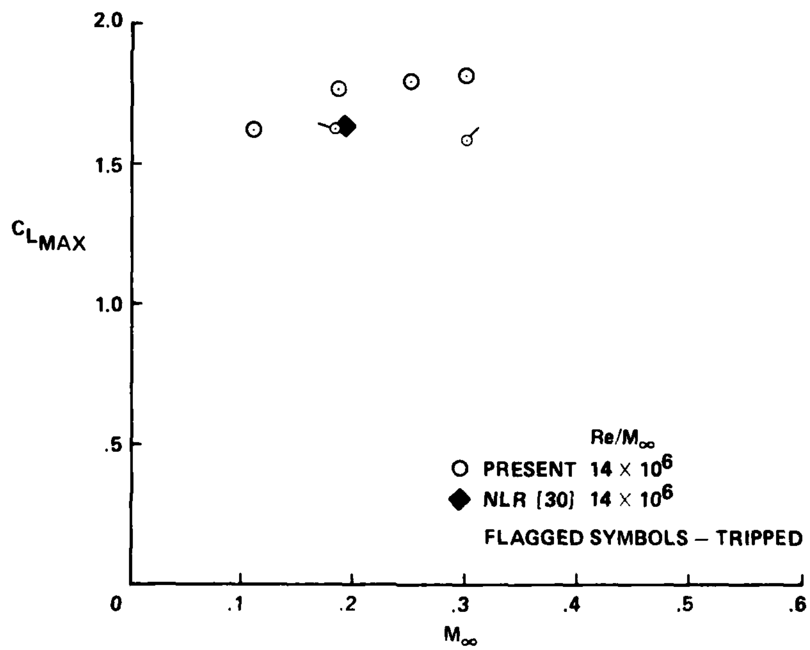

Figure 31.- Comparison of maximum static lift on the NLR-7301 airfoil.

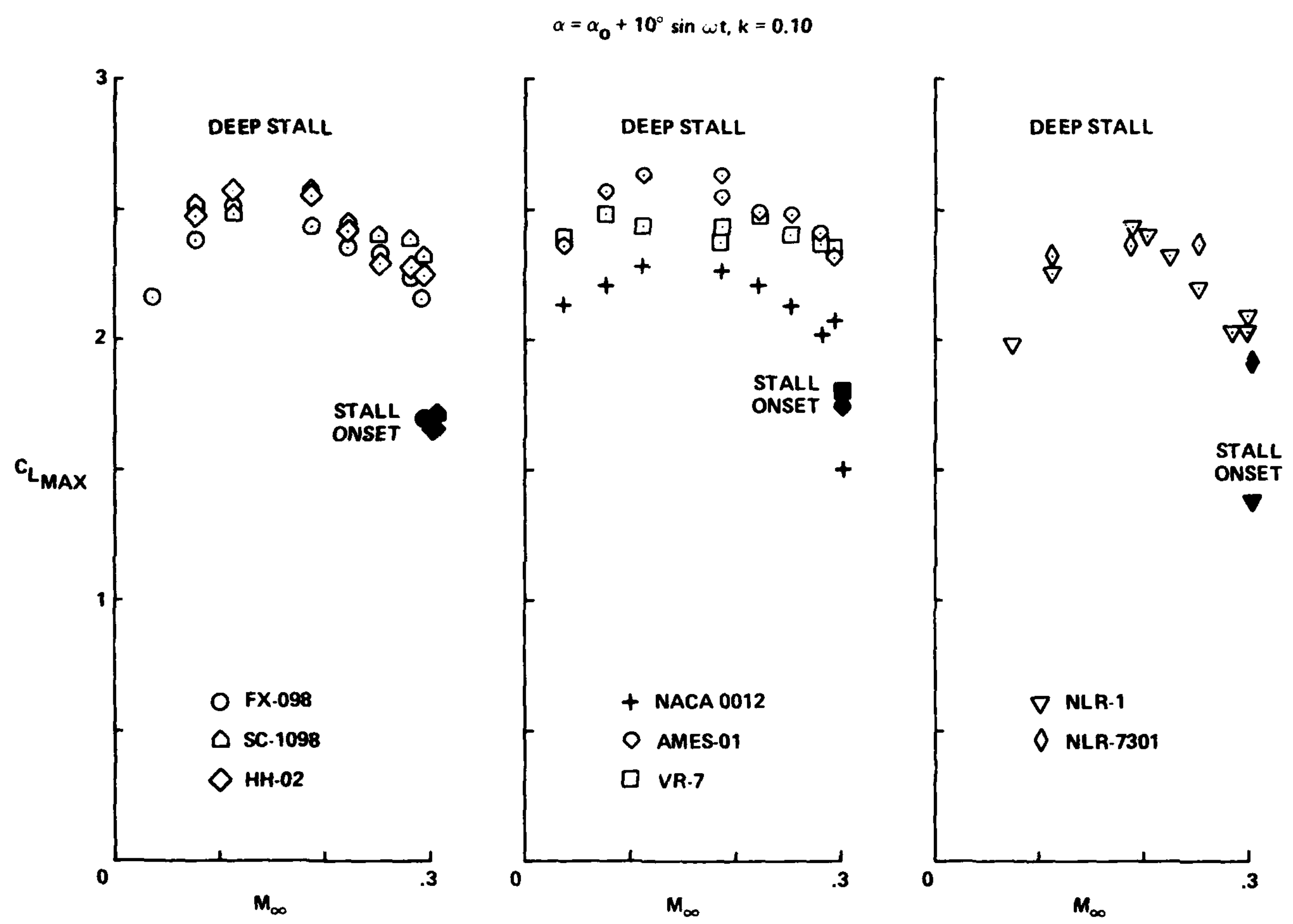

Figure 32.- Maximum unsteady lift on the eight airfoils: solid symbols = stall onset; open symbols = deep stall.

AD-A119 827 NATIONAL AERONUATICS AND SPACE ADMINISTRATION MOFFET--ETC F/G 20/4
AN EXPERIMENTAL STUDY OF DYNAMIC STALL ON ADVANCED AIRFOIL SECT--ETC(U)
JUL 82 W J MCCROSKEY, K W MCALISTER, L W CARR

UNCLASSIFIED NASA-A-8924-VOL-1 NASA-TM-84245-VOL-1 NL

2 of 2

END
DATE
FILMED
11 82
DTIC

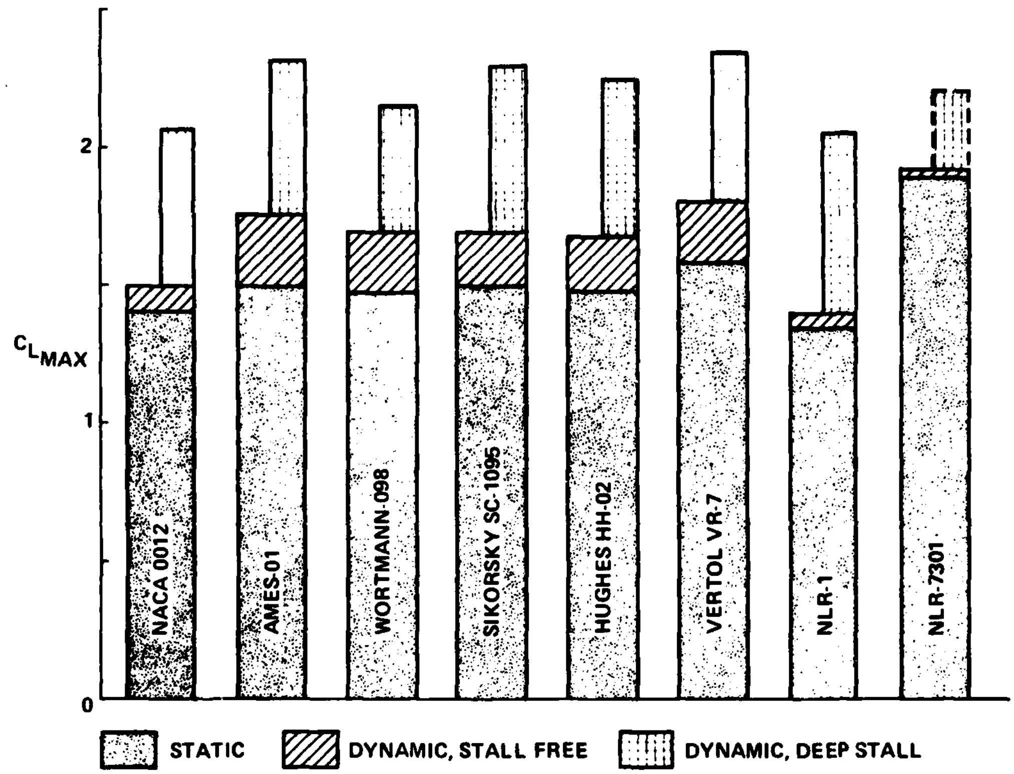

Figure 33.- Comparison of maximum lift on the eight airfoils at $M_\infty = 0.30$.

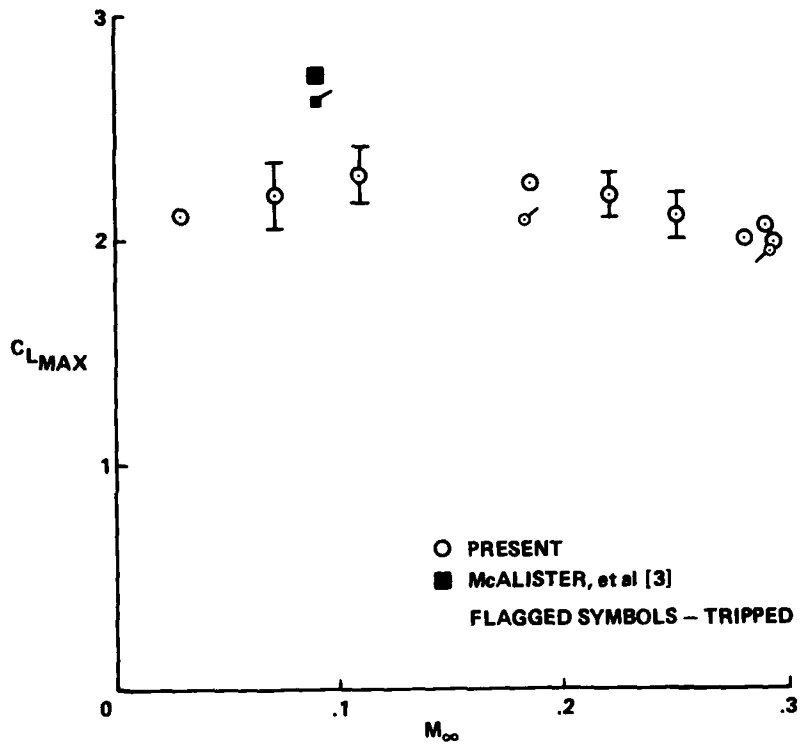

Figure 34.- Comparison of maximum lift on the NACA 0012 airfoil under deep-dynamic-stall conditions: $\alpha = 15° + 10° \sin \omega t$, $k = 0.10$.

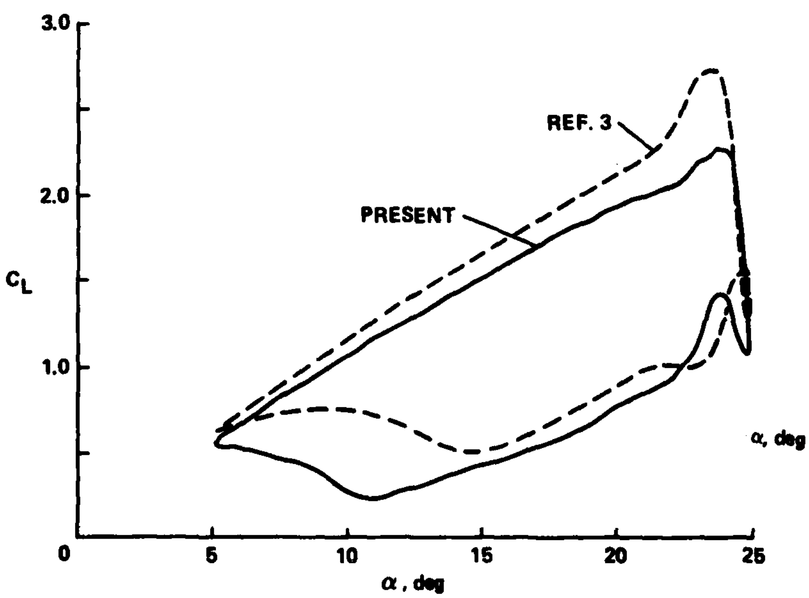

Figure 35.- Comparison of the lift hysteresis on the NACA 0012 airfoil: $M_\infty \approx 0.1$, $\alpha = 15° + 10° \sin \omega t$, $k = 0.10$.

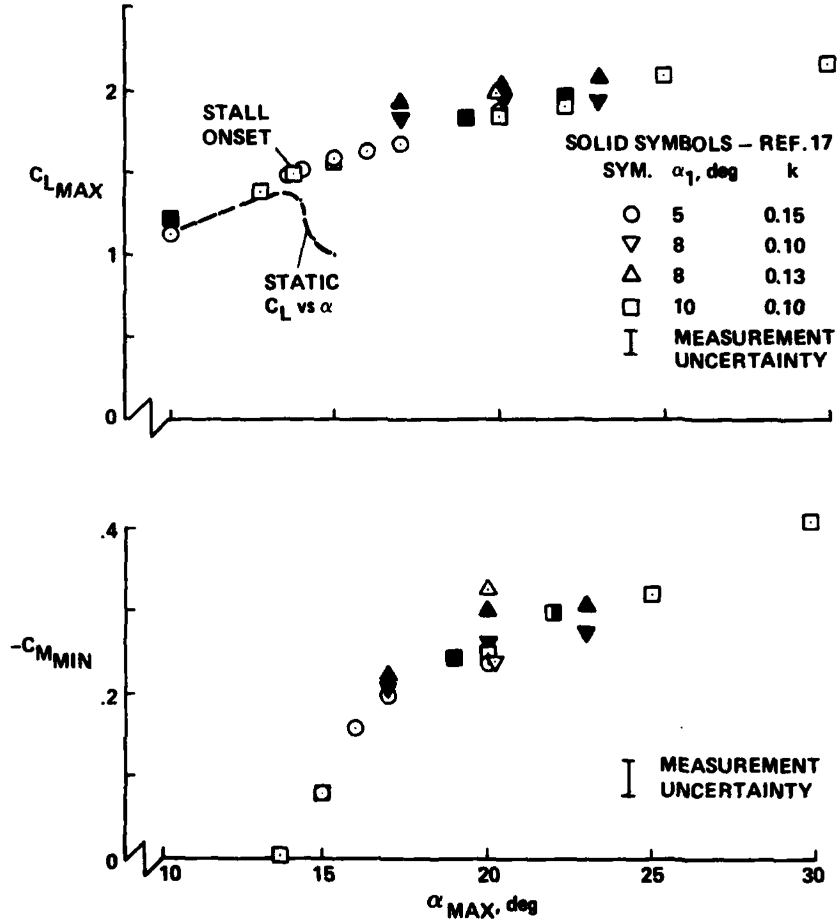

Figure 36.- Comparison of maximum airloads on the NACA 0012 airfoil at $M_\infty = 0.30$ and $\alpha_1 k^2 \cong$ constant.

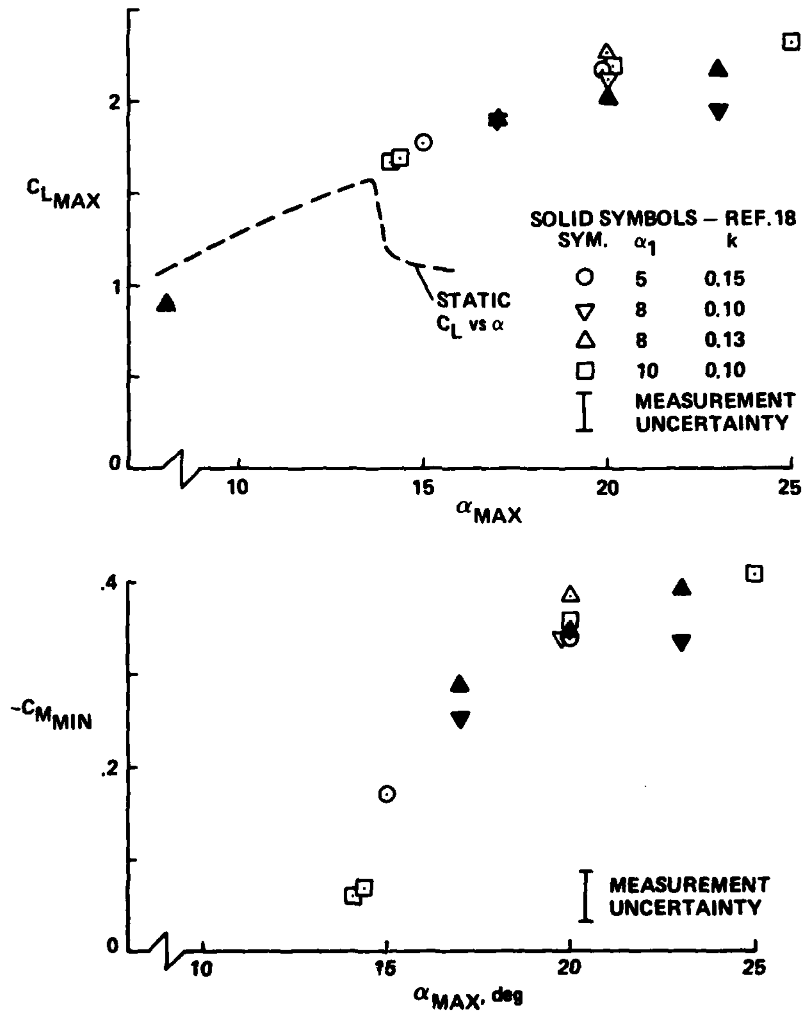

Figure 37.- Comparison of maximum airloads on the Sikorsky SC-1095 airfoil at $M_\infty = 0.30$ and $\alpha_1 k^2 \approx$ constant.

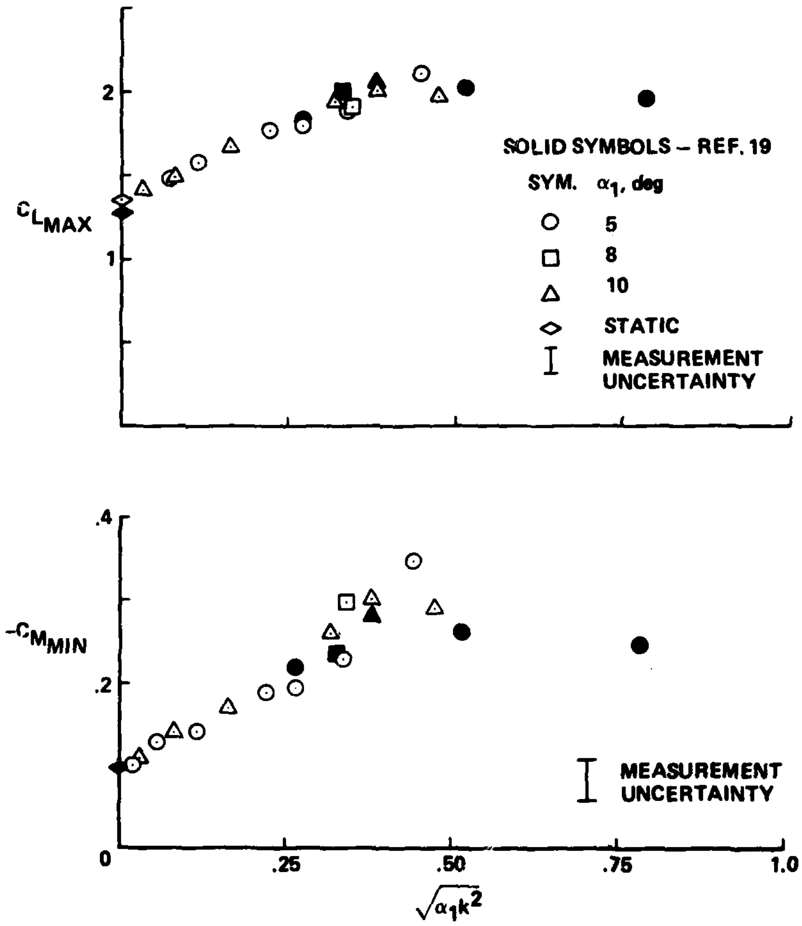

Figure 38.- Comparison of maximum airloads on the NLR-1 airfoil at $M_\infty = 0.3$ and $\alpha_{max} = 20°$.

1. Report No. NASA TM 84245
USAAVRADCOM TR-82-A-8

2. Government Accession No. AD-A119 827

3. Recipient's Catalog No.

4. Title and Subtitle
AN EXPERIMENTAL STUDY OF DYNAMIC STALL ON ADVANCED AIRFOIL SECTIONS
VOLUME 1. SUMMARY OF THE EXPERIMENT

5. Report Date
July 1982

6. Performing Organization Code

7. Author(s)
W. J. McCroskey, K. W. McAlister, L. W. Carr, and S. L. Pucci

8. Performing Organization Report No.
A-8924

9. Performing Organization Name and Address NASA Ames Research Center, Moffett Field, Calif. 94035, and U.S. Army Aeromechanics Laboratory (AVRADCOM), Ames Research Center, Moffett Field, Calif. 94035

10. Work Unit No.
K-1585

11. Contract or Grant No.

12. Sponsoring Agency Name and Address National Aeronautics and Space Administration, Washington, D.C. 20546, and U.S. Army Aviation R&D Command, St. Louis, MO 93166

13. Type of Report and Period Covered
Technical Memorandum

14. Sponsoring Agency Code

15. Supplementary Notes
Point of Contact: W. J. McCroskey, Ames Research Center, MS 202A-1
Moffett Field, Calif. 94035
(415) 965-6428 or FTS 448-6428

16. Abstract
The static and dynamic characteristics of seven helicopter sections and a fixed-wing supercritical airfoil were investigated over a wide range of nominally two-dimensional flow conditions, at Mach numbers up to 0.30 and Reynolds numbers up to 4×10^6. Details of the experiment, estimates of measurement accuracy, and test conditions are described in this volume (the first of three volumes). Representative results are also presented and comparisons are made with data from other sources. The complete results for pressure distributions, forces, pitching moments, and boundary-layer separation and reattachment characteristics are available in graphical form in volumes 2 and 3.

The results of the experiment show important differences between airfoils, which would otherwise tend to be masked by differences in wind tunnels, particularly in steady cases. All of the airfoils tested provide significant advantages over the conventional NACA 0012 profile. In general, however, the parameters of the unsteady motion appear to be more important than airfoil shape in determining the dynamic-stall airloads.

17. Key Words (Suggested by Author(s))
Dynamic stall
Oscillating airfoils
Boundary layer measurements
Unsteady pressure distributions
Maximum lift
Airfoil data

18. Distribution Statement
Unlimited

Subject Category — 02

19. Security Classif. (of this report)	20. Security Classif. (of this page)	21. No. of Pages	22. Price*
Unclassified	Unclassified	103	A06

*For sale by the National Technical Information Service, Springfield, Virginia 22161